DURBAN UNIVERSITY OF TECHNOLOGY

EVALUATION OF GRID-SCALE BATTERY ENERGY STORAGE SYSTEM AS AN ENABLER FOR LARGE-SCALE RENEWABLE ENERGY INTEGRATION

by

Nomhle Loji

Student Number: 20924909

A dissertation submitted in fulfillment of the requirements for the degree for the **Master of Engineering in Electrical Power Engineering**

In the Department of Electrical Power Engineering

Faculty of Engineering and Built Environment

2022

Supervisor: Prof. I.E. Davidson
Co-Supervisor: Dr. K.T Akindeji

DECLARATION 1 - PLAGIARISM

I, Nomhle Loji, declare that:

1. The research reported in this thesis, except where otherwise indicated, is my original research.

2. This thesis has not been submitted for any degree or examination at any other university.

3. This thesis does not contain other persons' data, pictures, graphs or other information, unless specifically acknowledged as being sourced from other persons.

4. This thesis does not contain other persons' writing, unless specifically acknowledged as being sourced from other researchers. Where other written sources have been quoted, then:
   a. Their words have been re-written but the general information attributed to them has been referenced
   b. Where their exact words have been used, then their writing has been placed in italics and inside quotation marks, and referenced.

5. This thesis does not contain text, graphics or tables copied and pasted from the Internet, unless specifically acknowledged, and the source being detailed in the thesis and in the References sections.

Signed: ..... Date 21/07/2022

Nomhle Loji.

As the candidate's supervisor / co-supervisor I agree to the submission of this thesis.

Signed: ..... Date 21/7/2022

Prof. I.E. Davidson

Signed: .... Date...**21 July 2022**.....

Dr. K. T. Akindeji

ACKNOWLEDGEMENTS

In memory of my late parents, Salome and Mbingeleli Makhoba, and my late son, Sibusiso.

To my kids, thanks for understanding through all challenges I had to face, finally it is done.

I would like to thank my husband, Kabulo Loji, for his undying support, advice and continuous encouragement for me to complete the Master's degree. It is an honour.

I thank my supervisor and co-supervisor for their contribution towards the completion of the thesis.

DECLARATION 2 - PUBLICATIONS

The following publications emanated from this research investigation and form part and/or include research presented in this thesis. This include publications in preparation, submitted, in press and published giving details of the contribution of each author:

[1] **N. Loji**, K. Loji, R. Tiako, I. E. Davidson and T. K. Akindeji, "Loadability Assessment of a Photovoltaic Penetrated Grid to Offset Intermittency and Reduce Total Losses using Battery Energy Storage System," 2021 Southern African Universities Power Engineering Conference/Robotics and Mechatronics/Pattern Recognition Association of South Africa (SAUPEC/RobMech/PRASA), 2021, pp. 1-6, doi: 10.1109/SAUPEC/RobMech/PRASA52254.2021.9377026.

[2] **N. Loji,** K. Loji, I. E. Davidson, M. C. Leoaneka, and G. Sharma, "Flexibility Assessment of a Solar PV Penetrated IEEE 9-Bus System Using Dynamic Transient Stability " submitted for 2022 Southern Africa Universities Power Engineering Conference (SAUPEC}, Durban, South Africa

ABSTRACT

Because of many substantial benefits over other renewable energy resources (RES), photovoltaic (PV) and wind technologies are the most important emerging renewable energy sources (RES) and they are rapidly and widely propagating. However, they are non-dispatchable and, the stochastic and intermittent natures of solar irradiation and wind, are some of the fundamental barriers and challenges to their development and their large-scale deployment. As a result, power systems operators have no control over DG's available resources and are compelled to operate conventional generators to both cater for normal changes in load demand and make provision for DG's output variations. These concerns lead to increase the uncertainty in power systems operation as they modify both the structure and the operation of the distribution network by affecting inter alia, the voltage profile and stability, the direction of network power flow and the overall performance of the power system. Enabling PV penetration into electrical grids require a balance of supply and demand that cannot be achieved by oneself. Because of the flexibility to control their real power output, batteries are suggested as a suitable and cost effective solution to mitigate the adverse effects of intermittency and shape the fluctuation of the system's output into relatively constant power. There is a need to quantitatively investigate and evaluate the performance of the use of BESS that adequately smoothen the output of the PV-BESS sub-system for over-voltage reduction and peak load shaving during the high PV generation – low consumption time in lieu of power curtailment or reactive power injection. Using *DigSILENT*™ - *PowerFactory*™ this research work investigated the impacts of BESS on voltage stability and power losses with the aim of increasing system loadability and enhancing stability.

A modified standard IEEE 9-Bus was used to perform the studies using four cases and various scenarios and the simulation results and comparative analysis first reveal that the combined effect of the Solar PV-BESS system has a substantial positive impact on the system loadability improvement and reduction of the total power system losses. Results further confirmed the BESS's ability to act as generator, or load, respectively during high load demand/lower PV generation and lower demand//higher Solar PV generation to contribute to the voltage regulation and power system stability, offsetting effectively the intermittency of Solar PV energy sources and subsequently enabling greater RE penetration.

TABLE OF CONTENTS

LIST OF FIGURES

LIST OF TABLES

CHAPTER 1: INTRODUCTION

1.1 Historical background

The main purpose of an electrical grid is to provide a stable supply of electricity viable for the economic growth in the country. The electric power industry had undergone profound changes influenced by technical, economic, and political factors [1, 2], resulting in high demands of electricity versus what could be supplied, over the past three decades. An increase in generation capacity was essential to meet the demand so as to achieve grid stability as required by the Transmission System Operator (TSO). Another factor was that the fossil fuel-based electricity generation contributed to greenhouse gases emissions and pollutants [3]. Change in electricity generation was desired to fight climate change by reducing greenhouse gases while improving energy security. Emphasis on advances around renewable energy sources (RES) i.e. solar photovoltaics (PV), wind turbines and biomass became of high priority and evaluated benefits of their integration to the existing grid as they are classified as clean energy technologies [4].

Electrical grids were first direct current (DC) based and only close neighbourhoods to power plants were supplied [5]. Local storage essentially constituted of batteries directly connected to the DC grid, which were partially used achieve balance in demand and supply of power. Later, with technological development leading to the discovery of AC grids, potential rise of power generated as well as transportation of power over longer distances became possible. Electric energy systems were designed and constructed to transport electrical energy, from production centres to load consumption centres that are situated kilometres away [6].The concept of power flow was then unidirectional, understood as transiting from bulk generating stations, currently constituted of greater percentage of coal fired stations, hydraulic or nuclear sources, toward medium and low voltage customers [7] at loads distribution centres essentially made of residential areas, industries and production plants facilities, commercial centres or a combination thereof [3],as shown in Figure1-1.

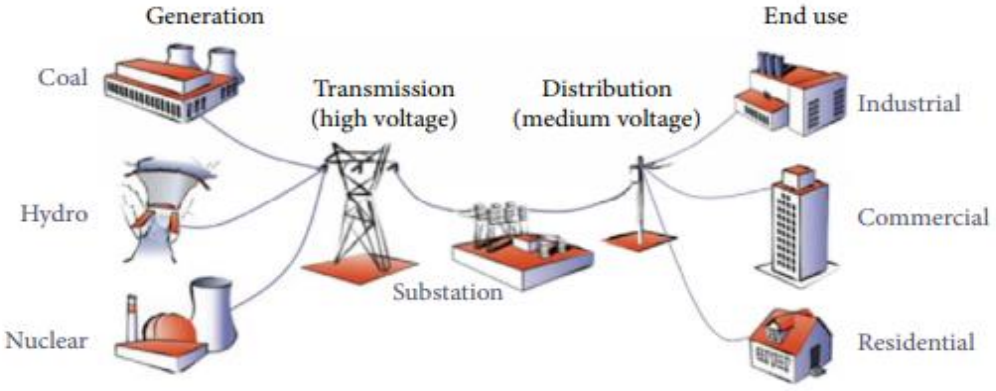

Figure 1-1: Elements of the electric power grid [3]

In today's power grid, generation units, transmission lines and loads are connected in power system (PS) networks that are becoming more complex [5]. The complexity is persistently increasing due to a growing number of interconnections and introduction of new technologies as shown in Figure 1-2.

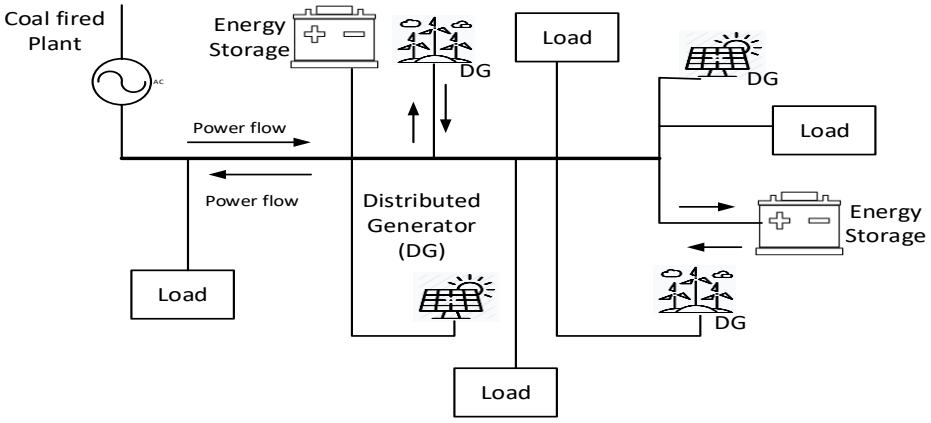

Figure 1-2: Power system topology with DGs and energy storage [9]

These new technologies mainly constitute of small-scale and decentralised renewable energy technologies, of which solar and wind together currently hold the major share [5]. Wind power and photovoltaic (PV) plants have grown rapidly, with power capacities increasing from small units used for domestic and commercial purposes, to large-scale grid applications [8], as shown from the global accumulated statistics in Figure 1-3. An integration of these RES to the main grid poses new challenges. such as voltage and frequency fluctuations, which result in grid instability as they are meteorologically dependent.

RES are non-dispatchable, meaning they cannot be controlled by operation as they originate and depend on the sun irradiation. Moreover, they are intermittent have random distribution depending on the weather pattern over a period of time and of stochastic nature, which implies that they may be analysed statistically but would not be predicted precisely, therefore unable to meet the continual daily and seasonal load demand [9].

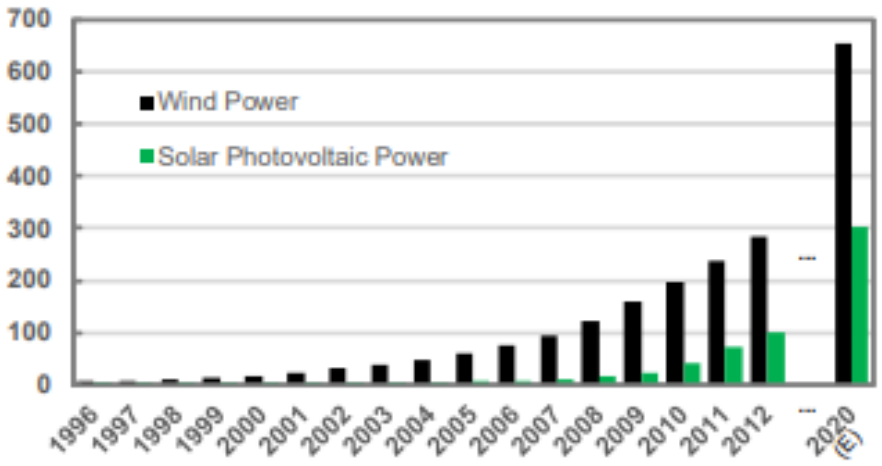

Figure 1-3: Global accumulated wind power and solar PV capacity (GW) over the years by 2020

An introduction of energy storage systems (ESS) features an advantage of storing energy generated by the RES and releasing it when there is a need. They are regarded as the future advancement in power networks as they can complement RES for future networks and smart grid applications. There are existing ESS within the grid which are mostly mechanical. Emerging ESS within transmission and distribution networks include flywheels, super-capacitors, large scale battery storage, compressed air and hydrogen[10]

1.2 Problem Statement

Enabling RES integration into electrical grids present several benefits for power system networks, including increased capacity generation, but require a balance of supply and demand that cannot be achieved due to their intermittent and stochastic nature. Because of the flexibility to control their real power output, batteries are suggested as a suitable and cost effective solution to mitigate adverse effects of intermittency and shape the fluctuation of the system's output into relatively constant power. There is a need to quantitatively investigate and evaluate the performance of the use of BESS to adequately smooth the output of the PV-BESS sub-system, in lieu of power curtailment or reactive power injection.

1.3 Aims and objectives

1.3.1 Aim

The aim of this research study is to evaluate impact of BESS use as an enabler for large-scale RES integration into power system networks.

1.3.2 Objectives

The main research objective of this study is the investigation of the system loadability of PS, with a particular focus on RES penetration and BESS incorporation. It proposes to analyse power systems stability et performance through the assessment of system loadability and power losses under the increasing influence of RES, namely PV systems, as well as to suggest probable ways of mitigating any violations. The impact of the combined PV-BESS system is analysed both in static and dynamic transient stability by considering the following factors:

(i) Load increase;
(ii) High PV penetration levels and BESS incorporation
(iii) Stability conditions before and after disturbances

The sub-objectives are to:

- Review the general voltage profile in relation with increased RES integration;
- Analyse the effects of DG units on voltage stability, system stability, system loadability and power losses;
- Explore system stability improvement techniques in utility grids with solar plants integration and compare levels of improvement;
- Investigate the effectiveness of the incorporation of BESS and its optimal location and size for great performance.
- Discuss the results and propose recommendations.

1.4 Key research questions

In relation to research aims and objectives above, the research questions that this study attempts to answer are:

1. To what extent does RES integration at the distribution ends impact voltage stability and system loadability?

2. Can DGs be used to effectively perform FACTS functions to enhance controllability, voltage support and stability, and increase power systems' loading margins, in addition to their primary function of increased capacity generation in response to increased power demand?
3. What measures can be taken to ensure that in the context of RES integration, voltage remains controlled and undisturbed at key buses under normal conditions and under disturbances?
4. Can the BESS perform a supportive function in mitigating the impact of the increased grid penetration of RES?
5. What is the optimal size and best location for the BESS to achieve its role of RES integration enabler, before stability limits and violations of standard codes are reached?

1.5 Limitations and delimitations

1.5.1 Limitations

It is almost impossible to conduct this kind of research on live power systems; thus the research is completed on computer-generated networks using simulation tools.

1.5.2 Delimitations

The following delimitations are to be considered:

1. This study work is limited to voltage behaviour, control and power system losses, due to increased penetration of intermittent DGs, considering the aspect of sizing and siting
2. The study will only focus on the effect of the load increase as the cause for voltage instability and possibly voltage collapse. The other causes: generators and static VAR systems (SVS) reaching their reactive power limits, tap changing transformers' action or contingencies such as line tripping or generator outages will not be considered.
3. Only the Solar PV is considered for the purpose of this study, even though other types of RES are briefly reviewed through the literature,
4. The impact on system frequency is also discussed and reviewed in the literature, but will not be considered for simulation purposes.
5. The impact on frequency, harmonics and flicker, protection system and philosophy and their economic impact do not form part of this work.
6. The study is limited to the use of *DigSILENT® PowerFactory* as the simulation tool.

1.6 Research methodology and design

An extensive literature review is carried out on the following contributing topics:

- Traditional electric systems and the challenges of power systems stability;
- The impact of RES integration to power quality and grid stability;
- Evaluation of energy storage systems and their effect to power system stability;
- BESS grid stability and economic issues, in line with specified grid code requirements; and

Mathematical design and /or modelling of systems is performed, including simulations of various case studies and scenarios using the DigSILENT® *Power Factory*® simulation tool, utilising static and dynamic analysis. Results are then presented and discussed.

1.7 Thesis Outline

The dissertation consists of 8 chapters as described below:

Chapter One provides an introductory overview of the research including the historical background, problem statement, the key research questions, the aim, the objectives and sub-objectives, the methodology, limitations and delimitations of the study.

Chapter Two defines a power system using literature review and opinions of different authors in the research context to compare the advances in technologies with previous studies. The main approaches and research techniques are also presented in order to establish similarities and differences within the core area of focus.

Chapter Three describes the classification of ESS. Comparison using technical characteristics and applications, also looking at developments in energy storage technologies are discussed.

Chapter Four elaborate on the BESS integration issues. The impact of grid-scale BESS on grid stability, grid code requirements and economic analysis are discussed.

Chapter Five defines the system network modelling elements and the reasoning behind the choice of components. The simulation tool, the parameter settings for the systems applied and the methodologies used will also form part of this chapter.

Chapter Six presents case studies and scenarios used in this research work and the corresponding simulations conducted on the network models presented in Chapter 5.

Chapter Seven The results of the case studies conducted are presented and discussed in this chapter using a comparative analysis approach.

Chapter Eight presents conclusions based on the research questions, findings based on simulations executed and further research topics and recommendations.

CHAPTER 2: LITERATURE REVIEW

Introduction

This chapter defines a power system, using literature review and opinions of different authors in the research context to compare the advances in technologies with previous studies. The main approaches and research techniques are also presented in order to establish similarities and differences within the core area of focus.

2.1 Power system overview

The electrical power system serves to generate, transport and distribute electrical energy to consumers in an efficient, economic and reliable manner. It should supply energy at minimum cost and minimum ecological impact and be able to meet continually changing load demand for active and reactive power [11]. The electrical grid must meet increasingly higher standards in reliability, security, efficiency, power quality and cost of service. However, in addition to these goals, the modern power system must address new global environmental issues, such as climate change, national security concerns, and a growing customer´s need to better manage their energy usage in order to reduce costs and decrease the environmental impact [1, 12, 13]

Power systems have some inherent level of flexibility designed to balance supply and demand at all times [14]. Flexibility of the electric power system is defined as "the ability to accommodate changes in the electric transmission system or operating conditions while maintaining sufficient steady state and transient margins" [15]. According to Lund [16] , flexibility relates closely to grid frequency and voltage control, delivery uncertainty and variability and power ramping rates. Huber[17] defines flexibility requirements using three metrics namely ramp magnitude, ramp frequency and response time.

The integration of intermittent resources into existing power systems varies according to the production and scale of the variable resource, its correlation with system load, and the flexibility of the power system in question [18]. In sufficient quantities, renewable energy will change the shape of dispatch requirements so that system flexibility must be reassessed, and high penetration levels of renewable energy may require increasing levels of flexibility [14]. Thus, the flexibility concept is denoted as the capability to balance rapid changes due to RES generation and forecast errors [19].

In terms of providing ancillary services to grid support, such as frequency control, reactive power control or voltage control during system disturbances, wind and solar PV plants provide lesser support than the conventional generation [20], and these services are required to ensure the safe and reliable operation of the PS [21]. Hence, large-scale RES integration leads to new requirements in the PS in order to achieve system security and stability [20] and, new strategies are obligatory for the operation of the electricity grid due to their short term variability and low predictability characteristics in order to improve and maintain power supply reliability and quality [22]. Reliability is measured by probability of failure, frequency of failure, or in terms of availability [23].

2.2 Power quality (PQ)

The power grid must meet certain standards by ensuring reliability, frequency and voltage stability to warrant the quality of power supply [11, 22]. Lopez [24] describes PQ, as an increasingly important issue and, generation is generally subject to the same regulations as loads. The IEEE defines PQ as "the concept of powering and grounding sensitive electronic equipment in a manner suitable for the equipment" [25]. It is also described as any power system problem demonstrated in voltage, current and frequency deviations which results in significant loss of performance in electrical equipment or life expectancy [25].

PQ refers to the presence of harmonic signals in bus voltages and load currents, spikes and momentary low voltages and other issues of distortion that can impact the performance of some sensitive pieces of equipment. This could cause instability in transmission lines resulting in loss of work output [26]. For example, in industrial firms, transient fluctuations in power can cause disruption in production processes. Tabatabaei et.al [27], noted that in an integrated and interconnected power system, a number of various electromagnetic field manifestations occur and effect, at any time/location, parameters such as currents, voltages, frequency or PQ, compelling users to be interested in its preservation. Good PQ is an important factor for a reliable supply of electricity to loads in a power system. However, the current electronic devices and nonlinear loads produce non-sinusoidal waveforms, which can result in poor PQ [28].

Studies have shown that the integration of RES to grids could potentially affect frequency and voltage, impact on voltage drop and power factor, as well as cause harmonic reduction, thus creating severe PQ problems in the system components [29]. Different types of PQ problems are classified based on their impacts on electrical systems as well as their duration [30]. The parameter variations are the main reason for PQ degradation and are hence of utmost

importance in reliable power systems operation [31]. Parameters to be considered in assessing problems in PQ are:

2.2.1 **Frequency variation**

Frequency fluctuation is a result of any imbalance between power production and power consumption [29] and any deviation of the frequency can cause equipment damage. Frequency variation is common in systems with poor power infrastructure and can be worse when the generator is heavily loaded [32]. A rapid drop in the frequency could also be sensed as a fault and subsequently causing the generating units to trip, leading to load shedding or even system collapse. Frequency variations are fairly rare in stable utility systems, but certain applications such as voltage source converters in the power system can cause frequency deviations due to the level of their harmonic emissions [33]. In DG integration, the main focus is on maintaining the PCC voltage within the permissible levels while the frequency at the PCC is expected to adapt to that of the grid [34].

2.2.2 **Harmonics**

These are voltage or current components that have frequencies of integer multiples of 50 Hz. Harmonics are classified based on their fundamental frequency and are categorized as integer harmonics, inter harmonics and sub harmonics. The respective harmonics classes are defined based on the relationship of their respective frequencies with the power system's frequency [31]. Harmonics are undesirable in power systems as they have adverse impacts on generation, transmission, distribution as well as on consumer's loads [34, 35]. Harmonics are mainly caused by non-linear loads where the ratio between voltage and current is not constant during periods.

Harmonic distortion, can be caused by power inverters used in RES networks with no application of proper filters [29]. The acceptable limits of the maximum harmonic distortion are set out by regulating bodies for different parts of the power system. According to IEEE standard 1250, the acceptable maximum total harmonic distortion allowable as per voltage level is:

5 % at 2,3 kV – 69 kV, 2,5 % at 69 kV – 138 kV and 1,5 % at voltage levels higher than 138 kV [36].

2.2.3 **Voltage fluctuations**

Voltage fluctuations are defined as continuous variations of the voltage or a series of random voltage changes normally with the magnitude within the voltage ranges [32]. Variations in voltage profiles in utility grids with RES integration are dependent on variables such as voltage level, grid type and strength, DG location and penetration level in the grid [37]. Some RES such as PV systems are usually intended to operate near unity power factor to optimize solar energy use. Therefore, they only inject active power into the utility side of the grid, which may change the rate of reactive power flow in the system, and the nearby buses may experience under/overvoltage problems because of the lack of reactive power [29]. An over-voltage occurs when rms AC voltage rises above 110 % of the nominal voltage for more than a minute, and under-voltage occurs when the rms voltage decreases to 90% of the of the nominal voltage [32].

2.2.4 **Voltage sags/voltage dips**

The incorporation of RES in grids can affect the functioning of over-current protection equipment, leading to events such as voltage dips [37]. These are described as transient voltage reductions ranged from 10% to 90% of the nominal voltage, normally lasting from 0,5 to up to 60 cycles [38]. The lost and retained voltage are considered in evaluating voltage dips. The lost voltage is the difference between the pre-fault voltage magnitude and that during the dip, while retained voltage is the percentage of the nominal rms voltage remaining at the lowest point of the dip. The seriousness of the voltage sag on power systems is determined by observing the magnitude and duration of the sag [34, 39]. Voltage dips depth of 10 % to 15 % may occur as a result of switching of loads whereas large voltage sags may occur as a result of faults in the system [40]

2.3 PS stability

PS stability is defined as an “attribute of the system that enables it to remain in a state of equilibrium under normal operating conditions and to regain the acceptable state of equilibrium after being subjected to a disturbance” [11, 41]. Because PS are non-linear, their stability depends on both the initial conditions and the size of the disturbance [42]. Power systems may experience small disturbances or large disturbances. Small disturbances are normal fluctuations of short amplitude, such as load variations leading to mild oscillations often not requiring any dumping, and large disturbances often caused by faults on transmission lines; the loss of one or

more generating units; or the insertion or loss of a huge load, developing into big oscillations usually requiring control actions [43].

PS stability can be classified as rotor angle, voltage or frequency stability as shown in Figure 2-1.

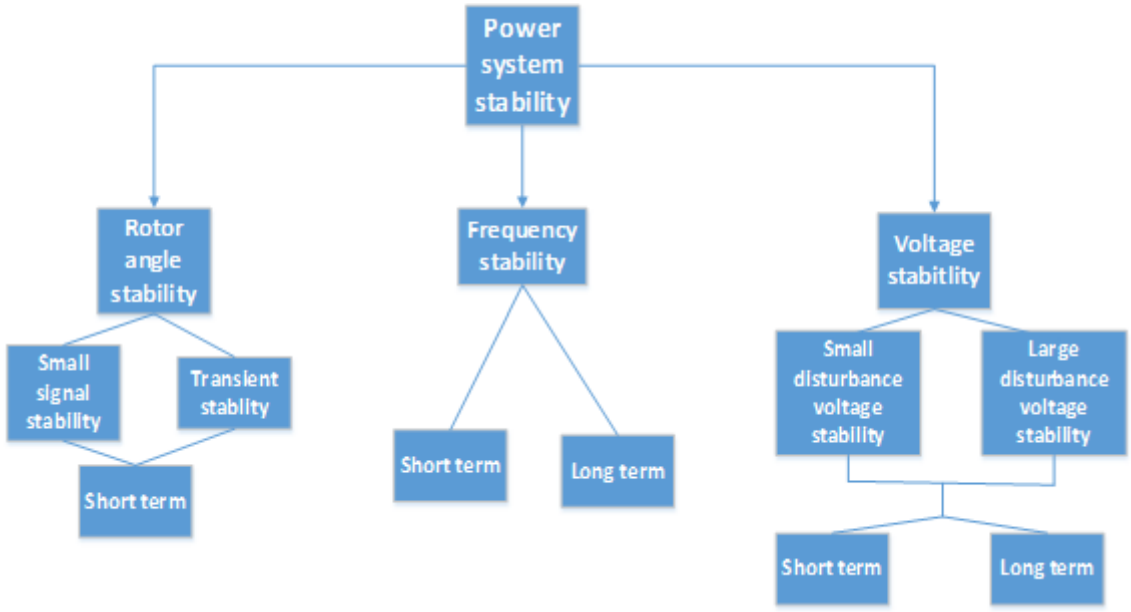

Figure 2-1: Classification of PS stability

2.3.1 **Rotor angle stability**

Also referred to as generator stability, rotor angle stability is the ability of interconnected synchronous machines in a PS to remain in synchronism under normal operating conditions or after being subjected to a disturbance [44].

Gupta [41] suggests that the term "stability" means maintenance of synchronism and these two terms may be used one at the place of the other. This form of stability is related to the manner in which synchronous machine power outputs fluctuate depending of their rotors' oscillation [11]. The voltages and currents' frequency must be equal while their rotor mechanical speed must be synchronized to this frequency[45].Hence, power systems dynamics are attentively associated to the mechanical and electrical dynamic state variables of all interconnected synchronous machines[46]. Increasing the angular swings of some of the machines may cause instability which leads to a likely loss of synchronism [44, 45].

Rotor angle stability phenomena is characterised in terms of small-signal or small-disturbance stability and transient stability [11]. In order not to lose synchronism, the electrical PS is designed and operate to sustain different types of contingencies [11, 47, 48]

2.3.1.1 Effect of RES integration on rotor angle stability

Rotor angle stability studies have been previously conducted both for transmission and distribution systems [49-51]. The author in [51] studied the impact of RES types on transient stability, comparing inverter-based and rotating-based types and they found a strong dependency between transient stability and technology employed. Reza et al in.[50] investigated the dependency of the rotor transient stability of a transmission power system to high RES penetration levels. Transient stability was tested using scenarios of faults in all possible branches and, in conclusion, it was found that the penetration level of the RES units affects power flow and hence the transient stability of the network [45].

2.3.2 Frequency stability

Kundur and the Taskforce [44] define frequency stability as the ability of the PS to maintain steady state frequency, after a severe system disturbance, that result in a considerable imbalance between generation and load. Loss of generation which may result from sudden imbalance between system generation and load demand can result in loss of system frequency stability[44, 48] therefore, frequency instability is due to electrical power deficiency [47].

With a sudden increase in load changes, the rotational inertia will initially provide the extra energy needed, subsequently decreasing the generator's speed, thus proportionally decreasing the frequency [52]. The control of frequency is therefore said to be closely linked to the system's active power control and balance. Frequency, or system's electrical speed is therefore firmly dependent on the rotational speed of the turbo-generator's shaft, which is also denoted as the mechanical speed of the machine [47, 52]. The rotational energy, also termed as inertial stored energy in the turbo-generator due to the substantial mass and high rotational speed, is directly dependent on the moment of inertia and the square of frequency [11, 52], as described in Equation 2-1.

$$E_{Rot} = \frac{1}{2} M^{\circ} . (2\pi f)^2 \qquad (2\text{-}1)$$

where, E_{Rot} equal to the rotational energy, M° is the moment of inertia and f the frequency.

2.3.2.1 Effect of RES integration on frequency stability

Most researchers established that a high penetration of non-synchronous generating resources, with non-rotating masses meaning no stored inertial energy, causes a reduction of the total system inertia [53-55]. It is eminent that PV systems have non-rotating masses. Daly et al[56] [53]noted that wind turbines, although having rotating masses, are often not synchronously connected to the grid as their connection is mostly achieved through power electronic devices. The reduction of system inertia due to an increased share of inertia-less resources has predominantly two frequency stability implications the Faster Rate of Change of Frequency (RoCoF) and the higher frequency deviations (nadirs/zeniths) or the time to maximum frequency deviation, which potentially leads to unpredicted load-shedding and in worst cases, blackouts [53, 57] .

This implies that, the higher the penetration of RES, the lower the system frequency and the higher the RoCoF, the shorter the time-frame to reach minimum frequency.

2.3.3 Voltage stability

This is referred to as the capability of a PS to preserve balanced and acceptable voltages at all system buses after being subjected to a disturbance from an initial operating condition and the factor contributing to instability is the lack of ability to compensate for reactive power demand [11]. Pure voltage stability is concerned with a large system feeding a load at the end of a radial configuration [58]as presented in Figure 2-2.

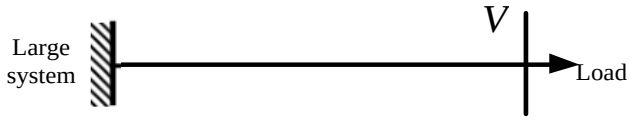

Figure 2-2 : Voltage stability : radial feed from a large system to a load

Voltage stability is predominantly associated with load stability and may be interpreted as the deficiency of any PS to transfer an infinite quantity of P to its loads [11, 46, 59, 60]. The main limiting factor for loading and for the power transfer capability of PSs at any point in time, a PS's operating condition should be stable, meeting various operational criteria and remaining secure in the event of any credible contingency [61]. A system is said to be voltage stable if all system operating conditions can be met after a small or large disturbance [58, 62] .

Voltage stability is also considered to be the maximum Megawatts (MW) capacity that the system is able to transfer to a load bus prior to voltage collapse [46].

2.3.4 **Voltage collapse**

Voltage collapse is the process by which the voltage falls to a low, unacceptable value as a result of an avalanche of events accompanying voltage instability [63]]. Chiang et. al [64] describe it as one type of system instability, which occurs when the system is heavily loaded. The event is characterised by a slow variation in the system operating point due to increase in loads, in such a way that voltage magnitudes gradually decrease until a sharp, accelerated change occurs. Voltage instability/collapse is caused by the power system inability to meet system MVAR demand [44, 59] in the presence of inductive loads or a disproportionate absorption of Q by the system itself, meaning high Q losses to keep desired voltages [65, 66].

The loading margin is the fundamental and extensively used traditional method to predict voltage collapse in a PS.

2.3.4.1 Voltage control measures used to offset voltage collapse

Measures to avoid voltage collapse include: the use of parallel bank capacitors, transformers with tap-changers, re-dispatching of generation capacity, use of secondary voltage regulation and in the extreme case, load shedding.

2.3.5 **Voltage stability analysis**

Voltage stability analysis for a PS involves the assessment of two areas namely [67, 68] : (1) Proximity to voltage instability, which is a measure of voltage security and (2) Mechanism of voltage instability. Voltage assessment requires a power monitoring tool to control the power system because of hourly changes caused by various situations that occur in the system [69].

Voltage stability analysis of a network can either be determined using a static method or dynamic analysis[66]. According to Taylor [63] ,the dynamic method with the use of time-domain simulations is essential for short-term voltage stability, but can also be valuable for long-term stability, with the purpose of performing coordination controls and greater accuracy and insight of the problem. A number of researchers noted that although stability studies in general require power system dynamic model, static methods are largely available and in use for voltage stability evaluation [70, 71] . They are less complex and require low computational

time to carry out a system stability analysis [72]. Static approaches are adequate for analysing due to the fact that the system dynamics that impact on voltage stability are frequently slow [73, 74], and the dynamical behaviour may be intently evaluated by a number of snapshots reproducing the system condition in the time domain at various time-frames [74].

2.3.6 **Variation of V on P-Q plane**

Let us consider a two-bus system as depicted below in Figure 2-3.

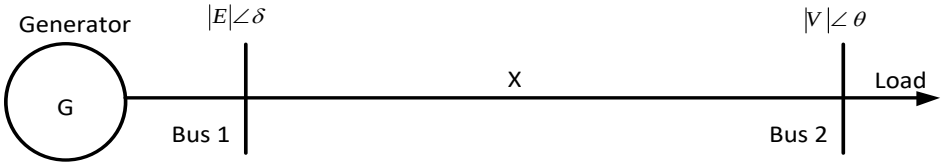

Figure 2-3: 2-Bus test system

P transfer from bus 1 to 2 is given by

$$P=\frac{EV}{X}\sin\delta \tag{2-2}$$

Q transfer from bus 1 to 2 is given by,

$$Q = -\frac{V^2}{X}+\frac{EV}{X}Cos\delta \tag{2-3}$$

Equations 2-2 and 2-3 are power flow or load flow equations for the lossless system [69] .

Where, E = ∠δ E is the voltage at bus 1, V = ∠V 0 is the voltage at bus 2, X= impedance of the line (neglecting resistance), δ = power angle.

After normalization, assuming that $v=V/E$, $p=P.X/E^2$ and $q=Q.X/E^2$ then,

$$p=v\sin\delta \tag{2-4}$$

$$q=-v^2+v\cos\delta \tag{2-5}$$

Squaring both equations, then the relationship $v=f(p,q)$ is expressed as in Equation 2-6:

$$v^4+v^2(2q-1)+(p^2+q^2)=0 \tag{2-6}$$

The possible solutions of *v* from Equation 2-6 are:

$$v=\sqrt{\frac{1}{2}-q\pm\sqrt{\frac{1}{4}-p^2-q}} \quad (2\text{-}7)$$

Figure 2-4 shows a plot of v on the p-q-v plane. Corresponding to each point (p, q), there are two voltage solutions: (1) For high voltage or stable solution and (2) For low voltage or unstable solution. Any increase in active and reactive powers beyond the maximum allowable power point makes the voltage unstable[58].

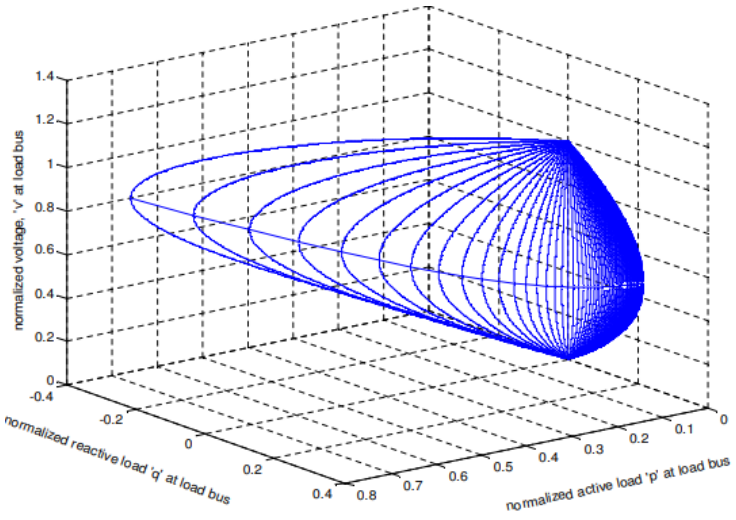

Figure 2-4: Variation of bus voltage with active and reactive loading for the 2-bus test system [58]

2.3.7 Tools for voltage stability analysis

Numerous means to carry out voltage stability assessment are discussed in different literature. Conventional means include: (1) P-V curve analysis, (2) the V-Q curve analysis and reactive power reserve, (3) the Jacobian matrix method and (4) the continuation of power flow method [58, 75].

2.3.7.1 The P-V curve method

This method provides the available amount of P margin before reaching the instability voltage point [58]. The curves describe the voltage path against the consumers' power demand [58, 76], and they allow the operator to effectively identify the loadability margin., as shown in Figure 2-5, which shows bus voltage changes versus system load change. The method relies on the accuracy of data to build up the curves [76]. This method can be used to analyse radial systems, large meshed networks, transmission interfaces or interconnections and consist essentially of monitoring the voltage at the critical bus, against the changes in real power in a radial system

[58]. In mesh networks the real power P can be the total active load in the load area and V the voltage at the critical or representative bus [58, 76]. Real power transfer through a transmission interface or interconnection also can be studied by this method.

The voltage stability margin (VSM) is defined as the proximity of the operating point to the point of voltage collapse in terms of power difference [70] as presented in Equation 2-8.

$$VSM = P_{o,i} - P_{max,i} \tag{2-8}$$

where, $P_{o,\,i}$ and $P_{max,\,i}$ are system operating load and loadability limit, under a given loading pattern i respectively.

The P-V curve analysis is used in this research work to assess system stability conditions of a PV-BESS penetrated network and to determine the limit of the system loadability, as well as the critical voltage collapse point.

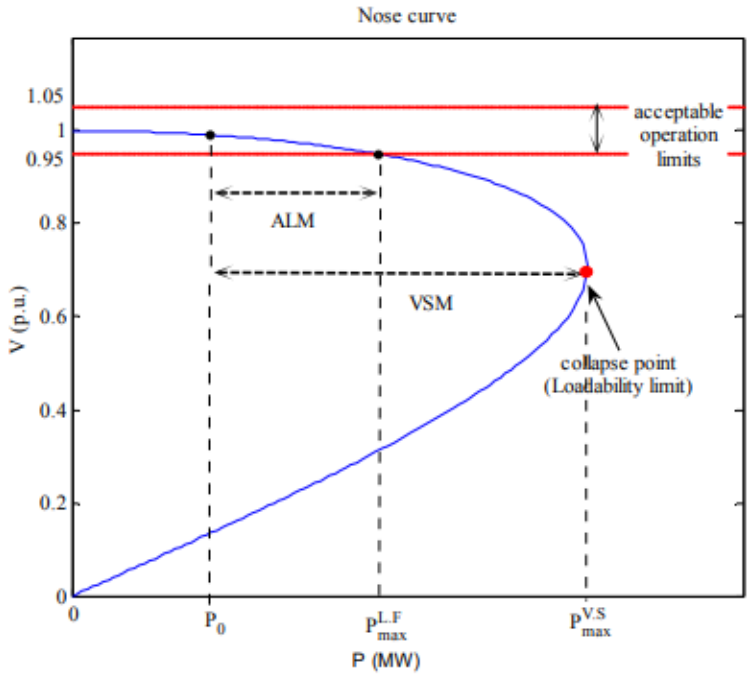

Figure 2-5: Typical P-V curve showing the voltage stability margin [70]

Considering the two-bus system given in Figure 2-3, equation 2-4 gives real solutions of v^2 as $(1-4q-4p^2)\geq 0$. If it is assumed at a constant power factor, meaning that:

$$\frac{q}{p} = \cos\theta = k \tag{2-9}$$

the inequality can be expressed as $p \leq \frac{1}{2}((1+k^2)^{\frac{1}{2}} - k)$,which determines the maximum value of the active power and can allow computing of the active power margin for a load with a suitable constant power factor. It is demonstrated that for different power factors, from lagging to leading power factor values, the knee point shifts toward higher values of real power and higher voltages, suggesting the improvement of voltage stability [60] , as presented in Figure 2-6.

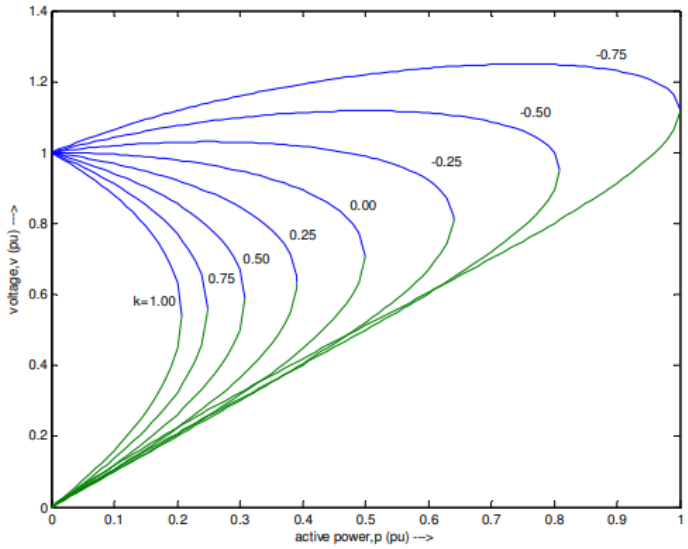

Figure 2-6: P-V curves for the 2-bus test system[58]

2.3.8 Effect of RES integration on voltage stability

The high penetration of renewable generations (RG) in the distribution system (DS) has presented more uncertainties and technical challenges in the operation of the grid-like voltage variation; degraded protection; altered transient stability; two-way power flow; and increased fault level [77, 78] .The reverse power flow may result to voltage rise ,which may not be effectively controlled by network operators [77]. The power network is no more passive as such, the power flow and voltage profile are determined by both generation and load [78]. Different techniques are used to mitigate the impact of RGs on the voltage profile, in order to overcome the voltage variations on DS with high penetration of RG [77]. Some are listed:

2.3.8.1 Power curtailment

Curtailment is a reduction in the output of a generator from what it could otherwise produce given available resources, classically on an involuntary basis [79]. It is regarded as one of the

practical solutions to reduce the RES power output to a manageable level for the grid capacity [80].The most common reason for renewable energy curtailment is transmission congestion, or constraints on the local network [81]. Curtailment can also occur in the distribution system to avoid high penetrations or back-feeding, in which a feeder produces more energy than it consumes, of distributed generation on feeders, which can lead to voltage control issues as a result of variability of the wind or solar resource [79] .

When load demand decreases, the intermittent RES peaks and the system will experience excess generation and bus voltages may exceed the grid operational limits. With respect to renewables and DG, power is becoming more widespread, expanding across countries and penetrations increase [79]. Power curtailments can result in operators or utilities commanding wind and solar generators to reduce output, with the aim of minimizing transmission congestion or otherwise managing the system or achieving the optimal mix of resources, and system accounting [82]. Analytical models are used to determine the need for curtailment[79] . Power curtailment can also be performed by means of an emergency load-shedding to economically prevent voltage collapse[83 , 90], but at the detriment of adversely affecting power supply reliability [84]. The negative impact of curtailment of variable renewable energy reduces the capacity factor and potentially the revenue stream of a plant[14].

2.3.8.2 Energy storage

For years, energy storage systems(ESS) have been used as stand-alone or grid formed. Energy storage is a method of changing electrical energy from an electric power network into a configuration that can be stored for changing it back into electrical energy when needed [85, 86]The production and consumption in a power supply system always needs to be balanced [11].

Energy storage can serve certain purposes such as system-level cost/price arbitrage, balancing power which is a frequency control element and power quality which is a voltage- & current-quality control factor[87]. It can mitigate the intermittency and fluctuation of RES[88], and offer an incredible technological solution to curb their stochastic nature, without having to resort to fossil fuel based technologies for back up[89].

The ESS is defined as the group of equipment that allows the conversion of several forms of energy into electricity that can be stored and later used by the grid [22]. ESS are regarded as valuable power system tools due their ability to time-shift the power delivery [3, 5]. They are

considered as effective mechanism to enhance the flexibility and controllability of the entire grid [90].

ESS can be integrated at different levels of the electricity system depending on the required services: at the transmission level, at the distribution level and at the customer/end-user side[1]. This involve different stakeholders, energy storage technologies and impact on the type of services provided [1]as shown in Figure 2-7, demonstrating the different applications of ESS in the electrical power grid.

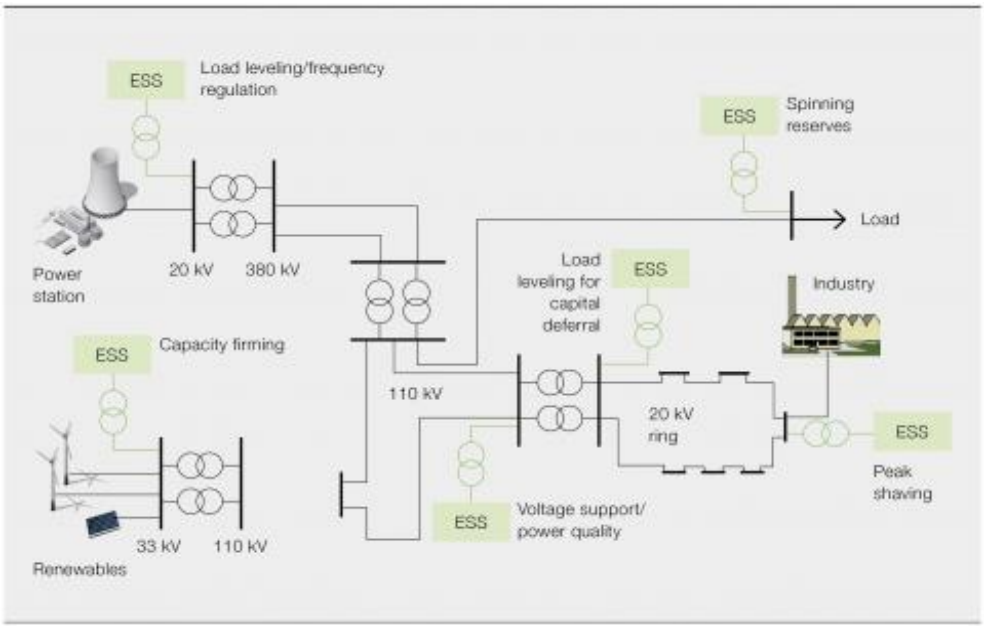

Figure 2-7: Main applications of ESS [91]

The classification of ESS, latest developments and comparison in technical characteristics are discussed in Chapter 3.

2.3.8.3 The Flexible Alternating Current Transmission System (FACTS)

The concept of FACTS was introduced in the late 1980's [28] as the result of related developments in electronic devices, designed to overcome the limitations of traditional mechanically controlled power transmission systems [92]. The IEEE defines FACTS as “the AC transmission systems incorporating the power electronic-based and other static controllers to enhance controllability and increase power transfer capability” [15, 93].

2.4 Renewable energy sources

Because of many substantial benefits over other RES, the photovoltaic and wind technologies are the most important distributed generation (DG) means and, they are rapidly and widely propagating.

2.4.1 The Photovoltaic (PV)

The PV is a solar energy based technology that uses the unique properties of semiconductors to directly convert solar irradiation into electricity [94].]The PV effect concept was discovered by the French scientist Alexandre-Edmund Becquerel in 1839 [94, 95]. Dunlop [94] acknowledged that space applications such as satellite were the first practical use of PV technology.

The development of solar energy conversion on a large scale became of interest in mid-1970s, certainly triggered by the energy crisis of that period [94, 95]. The availability of solar radiation resource at a particular location determine the feasibility of producing appreciable amounts of power [94]. The PV system delivers power directly to DC loads. For AC loads, an inverter coupled to the system will be needed. A PV system may be connected to a utility grid or as a standalone system. Interconnection to the grid is achieved via suitable interfacing circuitry to allow the PV system to deliver the excess of energy to the grid and/or to use the grid as back-up system in case of insufficient PV generation, as well as to disconnect it from the grid in the event of grid failure [96].

Sunlight is the fuel of solar cells, which are made from semiconductors and have much in common with other solid-state electronic devices such as diodes, transistors and integrated circuits [97].Photovoltaic cells are P-N junction type semi-conductor devices that have a large area which can be exposed to sunlight[98]. When the cell receives the illumination, the silicon crystalline absorbs photons from sunlight and releases them as electron-hole pairs by their interaction with the atoms. The electric field created by the cell junction causes photon-generated electron-hole pairs to separate, with electrons drifting into the N-region and holes drifting into P-region [96].

Figure 2-8 illustrates how cells are connected in a series-parallel configuration and then configured to modules, and modules to arrays.

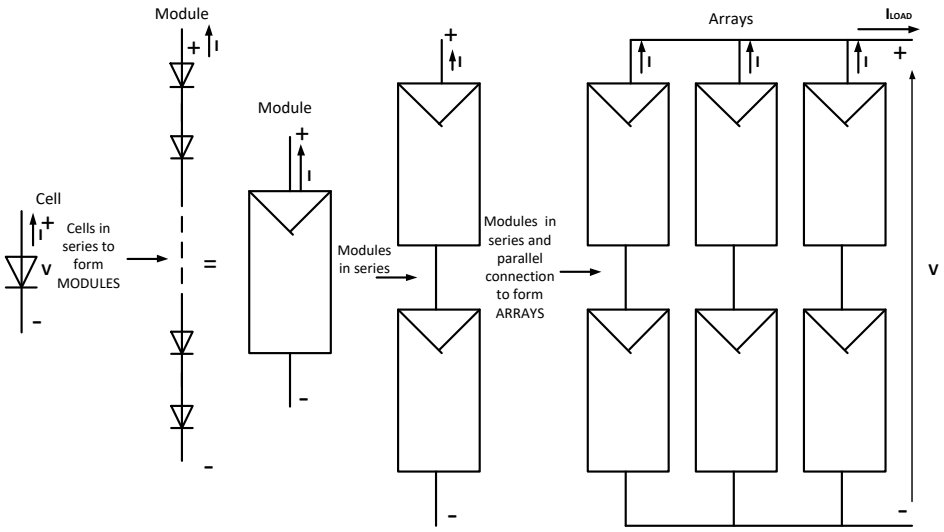

Figure 2-8: PV configuration ,cells , modules and arrays [94]

A single cell produces less than 2 watts at approximately 0,5 V and to produce enough power for high power applications. Module power may reach 300 watts, while arrays power can range up to some kilowatts.

2.4.1.1 Electrical characteristics of the PV

PV units electric characteristics are represented as I-V or V-P relationships in cells with the irradiance received by the cell and the temperature of the cell being the inputs upon which these characteristics are dependent upon [29, 99]. Consequently, a relevant model will be required to translate the irradiance and temperature effects on the current and voltage produced by the PV arrays in order to analyse the dynamic performance of PV system under various weather conditions [29]. Figure 2-9 shows the equivalent electrical circuit of a crystalline PV module.

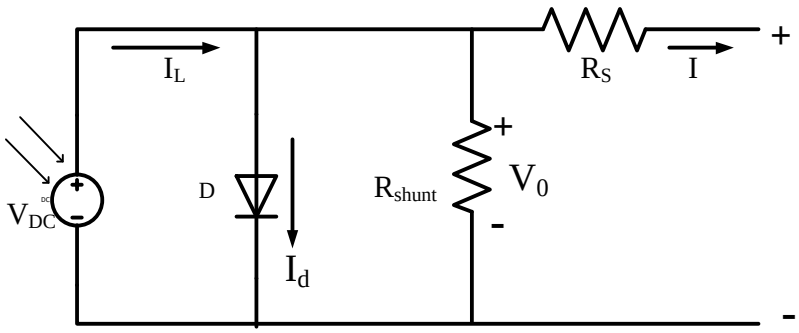

Figure 2-9: Equivalent circuit model of a PV module [29]

Equation 2-10 provides the output current I of a PV module.

$$I = I_L - I_d - \frac{V_0}{R_{shunt}} \quad (2\text{-}10)$$

where, I is the module's current, I_L is the photo current, I_d is the diode cell current, V_0 is open circuit voltage and R_{shun} is the shunt resistance.

The diode current I_d is expressed as in Equation 2-11:

$$I_d = I_0[e^{\frac{qV_0}{nkT}} - 1] \quad (2\text{-}11)$$

By substituting (2-3) in (2-2), the output current is then expressed as in Equation 2-12, assuming n=1.

$$I = I_L - I_0[e^{\frac{qV_0}{kT}} - 1] \quad (2\text{-}12)$$

where I_L is the component of the cell current due to photons or light-generated current, I_0 is the diode reverse saturation current, V_0 is the open circuit voltage, , $q = 1{,}6 \times 10^{-19} C$ is the charge of an electron, $k = 1{,}38 \times 10^{-23} J/K$ is the Boltzmann constant , T is the cell temperature in Kelvin [K]. Figure 2-10 presents the I-V and P-V characteristic curve of the solar cell.

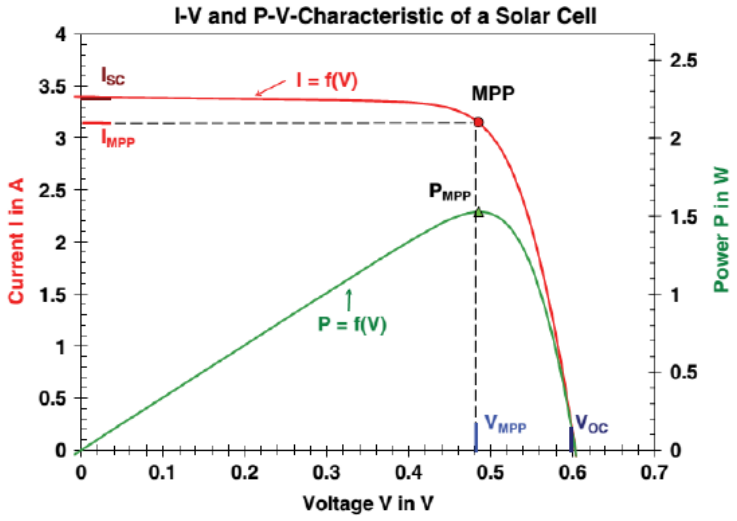

Figure 2-10 : Solar cell current-voltage and voltage-power characteristic curve [99]

The short-circuit current (I_{SC}), is the current that flows through the external circuit when the electrodes of the solar cell are short circuited. The I_{SC} depends on the solar cell area and the photon flux density incident on the solar cell, determined by the spectrum of the incident light. The open-circuit voltage (V_{OC}), is the voltage at which no current flows through the external circuit, which is the maximum voltage that a solar cell can deliver. The V_{OC}, corresponds to the forward bias voltage, at which the reverse saturation current compensates the photo-current [99]. The power produced by the cell at any operating point, is the product of its operating current and voltage, as illustrated on the graph in Figure 2-10.

Under open circuit conditions, voltage is highest but with zero current, thus no power is provided by the cell. Likewise, under short circuit conditions, current is largest but with no voltage, thus no power. Between these two extremes, a compromise condition combining relatively highest current I_m and highest voltage V_m will result in maximum power P_m ,which is a key parameter since solar cells are used to produce electrical energy and, it will always be smaller than the product of V_{OC} times I_{SC}.

The closeness with which maximum power approaches the product $V_{OC}I_{SC}$ is termed fill factor (FF), as expressed in Equation 2-13 . Hashim[99] defines the FF as a measure of the squareness of the current-voltage (I−V) curve and serves as an indicator for how the total internal electrical resistances effect the output current. A squarer curve indicates a greater maximum power and ideality [99].

$$FF = \frac{P_m}{V_{OC} * I_{SC}} \tag{2-13}$$

In a good cell, the fill factor is above 70 % [95-97].

Figure 2-11 shows the variation of P generated by a Solar PV system over twenty-four hours. It can be observed that output power from PV arrays is not available for nearly half of the time.

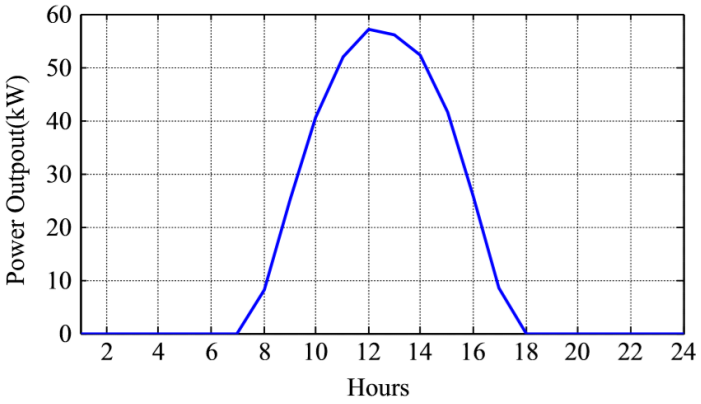

Figure 2-11: Variation of P generated by a Solar PV system over 24 hours [89]

Positive impacts of Solar PV on power systems include,

- Power loss reduction,
- System reliability improvement,
- Backup an emergency power,
- Voltage support,
- Transmission and capacity release,
- Deferments of new or upgraded transmission and distribution infrastructure,
- Lowering cost of expansion of HV lines and,
- Low emission of air pollutants [15-20]

The main demerits of PV systems are:

- Relatively high initial cost
- They require a relatively large array area to produce a significant amount of power and,
- Their need for electrical energy storage if 24-hour capability is required [21].

2.4.2 **Wind turbines**

Wind turbines convert wind kinetic energy into electric energy. Wind technologies have been propagating over the years, mostly for their ecological nature. The primary energy is free, with a greatly reduced environmental impact. Synchronous and asynchronous or Induction Generators are used for wind turbines and they can be configured and connected to the grid in many different ways [100]:

1. Fixed speed WT with direct grid-connected Induction Generator (IG)

2. Variable speed WT with variable rotor IG directly connected to the grid
3. Variable speed WT with direct grid-connected doubly-fed induction generator (DFIG) and DC/AC rotor converter
4. Synchronous machine and full scale AC/DC/AC converter

A schematic of the wind-generator concepts is presented in Figure 2-12.

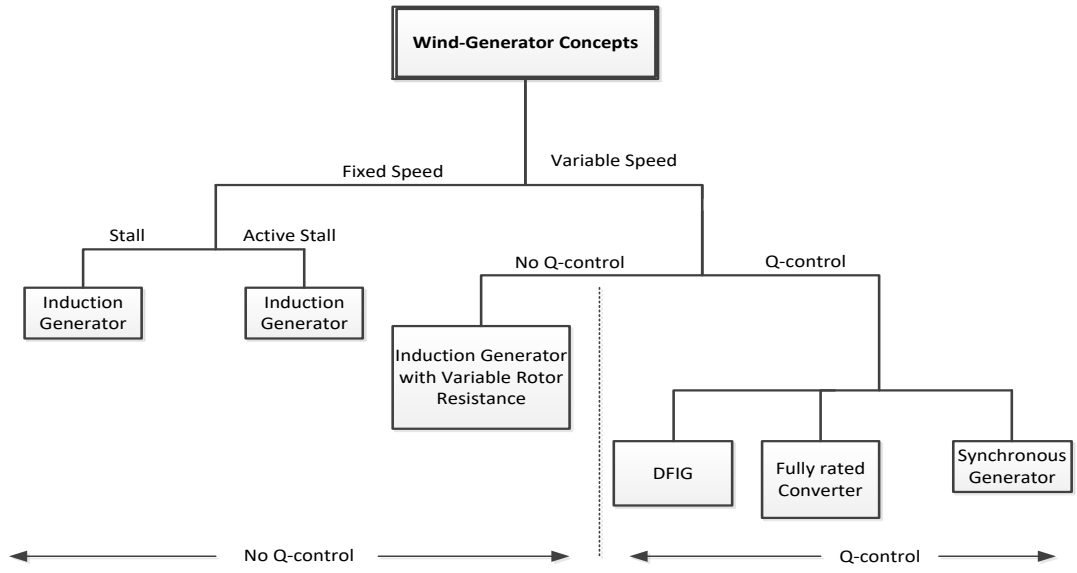

Figure 2-12: Wind generator concepts [89]

2.4.2.1 Merits and demerits of wind turbines [98, 101]

Their main merits include

- Less operating/generation costs,
- Fuel free,
- Minimal land use and
- Reduced environmental impact.

Demerits of wind turbines are

- High noise pollution,
- They have high initial installation cost,
- They cannot be used in all geographic locations,
- No power availability on demand due to their intermittent nature and,
- Their power production output is highly dependent on wind speed

Prakash and Paliwal [89, 101] compared the variation of output power of the wind turbine to other DGs, as seen in Figure 2-13. It can be observed that wind generator output is considerably intermittent in nature.

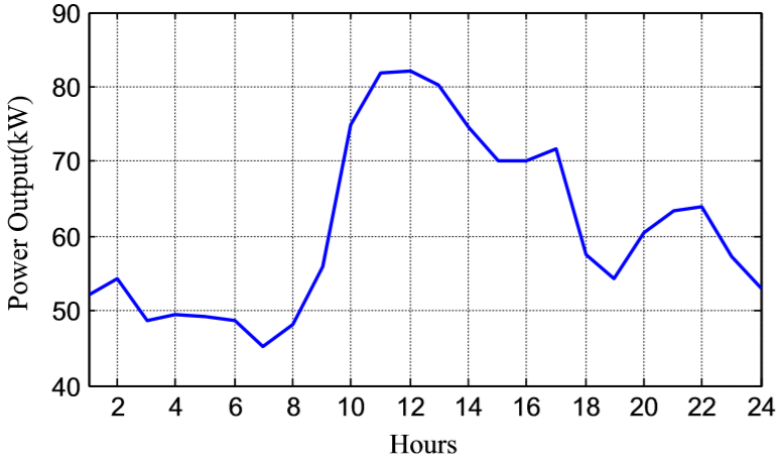

Figure 2-13: Variation of P generated by the wind turbine over 24 hours [89]

2.4.2.2 The power equation and modelling of the wind turbine

The power extracted by wind turbines is as presented in Equation 2-14 [98, 101]

$$P_W = \frac{1}{2} c_P \rho A v_W^3 \qquad (2\text{-}14)$$

where: c_P is the power coefficient, ρ is the air density of the wind in W/m^2, A is the swept area of rotor in m^2, V_W is the average velocity of rotor blades or wind speed in *m/s*.

2.5 Power electronics(PE)

PE serve as the key enabling technology in integration of RES into the electricity grid [102], facilitating the connection of ESS and command its response, ensuring grid codes and standards are met [103].The semiconductor devices such as IGBT, MOSFET, diode and Thyristor are building blocks of PE technologies. PE evolution resulted due to development of quick response semiconductor switches capable of handling high powers to minimize probability of grid instability and monitoring of real-time data [102]. They are widely used and swiftly become more advanced with developments in grid based systems and topologies classified according to the expected power conversion efficiency [23].

2.5.1 **Power losses and efficiency in PE topologies**

With the advancement in technology, inverter topologies have changed tremendously from large thyristor-equipped inverters to currently smaller IGBT-equipped ones. The IGBT enables the increase in power switching frequency with the result of extracting more energy and fulfil the connecting standards [102].

Switching devices power loss is a resultant of conduction and switching losses respectively. Conduction losses (P_{CT}) of the IGBT is approximated by a constant voltage drop and a series resistance [23] and calculated as in Equation.2-15.

$$P_{CT} = V_{CE0} * \bar{I}_T + R * I_T^2 \quad (2\text{-}15)$$

Where V_{CE0} is the forward voltage drop at zero current, R is the on-state resistance, $\bar{I}_T$ and I_T are the average and rms current respectively. V_{CE0} and R values are obtained from the datasheet. The average conduction losses of the anti-parallel diode (P_{CD}) can be calculated using Equation 2-16.

$$P_{CD} = V_{F0} * \bar{I}_D + R' * I_D^2 \quad (2\text{-}16)$$

Where V_{F0} and R' can be read from the diode losses characteristics. $\bar{I}_D$ and I_D are the average and rms values of the current through the diode, respectively.

The diode switch-on losses are normally neglected. The losses of the IGBT (P_T) and anti-parallel diode (P_D) are given by Equations 2-17 and 2-18 respectively [23].

$$P_T = V_{CE0} * \bar{I}_T + R * I_T^2 + [E_{ON}(\bar{I}_T) + E_{OFF}(\bar{I}_T)] * f_{sw} \quad (2\text{-}17)$$

$$P_D = V_{F0} * \bar{I}_D + R' * I_D^2 + [E_{REC}(\bar{I}_D)] * f_{sw} \quad (2\text{-}18)$$

Where f_{SW} is the switching frequency. The conversion efficiency is calculated using Equation 2-19.

$$\eta = \frac{1-n(P_T+P_D)}{P_{TOTAL}} \quad (2\text{-}19)$$

in which *n* is the number of IGBTs or diodes and P_{TOTAL} is the total input power [23].

2.6 The smart grid

The smart grid is the convergence of information and operational technologies, overlaid across the power grid, which intelligently incorporates generation and storage options to efficiently

deliver sufficient capacity of electricity to consumers within a specified coverage area in an accessible, safe, economic, reliable, efficient and allowing sustainable options [88, 104-106].

Authors in [104, 107] emphasize that increasing reliability and reducing environmental impacts are the most important goals of the smart grid. According to Phuangpornpitak [108] another benefit of the smart grid is voltage regulation and load following to reduce operational costs based on marginal production costs. Most authors [22, 88, 108-111], reason the necessity of the smart grid conception since it involves Information and Communications Technology (ICT). and to facilitate better integration of fluctuating RES such as wind or photovoltaics.

Energy storages supported by power electronics as an interface have considerable technical application and impact on future smart grid [77]. Figure 2- 14 shows functionalities of the smart grid.

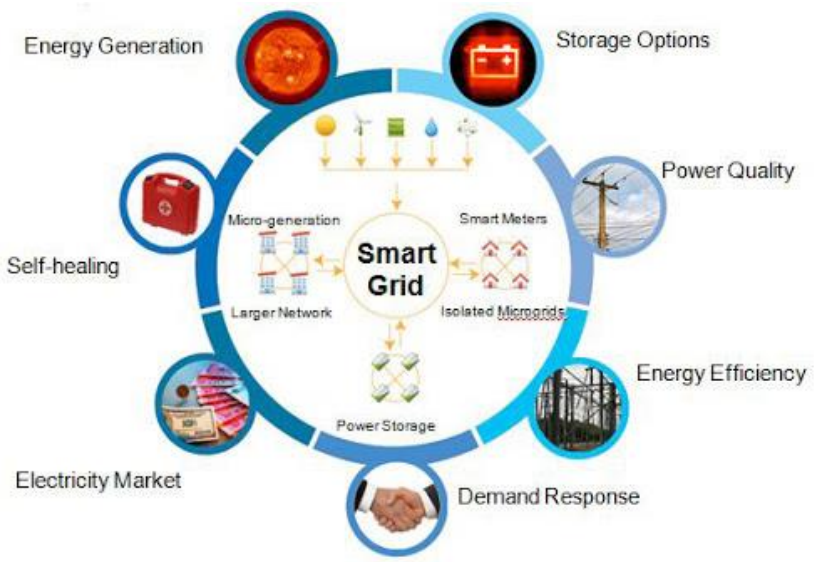

Figure 2-14: The smart grid concept [112]

Smart grid technologies pose an advantage of reduced reaction and restoration time [107, 108].Example of these technologies are: (1) Phasor Measurement Unit ,(2) Distance to fault estimator, (3)Smart monitoring and Measurement, and , (4)Feeder automation.

Summary

This chapter reviewed the relevant research on the historical development of traditional power systems with respect to flexibility, power quality and power system stability issues. The review included RES, considering the effect of power electronics and smart grid applications. Lastly,

voltage stability, using tools and also considering the effect of high RES penetration and subsequent mitigation techniques are analysed.

CHAPTER 3: EVALUATION OF ENERGY STORAGE SYSTEMS

Introduction

This chapter describes the classification of ESS and their impact on power quality and power stability. Comparison using technical characteristics and applications, also looking at developments in energy storage technologies are discussed.

3.1 Organisation of energy storage options

ESS are grouped according to the form of energy they can store and categorized by their energy storage and power capabilities[86, 90] Figure 3-1 shows the classification of energy storage options.

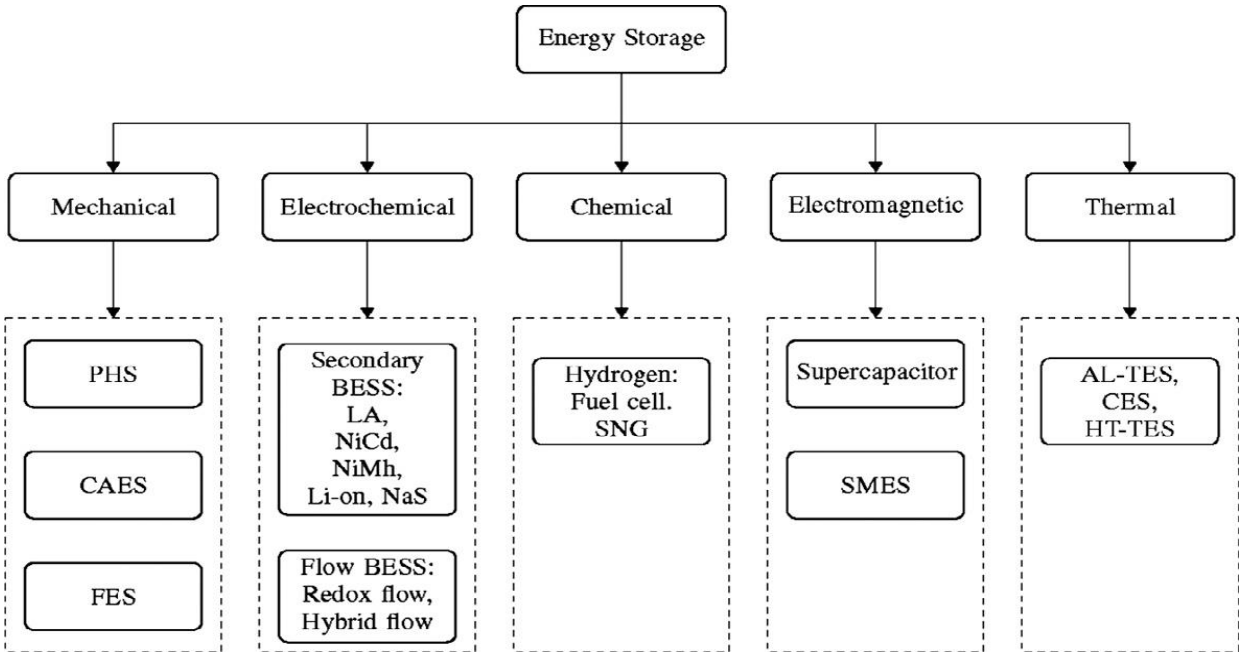

Figure 3-1: Energy storage classification[90]

3.1.1 Mechanical types of energy storage

These include storage in the forms of gravitational, potential and kinetic energy [113]. The major disadvantage is that they are limited to geographically appropriate sites. [85, 113].

3.1.1.1 Compressed air energy storage (CAES)

The system is based on the conventional gas turbine technology. Energy is stored as compressed air in designated underground storage location **[**[86, 113]. When there is a high energy demand, compressed air is drawn from the storage location, heated up, expanded and converted into rotational kinetic energy. It is then mixed with natural gas, to be released and fired to drive a turbine for electrical energy generation as described in Fig.3-2.

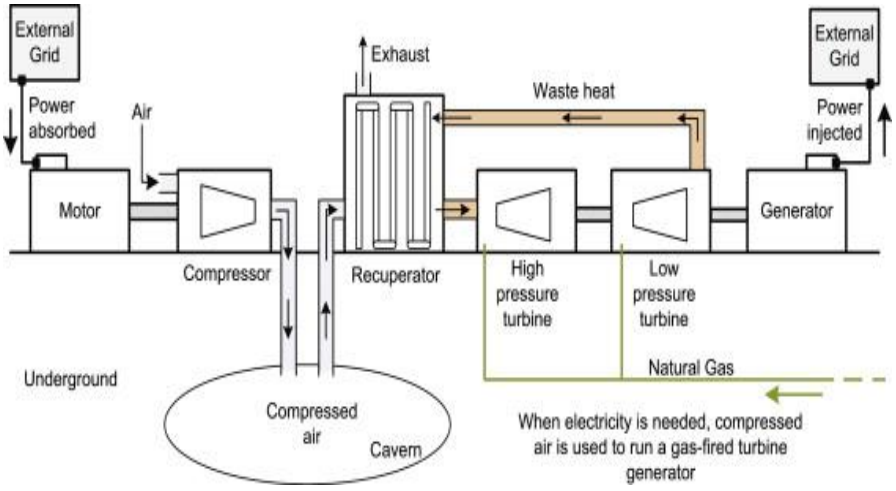

Figure 3-2: System description of the CAES [86]

There are few CAES worldwide but they are presented as the most suitable technology for large-scale energy storage. They can deliver up to 2700 MW of turbine power. The CAES energy efficiency is around 71% with low system self-discharge. Currently there are improvements in the technology. Their advantages are higher efficiency, and that they can switch between compressing or expanding or run both simultaneously, without emissions[113].

3.1.1.2 The flywheel

The flywheel utilizes kinetic energy principles. It is recognized as the most matured ESS due to its reliability and long useful life. The transformation in shapes, sizes, material, magnetic bearings and power electronics offered flywheels a competitive advantage from other energy storage applications [85, 113, 114]]. With increased integration of RES, flywheels are being effectively used for frequency regulation, reactive power support and spinning reserve [85, 90, 113] Energy is stored in the form of angular momentum of a rotating mass. Figure 3-3 shows the components of the flywheel system. [85]. During the charge, the flywheel is rotated by a motor and during the release phase, the same motor acts as a generator producing electricity

from the rotational energy of the flywheel. The power rating is dependent on the motor-generator. [85, 114].

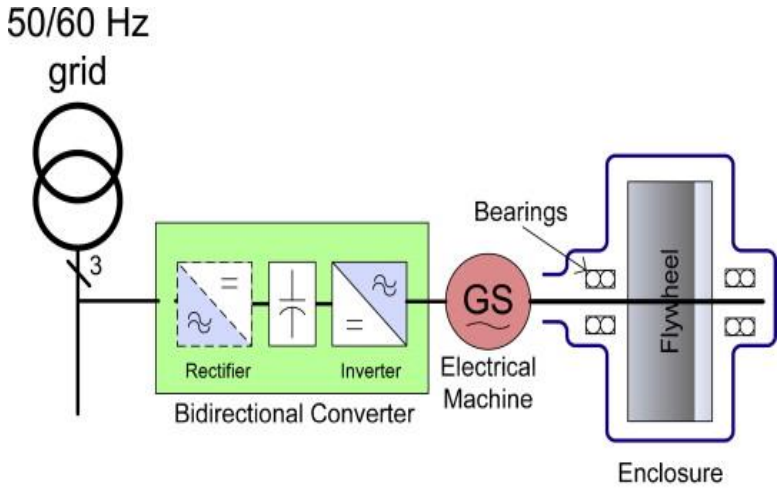

Figure 3-3: Components that form the FESS [85]

The full potential energy is a function of the moment of inertia l and spinning speed ω of the rotor as shown in Equation 3-1 .

$$E_c = ½ l\omega^2 \quad (3\text{-}1)$$

The moment of inertia is dependent on the flywheel mass and geometry

$$l = \int r^2 dm \quad (3\text{-}2)$$

In which *r* is the distance between the mass element and the axis in motion.

The spinning speed ω is determined by the material tensile strength, which is the material capacity to withstand centrifugal forces affecting the flywheel [114]

The energy density (e_v) and the specific energy (e_m) are calculated using Equations 3-3 and 3- 4 respectively [114]

$$e_v = K\sigma_{\partial\mu} \quad (3\text{-}3)$$

$$e_m = K\frac{\sigma_{\partial\mu}}{\rho} \quad (3\text{-}4)$$

Where e_v is the maximum energy per volume, e_m is the maximum energy per mass unit , $\sigma_{\partial\mu}$ is the material tensile strength , ρ is the mass density and, *K* is the shape factor., which is the measurement of the material utilization as shown in Fig.3-4 for different materials [114]

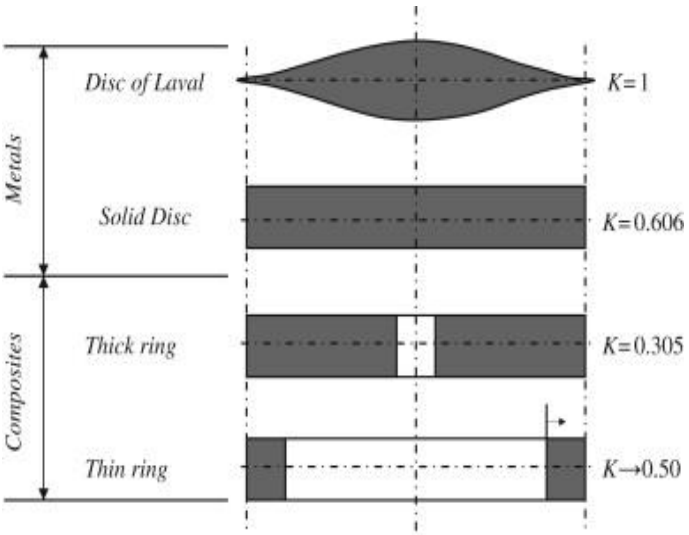

Figure 3-4: Different flywheel shapes [114]

The advantages of flywheels are that they can last long and have capability of providing many charge-discharge cycles at high efficiency (90-95%), quick response time less than 4seconds and offer relatively environmentally friendly technology solutions. Their limitations are high self-discharge losses and frictional loss restrict the flywheel systems from energy management applications [85, 114].

3.1.1.3 Pumped hydro storage (PHS)

PHS is based on the principles of potential energy from gravity. It I the most implemented large-scale energy storage consisting of two reservoirs located at different elevations. The storage schemes use water as a RES. During high peak period, water is released from the upper reservoir through the hydroelectric turbine and collected in the lower reservoir. During low energy demand, excess electrical capacity is used to pump water into the higher reservoir [85, 113]. The storage capacity is a function of the water fall height and available water volume [[26, 113], as shown in Fig 3-5. The system's performance is compromised by two types of losses namely: (1) the exposed water surface evaporation losses and (2) the mechanical conversion losses [26, 85, 113]. The only existing within the Eskom network are Ingula in KwaZulu-Natal and Palmiet in the Western Cape. Since South Africa is a water-scarce country it puts such an ESS at a disadvantage.

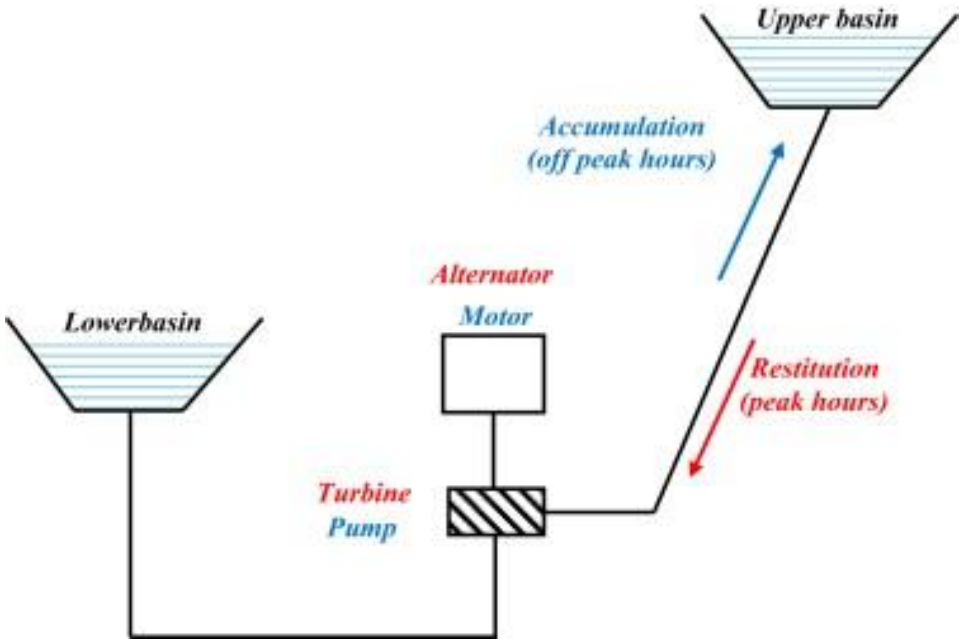

Figure 3-5: The pumped hydro storage system [[26]

The PHS are rated around 1000 MW up to 5 GW per year throughout the world. The advantage is that the storage system is economical as it injects significant power into the grid to balance out the electricity demand, with rapid response time . The limitation is that it is geographically constrained.

3.1.2 **Electromagnetic energy storage (EES)**

EES is the technique of directly storing electrical energy into electrical current. It can be achieved in the forms of electrostatics such as superconducting magnetic energy storage (SMES), capacitors and super-capacitors [85, 113].

3.1.2.1 Capacitors / super capacitors

The capacitors store energy in an electric field between the two metal plates separated by an insulating material called the dielectric. The major disadvantage is short durations and high energy dissipation. [113].

The super capacitor is the electric double-layer capacitor (EDLC) with absorbent carbon materials with a large specific surface [85]. A super capacitor stores energy using the an electrolyte solution between two solid conductors as shown in Fig.3-6 ,which describes the energy storage based on the super capacitor [85, 113] . They have extremely high power density,

high cycle life,quick recharge and their temperature operating range is wide(-40 to 70^0C). It is a technology that shows more development [86, 113].

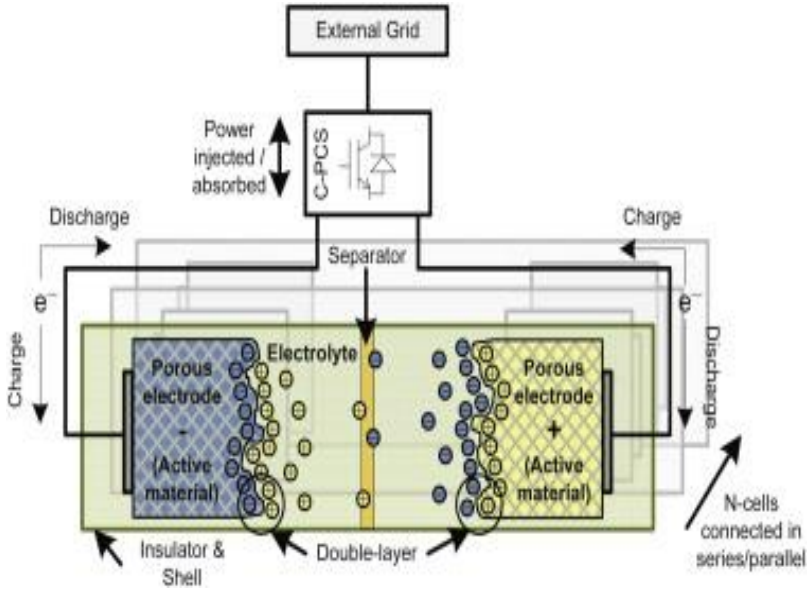

Figure 3-6: Energy storage based on a super capacitor [86]

The energy stored in the capacitor/super capacitor is directly proportional to its capacity (C) and the square root of the terminal voltage. C on the other side is directly proportional to the area of the plates and inversly propotional to the distance between the electrodes as described in Equations 3-5 and 3-6 respectively,thus the supercapacitor provides high energy density due to its carbon-activated surface area (up to 2000 m^2/g) added to a very small distance separating the plates [86, 113].

$$E = ½CV^2 \quad (3\text{-}5)$$

$$C = \frac{A\varepsilon_r\varepsilon_0}{d} \quad (3\text{-}6)$$

Where C = capacitance, V = voltage between the terminals, A = surface area, E = energy, is the relative permittivity, ε_0 = absolute permittivity = $8.85x10^{-12}$ F/m and, d is the distance between the electrodes.

Advantages are rapid response time and high power density, with limitations of being expensive[86].

3.1.2.2 Superconducting magnetic energy storage system (SMES)

Their operating principle is based on storing electric energy in a magnetic field. Direct electric current passes through an inductor made from superconducting material and circular so that current can circulate indefinitely without any loss. The inductor is kept in a superconducting state by immersing it in liquid helium or contained in a vacuum-insulated cryostat. Fig. 3-7 demonstrates the three major components of the SMES system, the cryostat system which consists of cryonic refrigerator and a vacuum-sealed vessel, the superconducting unit and the power conversion unit. The charging and discharging [85, 86, 113, 115].

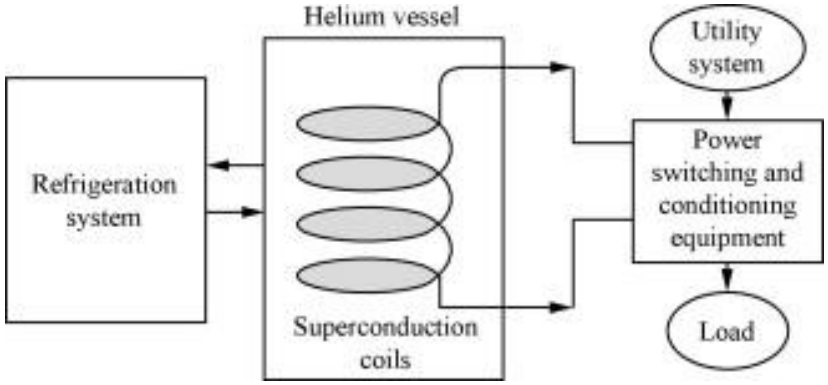

Figure 3-7: The SMES [85]

The SMES is used for regulating power quality and voltage stability [86]. Energy stored in the SMES is calculated using Equation 3-7.

$$E = ½LI^2 \quad (3\text{-}7)$$

Where, L = inductance of the coil and I = current passing through the conductor.

Advantages are ability to exhibit higher energy efficiency (≥97%), quick response, within milliseconds, delivering 100 MW of power and high cycle life. Limitations are high cooling requirements and strong magnetic field associated environmental issues [85, 86, 114].

3.1.3 Chemical energy storage

Chemical energy storage is considered as a secondary energy carrier using hydrogen or synthetic gas, where hydrogen is electrolyzed, and synthetized into natural gas (i.e. methane) with carbon dioxide [[116]. An example is the fuel cell, which consume reactants and must be refilled [85, 117]. This green technology without any pollution could lead to formation of large-scale energy storage which can store more than 100 GWh energy [116].

3.1.3.1 The fuel cell

A fuel cell is regarded as an electrochemical energy conversion device. It produces electricity from an external fuel supplied anode and an oxidant based cathode, with the electrolyte present. There are different combinations of fuels and oxidants used for fuel cells such as phosphoric acid (PAFC) utilizing phosphoric acid, direct methanol (DMFC) using non-reformed methanol, the molten carbonate (MCFC). The most efficient and practical is the hydrogen fuel cell due to its non-polluting value since it uses hydrogen as fuel and oxygen as an oxidant to produce electricity and water. The process is reversible to produce hydrogen and oxygen [[1, 86, 113, 117].The hydrogen based energy storage system consists of an electrolyser unit, which is powered by the off-peak renewable power to convert the electrical energy , when needed. During the charge and discharge process the electrodes remain catalytic and stable [85, 86, 113, 117]. Fig.3-9 describes the formation of the hydrogen fuel cell.

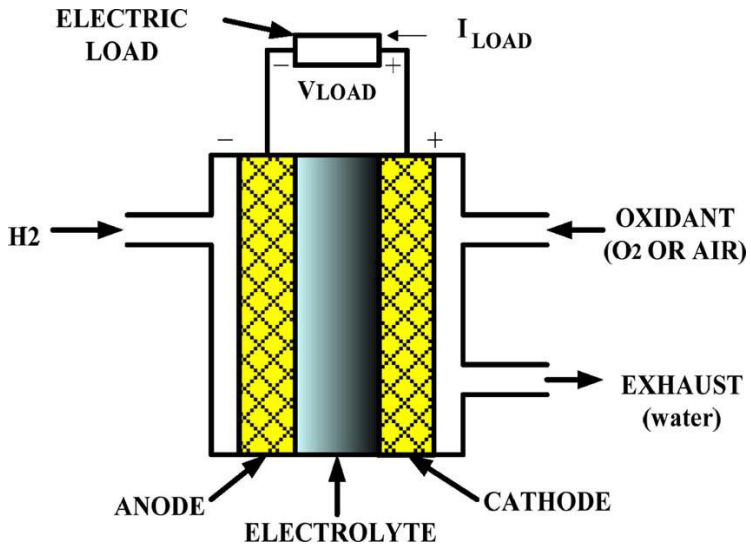

Figure 3-8: Configuration of a hydrogen fuel cell [117]

Fuel cells possess high conversion efficiency and quiet operation with good reliability since the power quality doesn't degrade over time. Electricity production is continuous so long as necessary flows of fuel and oxygen are maintained and their modular construction allows further addition of modules in future [118, 119],

Disadvantages are low round-trip efficiency (20-50%), with high operating costs and low security[119].

3.1.4 **Electrochemical Energy Storage**

Electrochemical energy storage involves the conversion of chemical energy to electrical energy. The ESS are batteries and they store electrical energy chemically in a closed system [85, 117]. Batteries offer another means of grid-level energy storage by converting electricity to chemical energy during times when electrical supply exceeds demand[85].

The BESS is a chemical-based energy storage system using shunt connected, voltage sourced converters capable of rapidly adjusting the amount of energy which is supplied to or absorbed from an ac system [15]]. The BESS have an advantage of being feasible for any geographical location [120]. They have an ability of quick response to load changes and accept co-generated and /or third party power consequently improving system stability [85]. They are categorized by their operational modes, energy density, cycle capability, efficiency of charge and discharge [115]. Figure3-10 shows the operation of a BESS, which is made up of a set of low-voltage/power battery modules connected in parallel and in series depending on the anticipated characteristic. During the charge process batteries undergo an internal chemical reaction due to a potential applied to the terminals and the discharge process is achieved when the chemical reaction is reversed [105, 115, 121]. Energy is stored as chemical energy in the active materials, whose redox reactions produce electricity when required [122].

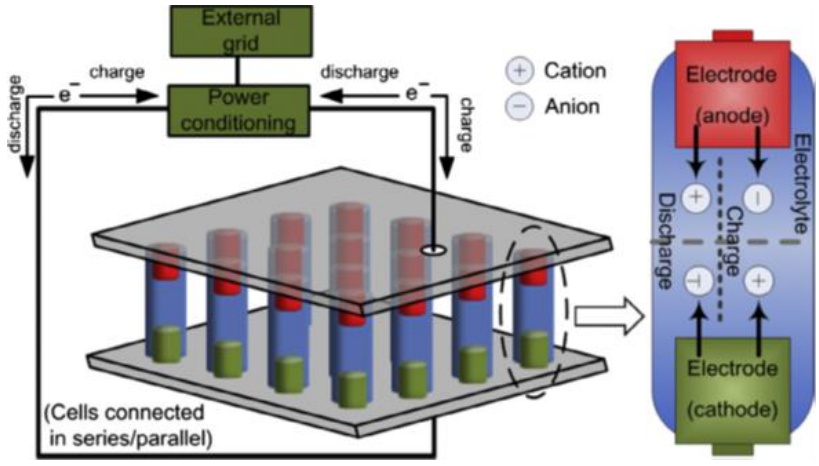

Figure 3-9: Schematic diagram of a BESS operation [105]

The grid-scale battery energy storage system (GSBESS) is a form of storage power plant which utilize the electrochemical principles for energy storage and possess an advantage of not requiring mechanical mass movement to inject power [123]. The impact of GSBESS on grid stability, grid code requirements and economic analysis are discussed in Chapter 4.

There are different materials which have a track record for being used for large-scale energy storage and they vary in characteristics. Some of the battery materials for grid-scale energy storage are listed:

3.1.4.1 Lead Acid batteries

Lead–acid is the oldest and most commonly used rechargeable BES [85]. It consists of series-connected cells, an electrolyte, and the positive and negative electrodes [85, 124]. In the charged state, the battery consists of lead (Pb) and lead oxide (PbO_2) in Tetraoxosulphate VI acid (H_2SO_4); and, in the discharged state, lead sulphate ($PbSO_4$) is produced both at the anode and the cathode, while the electrolyte changes to water [85]. A porous separator is placed between the electrodes to prevent them from having a contact [121, 124]. The chemical reactions at anode and cathode are as represented in Equations 3-10 and 3-11, respectively [85, 121].

$$Pb + SO_4^{2-} \leftrightarrow PbSO_4 + 2e^- \quad (3\text{-}8)$$

$$PbSO_2 + SO_4^{2-}4H^+ + 2e^- \leftrightarrow PbSO_4 + 2H_2O \quad (3\text{-}9)$$

The battery's state of charge (SOC) could be determined by measuring the concentration of the electrolyte through the specific gravity (SG) method [85, 125]. This battery chemistry requires an operating temperature of about 300°C to maintain the active materials in a molten state [124]. Of emerging battery technologies suitable for utility applications, sodium sulphur batteries are the most technologically mature, and are deployed on a limited scale in Japan and in the United States. [26, 85]. They are suitable for cost-sensitive' applications such as automotive starting, lighting and ignition and uninterruptible power supplies [126]. Figure 3-11 shows the lead acid battery storage. Latest modernizations in lead acid technology demonstrated three to four times the energy density with improved lifetimes over conventional lead acid batteries. With additional research and demonstration, other battery technologies also could prove useful for large-scale energy storage [[113].

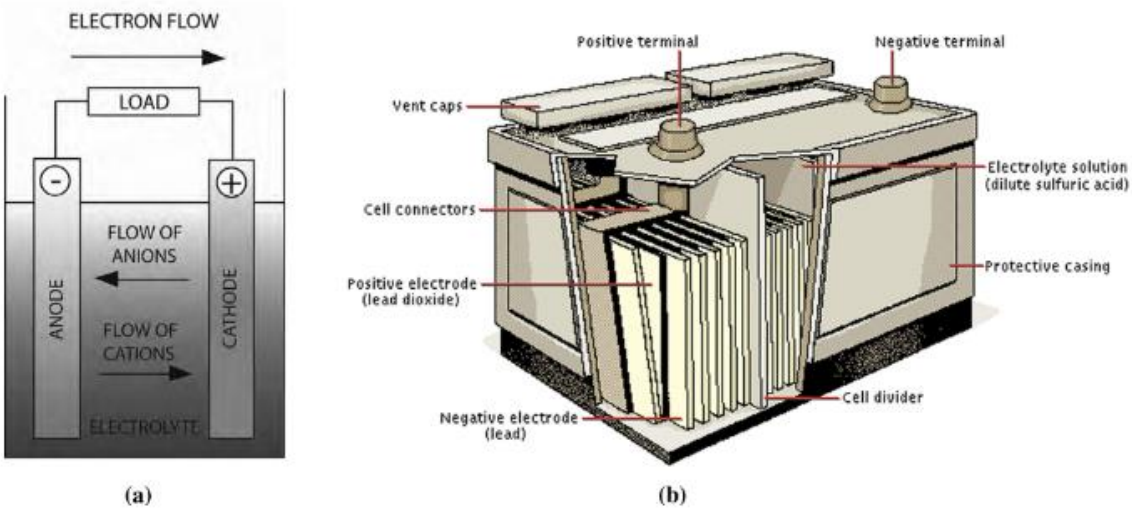

Figure 3-10:Lead acid battery storage [121]

3.1.4.2 Lithium ion batteries

The lithium ion battery technology is approximately 40 years old, and it is recognized in electronics and transportation industries, especially in the operation of plug-in hybrid electric vehicles (PHEVs), and power grid applications [121]. The Li-ion battery consists of the lithiated metal oxide cathode and the anode made of graphite carbon with a layering structure. The electrolyte is made up lithium salts dissolved in organic carbonates. During the charge process, the Li atoms in the cathode becomes ions and migrate through the electrolyte towards the carbon anode to mix with the external electrons. They are then deposited between the carbon layers as Li atoms. The process is reversed during the discharge process[85, 113, 121]. Figure 3-12 shows the schematic diagram of the Li-ion battery. With the continuing research and developmental efforts, lithium-ion battery prices are expected to drop in future. The 25%and 50% reductions in battery price are chosen. These choices are consistent with the target of $100/kWh to $150/kWh set by US Advanced Battery Consortium [127].

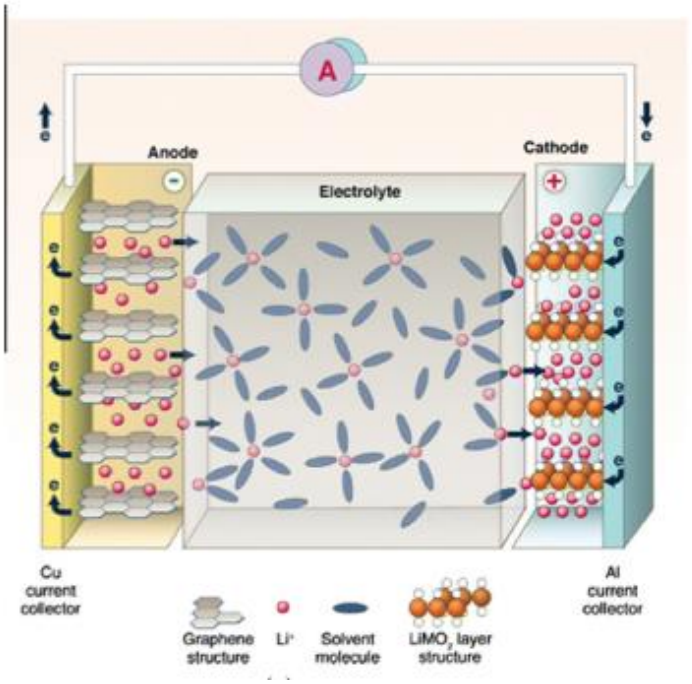

Figure 3-11: Schematic diagram of the Li-ion battery [121]

Equations 3-12 and 3-13 show the reversible reactions involved in the charged/discharged states, at anode and cathode, respectively [121].

$$C^{+}xLi^{+} + xe^{-} \leftrightarrow Li_{x}C \quad (3\text{-}10)$$

$$LiMO_{2} \leftrightarrow Li_{1-x}MO_{2} + Li^{+} + xe^{-} \quad (3\text{-}11)$$

Li ion batteries have highest efficiencies (approx. 100%), high energy density (75–200 Wh/kg), high cycle life (10 000 cycles), high 'energy-to-weight' ratio and low self-discharge loss with limited discharge depth[85].

3.1.4.3 Development in battery technologies

- There is a development in technology where the combination of ultra-capacitors and lead acid batteries into integrated energy storage devices is tested and it is referred to as "ultra-batteries." [85, 86].
- The long life aqueous electrolyte battery is the newest development. The potassium ion is inserted into the copper hexacyanofferate cathode and novel activated carbon polypyrrolehybrid (PPy) anode. It is demonstrated to be safe, fast, and inexpensive. It has a high rate, 95% round trip energy efficiency with zero capacity loss after 1000 deep-discharge cycles [128].

3.2 Impact of energy storage to power quality and stability

ES integration to the DS can be used to improve local power quality and reliability, voltage support, provide ancillary services and backup power, reduce losses, and defer DS upgrade[77]

In order to mitigate the effects of power fluctuations, an electrical storage system can be used. Flywheel, batteries excluding conventional lead acid batteries, capacitors and super capacitors, superconducting magnetic energy storage system (SMES) have fast response rated in milliseconds [85]. The most suitable for bridging power are flow batteries and fuel cells due to the fact that they have quite fast response and long discharge time [85, 121].

Summary

This chapter explored on categories of energy storage. Their advantages and disadvantages were highlighted, including some technical capabilities. Their impacts on power quality and stability is mentioned as well as battery technological developments.

CHAPTER 4: BESS GRID STABILITY AND ECONOMIC ISSUES

Introduction

This chapter will elaborate on the BESS integration issues. The impact of grid-scale BESS on grid stability, grid code requirements and economic analysis are discussed. Like any other DG, the issues are classified into three categories namely, technical, commercial and regulatory. Commercial and regulatory issues are affected by government policies and operating requirements.

4.1 Impact of BESS to grid stability

Battery energy storage is one technology that is now attracting considerable interest for autonomous applications as well as for large scale deployment on the grid [89], due to its versatility, high energy density, and efficiency [100]. It can be used for load following applications thereby dealing with essentially intermittent nature of PV and wind sources [89]. Moreover, integrating battery energy storage systems with renewables helps to increase the reliability and defer capital cost investments of upgrading the ratings of transmission lines and other electrical equipment [68]. More grid applications have become suitable for BESSs as battery costs have decreased while performance and life cycle have continued to increase [125].

4.1.1 The BESS architecture

The BESS comprises mainly of batteries, control and power conditioning system and rest of plant [100]. It requires a battery management system to monitor and maintain safe, optimal operation of each battery pack and a system supervisory control to monitor the full system [129]. Figure 4-1 shows the BESS functional block diagram.

.

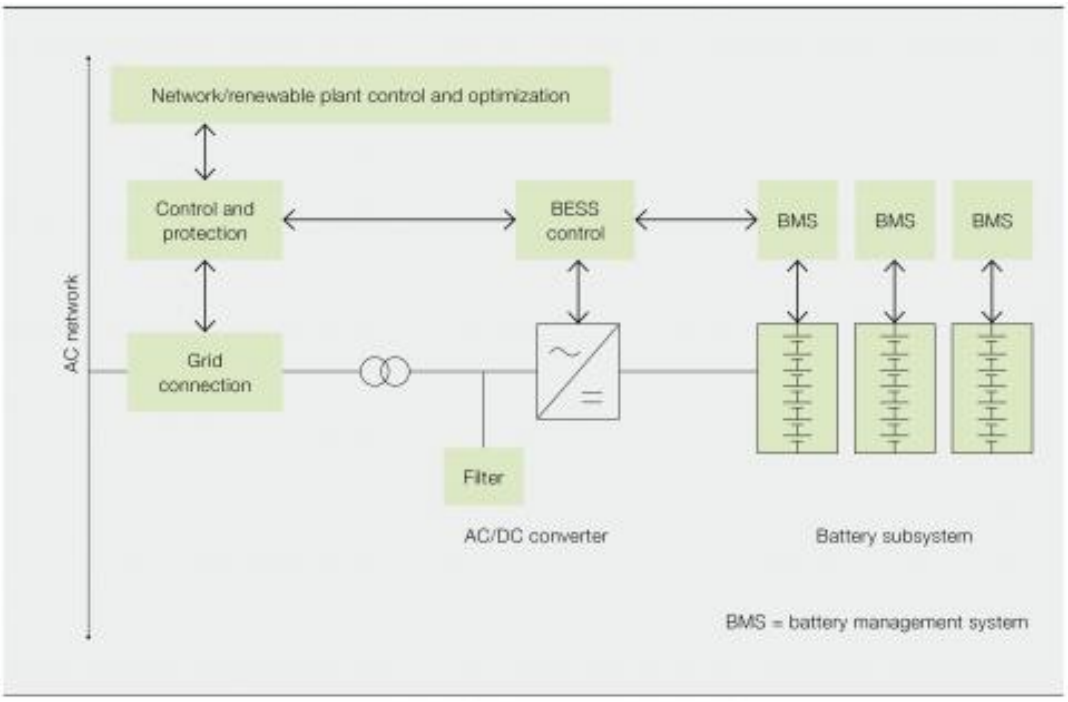

Figure 4-1: Functional block diagram of the BESS[91]

4.1.2 The BESS applications

Many authors have researched various aspects of effective incorporation of BESS to support RES technology, most of them aiming to their optimization use to permit higher penetration [9]. Begovic and Hill [130, 131] present challenges inherent to integrating solar energy into power systems and developed a variety of real-time control modes of operation for BESS in grid-tied solar applications. To alleviate possible adverse effects for increased penetration and maximizing economic benefits smart grid developers and power systems planners are required to broaden the understanding of BESS applications [9]. BESS may be used as bulk storage, distributed storage or mobile storage units. Some of the benefits provided by the BESS are:

4.1.2.1 Frequency regulation

Frequency regulation is the constant second-by-second adjustment of power to maintain system frequency at the nominal value (50 or 60 Hz) to ensure grid stability [132].The BESS can provide regulating power with sub-second response times, by charging and discharging in response to an increase or decrease in grid frequency caused by misalignment of energy supply and demand [91]. Figure 4-2 shows the frequency containment and subsequent restoration following a contingency such as an outage at a large power station.

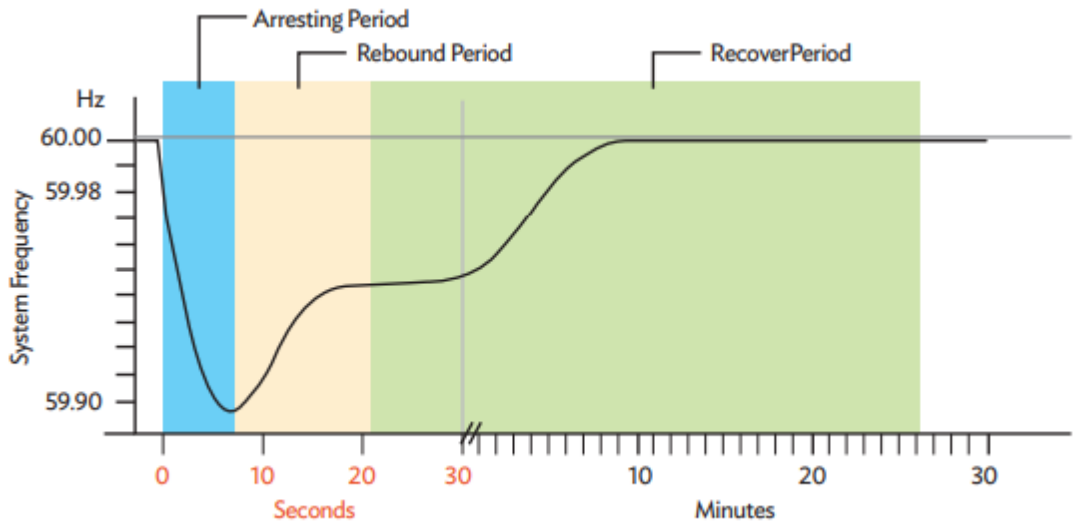

Figure 4-2: Frequency containment and subsequent restoration[133]

Frequency regulation and black start BESS grid applications are sized according to power converter capacity (in MW), as demonstrated in Equations 4-1 and 4-2.

$$BESS\ capacity(MW) = Frequency\ gain * Governor\ droop * System\ frequency \quad (4\text{-}1)$$

And,
$$S = 100\% * \frac{\Delta f}{\Delta f_n} * \frac{P_{ref}}{\Delta p} \quad (4\text{-}2)$$

Where S = Droop in %, Δf = System frequency change, where the BESS must provide a frequency response, f_n = Nominal system frequency, P_{ref} = Nominal power of the BESS, and ΔP = The change in active power performed by the BESS [134]

4.1.2.2 Voltage regulation

BESS can be used to balance load and generation and minimize the voltage fluctuation issues by serving as a supplementary controller and improve the efficiency of voltage support in low-voltage network, as demonstrated in Figure 4-3. Yang in [135] proposed a method for BESS design optimization and sizing strategy considering voltage regulation, peak shaving and annual cost for distributed PV systems.

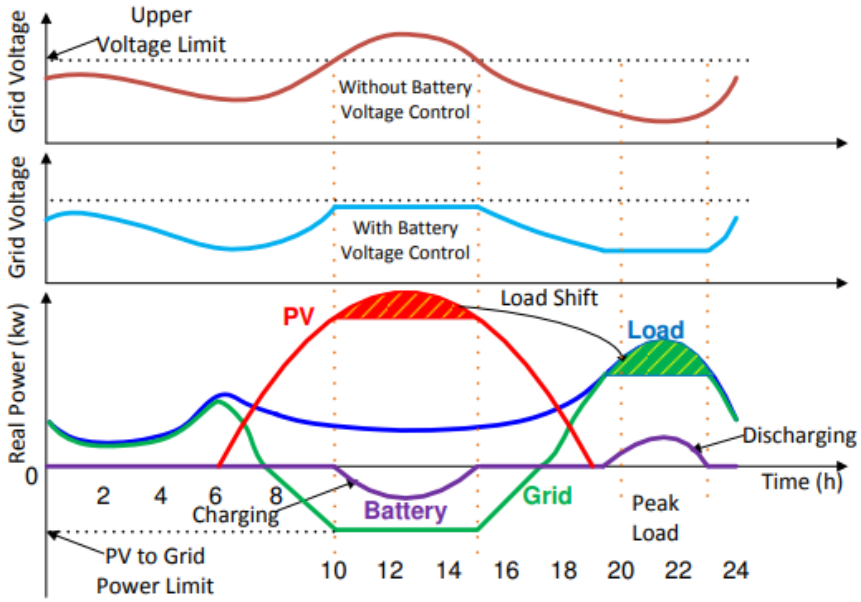

Figure 4-3: Energy management system for the PV integrated grid [136]

4.1.2.3 Peak shaving

Peak shaving is the reduction of electric power demand during times when network capacity is stressed [137]. As bulk storage in grid applications, BESS are used for peak load shaving, acting as generator to discharge energy in the network during load peak hours and/or relieve lines congestion, RES integration enabler, acting as loads to store the extra energy from intermittent DG sources and, provide ancillary services and power quality to support distribution networks in a fast and reliable manner [138]. The BESS can be used to adequately smooth the output of the Solar PV-BESS sub-system for over voltage reduction and peak load shaving during high PV generation/low consumption or high demand/low solar PV generation time, and are suggested as a suitable and cost effective solution to mitigate adverse effects of intermittency and shape the fluctuation of the system's output into relatively constant power [139].

Peak shaving is similar to load leveling but is for reducing peak demand rather than for economy of power system operation [91]]. Figure 4-4 shows optimal charging and discharging of BESS for peak shaving and load leveling. The batteries are charged with the produced energy from the power plant during off-peak demand and discharged to inject energy into the network during periods of high electricity demand, so as to achieve peak shaving and load levelling, thus helping in smoothing the distinctive mountain and valley shape of the load curve [140].

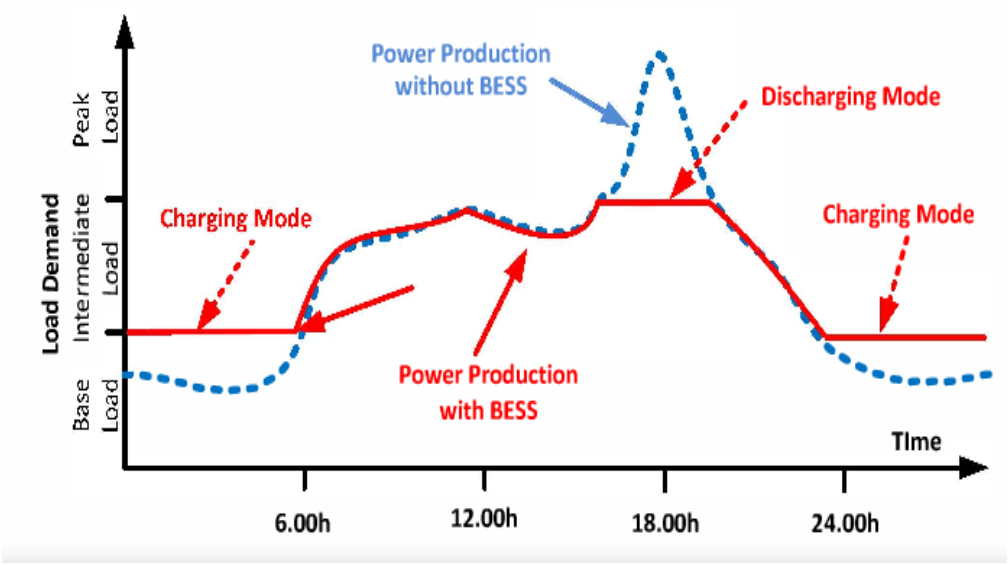

Figure 4-4: Optimal charging and discharging of the BESS for peak shaving and load leveling [140]

4.1.2.4 Load leveling

Load leveling is a promising application of storage unit, which involves storing power during periods of light loading on the system and delivering it during periods of high demand. During the periods of high demand, the BESS supplies power, reducing the load on less economical peak generating facilities [124]. The BESS is strategically located next to the load to allow for the postponement of investments in grid upgrades or new generating capacity [141]. This facilitate reductions in transmission losses, reduces the requirements for expensive peaking generation, delay the installation of extra generating capacity and improve system power quality and reliability [124, 142].

4.1.2.5 Power quality

The BESS are capable of increasing the quality of power to a facility by maintaining nominal voltage and frequency values[123]]. One of the merits of BESS use in power systems is their versatile ability to act as load or as generator with additional increased advantages when connected to the grid through power electronic inverters [9]. The BESS can bridge the power gap between RES and the loads by supplying power during periods of unavailability as well as storing the excess power during high periods of wind and/or sun accessibility [89]. They serve as an uninterruptable power supply(UPS) that can facilitate for unplanned disruptions and enhance system reliability [91]. A BESS can be used to absorb the supply of renewable energy and keep the voltage below the upper limit prescribed in the grid code [137].

4.1.2.6 Spinning reserve

Utility-scale BESS feature fast response characteristics can provide an economic and alternative to smooth the output power of RES and provide operating reserves [103]. The BESS is maintained at a level of charge ready to respond within milliseconds to a generation or transmission outage to maintain network continuity while the backup generator is started and brought online. This enables generators to work at optimum power output, without the need to keep idle capacity [91]. There is practically no cost to the system when BESS are in reserve state. [23]].

4.2 Grid code requirements for BESS

National grid codes are used to define the electrical performance requirements of generating assets, operational and dispatch rules, technical requirements for interconnection to the grid and energy market operation [143, 144]. To improve frequency stability, in the future, grid codes could extend frequency control requirements applied only to conventional power plants and DGs [144].

Most grid codes and standards provide permissible frequency ranges for desirable power systems. The South African grid connection code for DGs specifies the operating frequency range of 49 Hz to 51 Hz for all categories of RES and energy storage [145], and the nominal systems' frequency is 50 Hz, which was decided based on the design and operating characteristics of the main power system components.

The "Grid Connection Code for Battery Energy Storage Facilities (BESF) Connected to the Electricity Transmission System (TS) or the Distribution System (DS) in South Africa." sets the requirements for BESF as specified in terms of the Electricity Regulation Act (Act 4 of 2006).

BESS are classified into three main categories based on their rated power and the voltage level at which they are connected. These categories are A, B and C. Category A are BESS connected to low voltage (LV) networks, with rated power greater than 0 and less than 1 MW, within the 3 sub-categories A1, A2 and A3. Category B includes BESS connected to medium voltage (MV) networks, with the rated power greater or equal to 1 MW and less than 20 MW with 2 sub-categories B1 and B2. Category C is for BESS connected to medium or high voltage (MV/HV) networks, greater than or equal to 20 MW. A summary of grid code requirements for these categories is presented in Table 4-1.

Table 4-1: Summary of grid code requirements for BESS categories[134]

Category	**A1**	**A2**	**A3**	**B1**	**B2**	**C**
Rated power [kW]	0 -13,8	13,8-100	100-1000	1000-5000	5000-20000	≥20000
Voltage level	LV			MV/HV		HV
Operating frequency	49-51 Hz					
Operating voltage range	-15% to +10%			within the POC voltage range specified by U_{min} and U_{max}		
High voltage ride through	N/A			120% for 2seconds		

The technical operating requirements for BESS are presented for normal and abnormal network operating conditions.

4.2.1 **Normal operating conditions**

BESF of Category A shall only be allowed to connect to the NIPS, at the earliest, 60 seconds after the following conditions have been satisfied: The frequency in the NIPS is within the range of 49.0 Hz and 50.2 Hz, as shown in Figure 4-5.

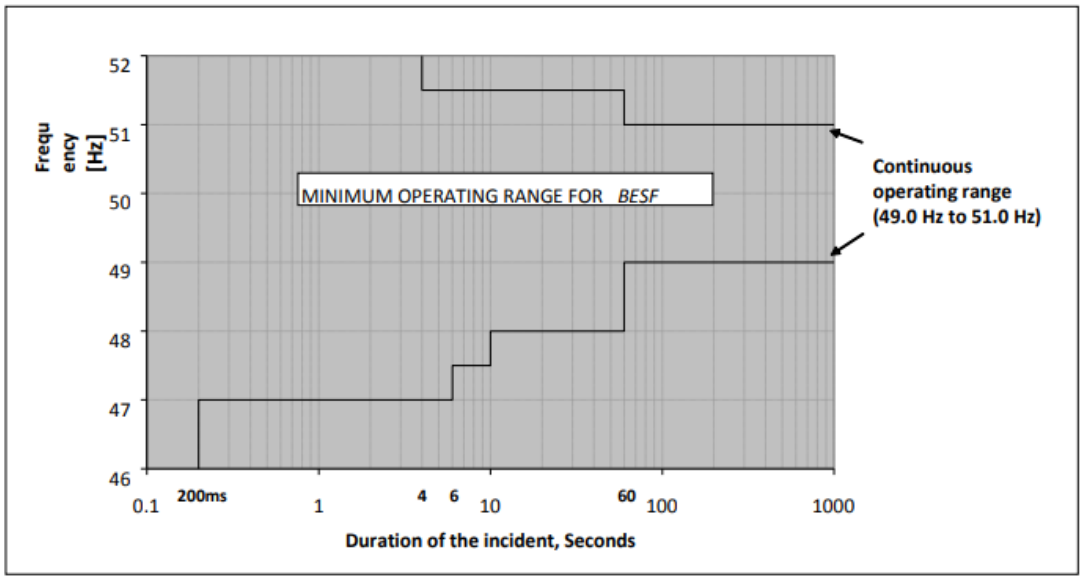

Figure 4-5: Minimum frequency operating range for a BESF during system frequency disturbance [134]

The BESF of category A, the voltage at the point of connection (POC) is in the range -15 % to +10 % of the nominal voltage.

BESF of Category B1, B2 and C, the voltage at the POC is within the specified U_{max} and $U_{min.}$ The minimum operating voltage that can be reached at the POC should be 0.9 p. u for BESS integrated on 11 kV up to 44 kV networks and the maximum operating voltage at 1.08 p.u. For BESS integrated on 66 kV up to 132 kV networks, the minimum operating voltage that can be reached at the POC should be 0.9 p. u and the maximum operating voltage at 1.0985 p.u.

4.2.2 **Abnormal operating conditions**

The BESF of category C shall be able to withstand voltage peaks up to 120% of the nominal voltage, measured at the POC, for a minimum period of 2 seconds without disconnecting

The voltage ride through is a capability that BESF needs to have in order to stay connected to the National Grid and keep operating following voltage dips or surges caused by short-circuit faults, or disturbances on any or all phases in the Transmission, or a Distribution System [134]. It is a requirement, under abnormal conditions and, is applicable to all types of faults (symmetrical and asymmetrical, i.e. one-, two- or three-phase faults) [134]. Figure 4-6 shows the voltage ride through capability for Category AI and A2 BESFs.

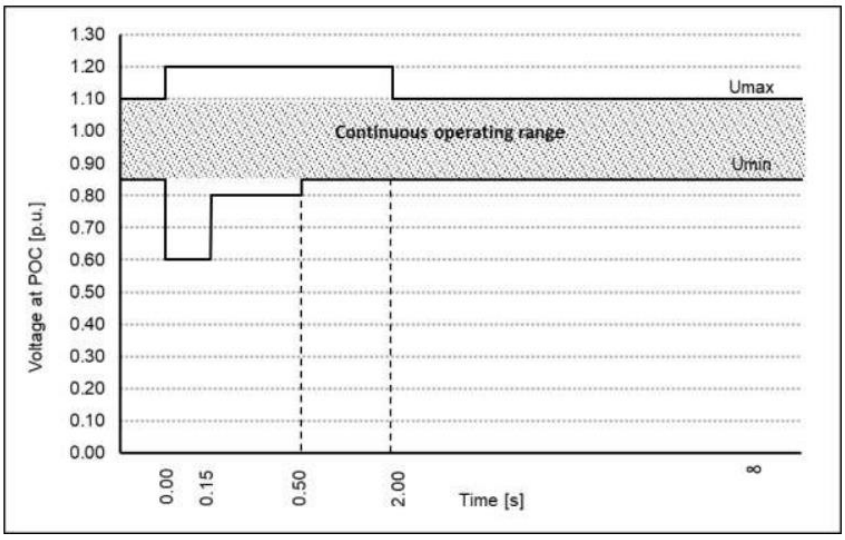

Figure 4-6: Voltage ride through capability for Category AI and A2 BESF[134]

For asymmetric faults, the BESF must be able to withstand voltage drops to zero, measured at the point of connection, for a minimum period of 0.15 seconds without disconnecting. Thereafter, the reactive power follows the control characteristics with a tolerance of ± 20% after 60 ms. [134]. Figure 4-7 represents voltage ride through capability for BESF of category A3, B1, B2 and C. The operating areas A-D illustrate. the minimum voltages on all phases that the BESFs must withstand.

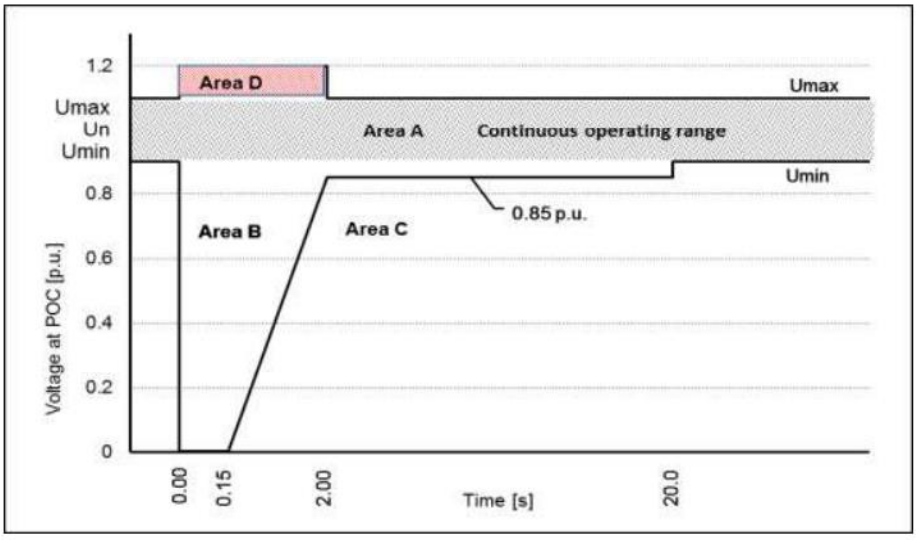

Figure 4-7:Voltage ride through capability for BESF of category A3, B1, B2 and C[134]

4.3 Economic analysis of BESS

A storage facility's greatest strength is to improve the economic efficiency of the existing system, not replace it [142]. Energy storage economics is highly dependent on the technology, costs and potential revenues for both the discharge capacity (MW) and energy storage capacity(MWh). The energy storage costs are calculated assuming one full cycle per day [146]. It is found that regulatory framework can be of paramount importance in ascertaining the economic feasibility of energy storage [127].

The development and application of the energy storage technology in future smart grids depends not only on the improvement in energy storage and power electronics features, but also on the cost reduction and the market policy required from the power industry[Molina]. As the intermittent renewable energy has become more prevalent, the large-scale implementation of energy storage system is gaining much attention [122]. Figure 4-8 presents the global cumulative energy storage forecast for 2040 according to the Energy Storage Outlook 2019, which predicts that the worldwide capacity of energy storage will increase prolifically from 9 GW/17 GWh (2018) to 1095 GW/2850 GWh

(2040) [122].

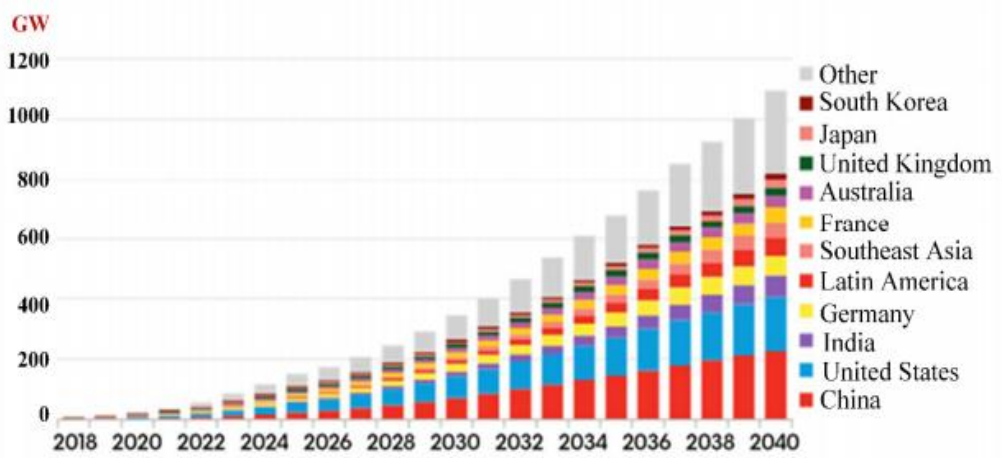

Figure 4-8: The global ESS forecast according to the Energy Storage Outlook 2019 by Bloomberg NEF [122]

Cost reductions in BESS technology are widely expected to become a key determinant of their increased installation. It is expected that the cost of lithium-ion BESS will decrease significantly, namely by 54–61%, between 2016 and 2030 or by 52% between 2018 and 2040 [147], as predicted by Bloomberg, in Figure 4-9. Battery costs, while falling, are still the most

significant driver of project viability, and costs depend on the MW/MWh ratio of the battery [137].

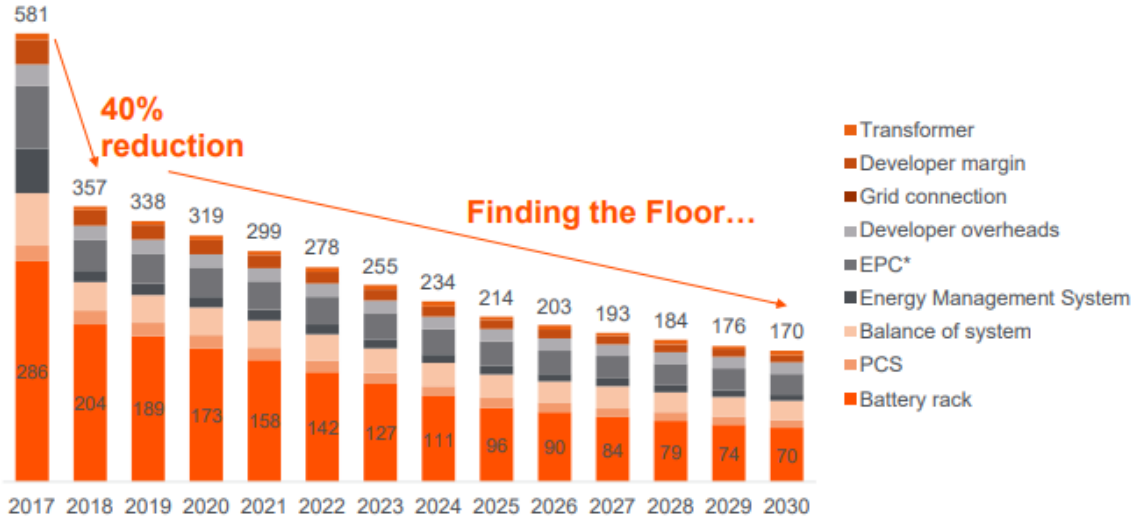

Figure 4-9: Bloomberg NEF estimate real 2018 $/kWh[148]

4.3.1 Cost characterization of the BESS

The BESS lifetime varies a lot under different scenarios, the lifetime levelized annual cost analysis method is adopted [98]. The levelized annual cost of BESS varies depending on the user case for battery services, charge/discharge cycle, depth of discharge, life assumptions, charging cost, assuming capacity augmentation is included in the agreement [148].

The levelized cost(C_L) over its lifetime is given by

$$C_L = Q\left[\frac{d*(1+d)^n}{(1+d)^n-1}\right] \quad (4\text{-}3)$$

Where Q = current cost; n = BESS lifetime (years) and d = discount rate, the levelized factor (LF_N) over n years is denoted [98] as:

$$LF_N = \frac{d*(1+d)^n}{[(1+d)^n-1]} \quad (4\text{-}4)$$

Therefore, the levelized annual cost of BESS on a particular bus i can be expressed as [135]:

$$LC_{BESS_i} = \left(C_{PCS} * P_{BESS_i} + \frac{C_W + W_{BESS_i}}{\eta}\right) * (1 + CF_{install}) * LF_{ni} \quad (4\text{-}5)$$

Where *i* = bus number; BESS*i* = BESS on a bus *i;* C_{PCS} = The unit cost of the power conversion system (PCS); C_W= Unit cost of the battery; ŋ = system efficiency; LF_{ni} =The levelized factors related to the BESS*i*'s lifetime.

The price for BESS service will be capped by the energy storage benefit to cost(B/C) from a utility/grid company [148], which is calculated as in Equation 4-6.

$$BESS\ \frac{B}{C}ratio = \frac{BESS\ benefits}{Cost-(Revenue+Incentives)} \quad (4\text{-}6)$$

Summary

This chapter addressed the effective ways of dealing of the intermittency of the energy source and the impact of BESS to grid stability. The grid code requirement issues and economic aspects are highlighted, in the context of BESS.

CHAPTER 5: NETWORK SYSTEM MODELLING

Introduction

This chapter covers discussions on the system network modelling and the justification for the choice of components. Parameter settings for the techniques applied and the methodologies used are also presented in this chapter.

The components of the system at both transmission and distribution levels include generators, transformers, transmission lines, loads and the DG system to be integrated into the grid system. Models of voltage regulator equipment, other additional components such as the inverter and other sub-components of the DG system including DG power output enhancing devices are also discussed in this chapter.

5.1 Tools for integrated system studies

5.1.1 The DigSILENT PowerFactory simulator [149]

The DigSILENT Power Factory simulator is a power system analysis software application. It is used in analysing generation, transmission, distribution and industrial systems. It covers the full range of functionality from standard features to highly sophisticated and advanced applications including wind power, distributed generation, real-time simulation and performance monitoring for system testing and supervision [149]. For this research, load flow analysis will be conducted for different network set-ups.

5.2 The test network system

DigSILENT™ PowerFactory™ IEEE-9 Bus model[150] is the IEEE standard test system model that will be used to assess the role BESS integration into grid power systems with regards to voltage stability and power quality enhancement. The system represents a small transmission system which consists of nine buses (nodes), three synchronous machines representing conventional generators supplying the network, three two-winding transformers, six lines and three loads[150].

The base kV levels are respectively 13.8 kV, 18,45 kV, 16,5 kV at generator buses and 230 kV at the remaining buses. The sub-transmission network is represented by the part at which loads

are connected to. For the purpose of this study, the network will be subjected to modifications according to test scenarios required to demonstrate BESS and PV integration.

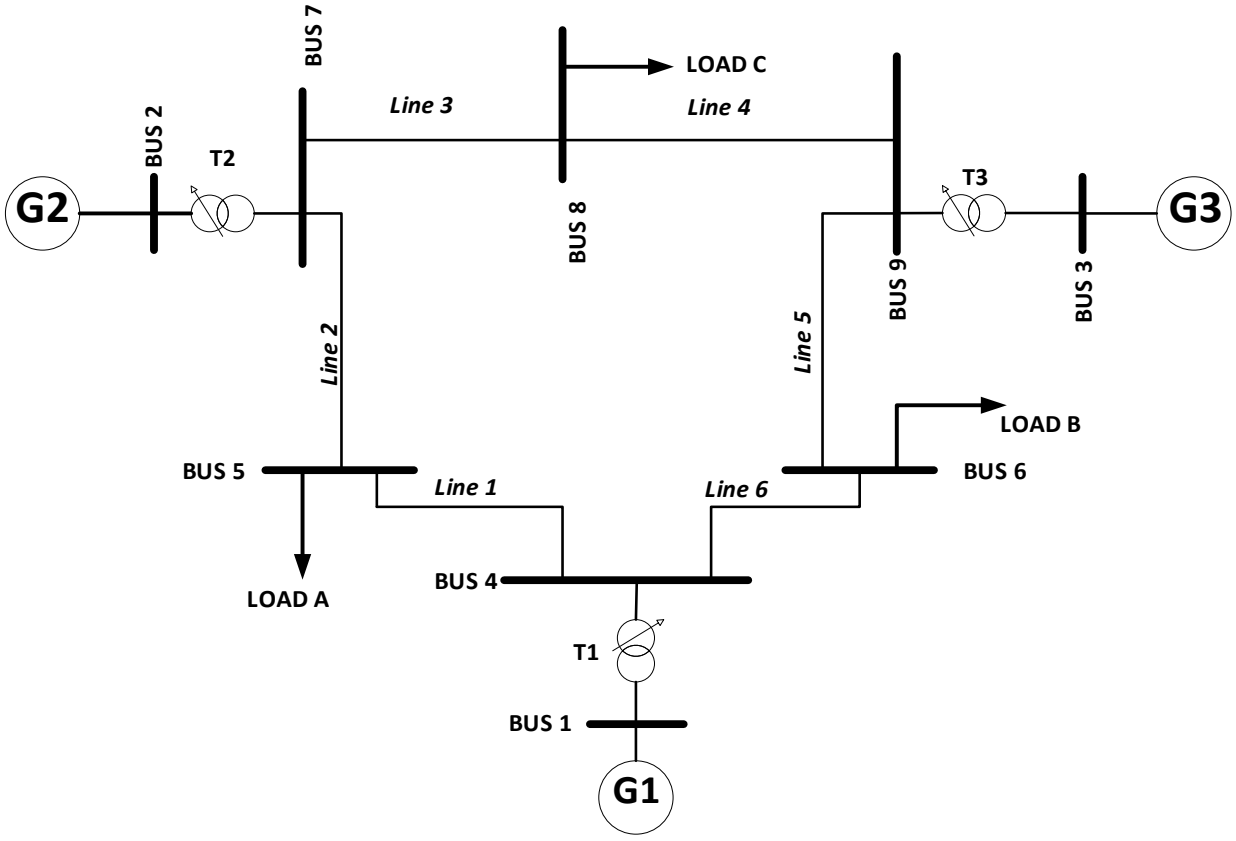

Figure 5-1: Single line diagram of the IEEE 9-Bus system

5.2.1 System model parameters

5.2.1.1 The generator model characteristics and settings

Table 5-1 shows the generator characteristics for the IEEE 9-Bus system.

Table 5-1: Generator characteristics of the IEEE 9-Bus system

Bus	V[97]	δ[151]	P[p.u.]	Q[p.u.]
1	17,1600	0,0000	0,7163	0,2791
2	18,4500	9,3507	1,6300	0,0490
3	14,1450	5,1420	0,8500	-0,1145

Each generator is represented as voltage source with its source impedance set arbitrarily as one Ohm. The generator model settings in *DigSILENT*™ - *PowerFactory*™ model are as shown in Table 5-2.

Table 5-2: Generator model settings in DigSILENT PowerFactory[152]

Parameters	Generator 1 (G1)	Generator 2 (G2)	Generator 3 (G3)
Set up	Reference Machine	To control P and V magnitude	To control P and V magnitude
Local controller mode	"constant V" at 1,04 p.u. at Bus 1	"constant Q"	"constant Q"
Generation adequacy	Based on the nominal power which is 247,5 MW at nominal voltage of 16,5 kV with power factor = 1	Stochastic: based on the nominal power which is 163,2 MW	Based on the nominal power which is 108,8 MW at nominal voltage 13,8 kV
Load flow parameters	P = 71,6 MW and Q = 27 MVAr	P = 163,2 MW and Q = 6,7 MVAr	P = 85 MW and Q = -10,9 MVAr
Plant category	Hydro power plant	Steam plant	Steam plant

5.2.1.2 The load model

For the purpose of this study, loads are considered as PQ loads, meaning they are modelled to have constant active and reactive power demand. They are assumed to be voltage-dependent under normal conditions and not voltage-dependent only during load flow calculation by disabling the load option “Consider Voltage Dependency of Loads” under the load flow calculation command in the *DigSILENT™ PowerFactory™ 2017* tool. Initial load data given in per units of P and Q are listed in table 5-3.

Table 5-3: Per unit load demand of the IEEE 9-Bus system

Load	Bus	P[MW]	Q[MVAr]
Load A	5	1,25	0,50
Load B	6	0,90	0,30
Load C	8	1,00	0,35

For the Quasi-Dynamic Simulation, the loads were modified into time characteristics loads and a 24-Hour load profile was assigned to the three loads based on typical residential, commercial and industrial load profiles.

5.2.1.3 The transmission line model

In the *DigSILENT™ PowerFactory™ 2017* model the transmission lines are modelled using the Bergeron model and table 5-4 provides the per unitised line data on a $S_b = 100$ MVA system base at nominal voltage $U_n = 230$ kV. However, since for the *PowerFactory* model input data are required in Ω/km and $\mu F/km$ respectively, line parameters are recalculated for the network model at the nominal voltage using Equations 5.1 -5.3. .

$$R[\Omega] = r[p.u.] \cdot \frac{U_n^2[kV^2]}{S_b[MVA]} \quad (5\text{-}1)$$

$$X[\Omega] = x[p.u.] \cdot \frac{U_n^2[kV^2]}{S_b[MVA]} \quad (5\text{-}2)$$

$$B[\mu S] = b[p.u.] \cdot \frac{S_b[MVA]}{U_n^2[kV^2]} \cdot 10^6 \quad (5\text{-}3)$$

Table 5-4: Transmission line characteristics of the IEEE 9-Bus system

Line				
From Bus	**To Bus**	**R[p.u./m]**	**X[p.u./m]**	**B[p.u./m]**
4	**5**	0,0100	0,0850	0,1760
4	**6**	0,0170	0,0920	0,1580
5	**7**	0,0320	0,1610	0,3060
6	**9**	0,0390	0,1738	0,3580
7	**8**	0,0085	0,0576	0,1490
8	**9**	0,0119	0,1008	0,2090

The lines are assumed to be overhead. The length of each line and the rated current have been set to respectively one km and one kA [149]

5.2.2 The PV model

DigSILENT™ - PowerFactory™ has an already developed and available PV system generic model (*ElmP*vsys) that includes some basic control and design features. Because of the absence

of rotating machinery, the PV system generic model can be assimilated to a static generator (*ElmGenstat*), easy to use for even other applications such as photovoltaic generators, fuel cells, storage devices, HVDC terminal, reactive power compensators and wind generators. It has been modelled as an array of PV panels that can be connected to the grid via a single inverter, as shown on Figure 4-4. The PV system can be seen as a DC source behind some inverters.

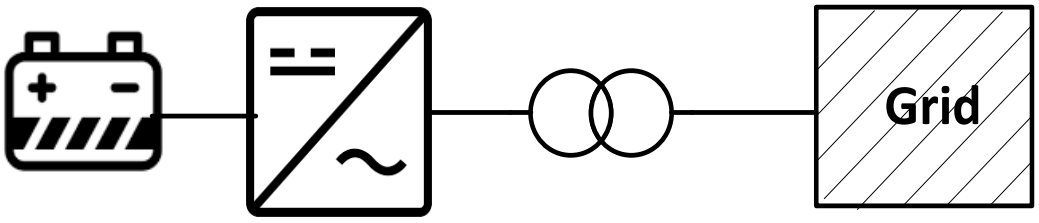

Figure 5-2: PV model representation

The PV output current I is represented by an exponential function derived from the physics of the P-N junction and dependent of several other parameters such as the short circuit current of the cell, the solar insolation, the number and the configuration of connected PV cells[34]. The expression of the output current is provided in Equation 5-4 below:

$$I_{PV} = I_{SCA}(G) - N_p x I_0 [e^{\frac{(V_A + I_{PV} R_S) q}{n N_S k T}} - 1] \qquad (5\text{-}4)$$

Where I_{PV} is the array current [A], I_{SCA} is the total short circuit current of the array, V_A is the array voltage [V], I_0 is the reverse saturation of the diode, R_S is the array series' resistance, is the solar insulation G V_0 is the open circuit voltage, $q = 1{,}6 x 10^{-19} C$ is the charge of an electron,

The PV system element is represented in figure 5-3 below. On each PV system with a single inverter, a number of panels can be entered with the option of parallel, series or series-parallel connections. Input choice of number of parallel inverters and MVA rating per single inverter can also be entered. The total MW and MVAR outputs of the PV system is determined by Equation 5-5.

$$MW_{(PV)} = MW_{(P)} x N_{(Inv)} \qquad (5\text{-}5)$$

where $MW_{(PV)}$ is the total PV active power output, $MW_{(P)}$ is the active power rating of one panel and $N_{(Inv)}$ is the number of parallel inverters. The choice of connection type, parallel or series, or a combination of both, depend on the required output power, the control strategy and the topologies of the inverter that is employed in the integrated PV systems. Voltage oriented control is the most common control strategy applied to grid-connected PV systems. Since it is capable of controlling the DC-link and regulate the current injected into the grid [153]

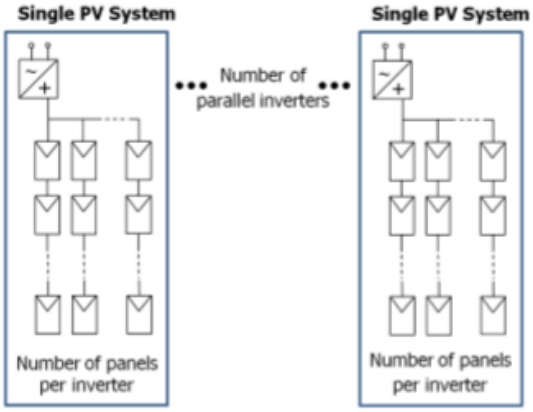

Figure 5-3: Photovoltaic system as built in PowerFactory[149]

For the purpose of this study, manual input sets method was used in all the simulation study cases. The PV systems were set as constant V machines with nominal S=250 kVA and twenty parallel inverters considered

5.2.2.1 The DC-DC converter model

The DC-DC converter model is built in the solar PV generator model *DigSILENT™ PowerFactory™ 2017*. For load flow or RMS calculations, the basic model is a boost or buck converter with no losses and controlled using pulse width modulation PWM. Various DC-DC converter models have been developed to produce a regulated output voltage from the PV array since a single cell voltage is limited to a very low value and cells cannot, due to reliability issues, be increasingly connected in series to achieve higher voltage level [154].

Solar cells have internal impedances that vary throughout the day depending on solar irradiance and the temperature of the cell. To overcome these issues, a boost converter is inserted between the PV source and the DC bus or the AC module as illustrated in Figure 5-4 below. The converter will temporarily store the input energy and release it to the output end at different voltage. The main design criterion of the maximum power point tracker (MPPT) is to

adequately and correctly feed the AC module or the battery at the required voltage and current for optimal power delivery and high efficiency operation. MPPT are high-frequency DC to DC converters aiming to maximize the available energy exerted from the solar arrays at any time of its operation.

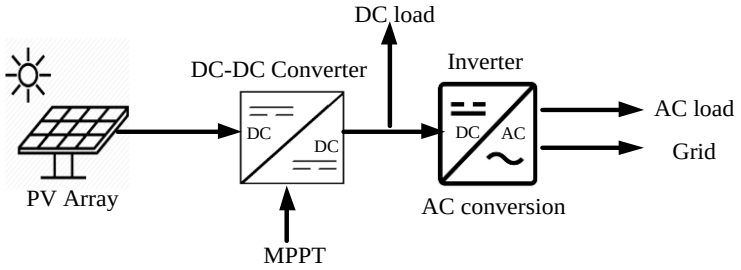

Figure 5-4: Position of the DC-DC converter and the inverter in the mini-grid

5.2.3 The Battery Energy Storage System model

The PowerFactory BESS consists of two parts. A storing part, which is a rechargeable battery and the rectifier/inverter part, which transforms the DC-voltage from the storing part to the AC-voltage needed for the grid and vice versa. It is based on a voltage source converter (VSC) combined with a pulse width modulation (PWM). Figure 5-5 shows the BESS structure.

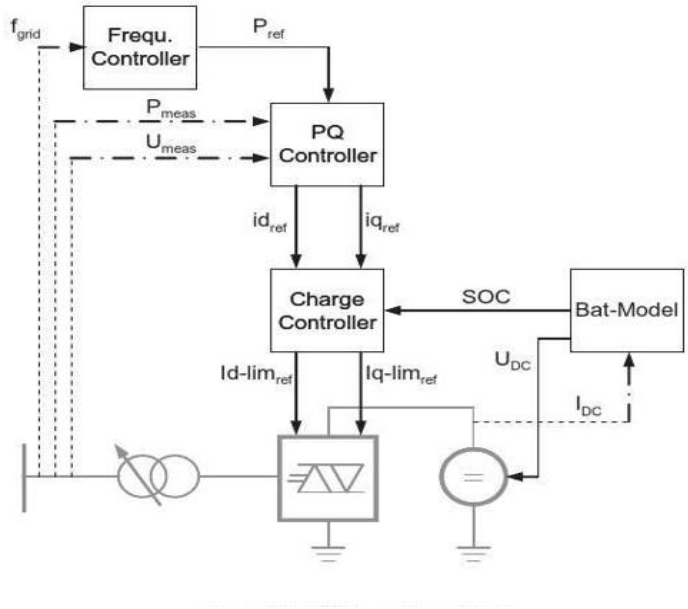

Figure 5-5: Structure of the BESS

5.2.3.1 The battery model

Peukert's Law defines the battery capacity in terms of the rate at which it is discharged. As the rate increases, the battery's available capacity decreases, as expressed in equation 5-6.

$$C_p = I^k t \tag{5-6}$$

Where Cp is the capacity according to Peukert, at a one-ampere discharge rate (Ah), I = discharge current (A) and, k = Peukert constant, dimensionless. The value of k is between 1.1 and 1. 3, for a lead-acid battery.

Energy efficiency of the battery is defined as in Equation 5-7 [155]

$$\eta_{energy} = \frac{\int_0^{t_1} I_1 E_1 dt}{\int_0^{t_2} I_2 E_2 dt} \tag{5-7}$$

Where I_1 = battery discharge current, E_1 = battery discharge terminal voltage, t_1 = battery discharge time I_2 = battery charging current, E_2 = battery charging terminal voltage and t_2 = battery charging time.

5.2.3.2 Charging and discharging of the battery

A battery model should depict the terminal voltage and the internal resistance which are a function of several intern-related variables such as the Battery State of Charge(SOC), the age and temperature of the battery [156]. The State of Charge corresponds to the current loading state of the battery. The battery is fully loaded if the SOC is one and it is zero if the battery is empty.

$$U_{DC} = U_{max} * SOC + U_{min} * (1 - SOC) - I * Z_i \tag{5-8}$$

Figures 5-6 and 5-7 shows the simple battery model and the general battery model with a parasitic branch respectively.

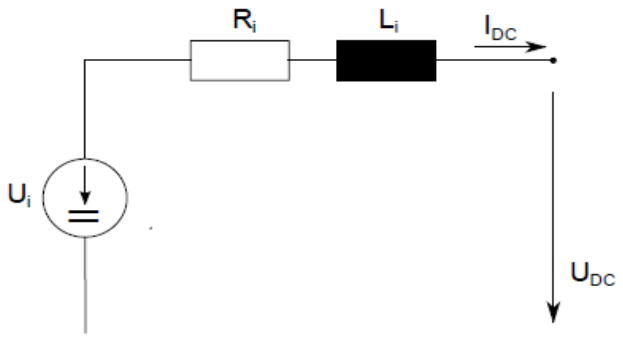

Figure 5-6: The simple battery model[156]

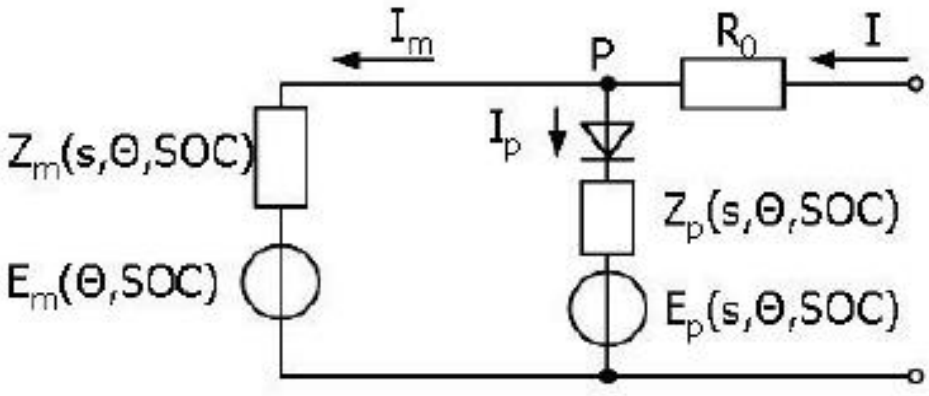

Figure 5-7: The general battery model with the parasitic branch[156]

The SOC is measured as the fraction of the charge remaining in the battery and the Depth of Charge (DOC) measured the fraction of usable charge remaining per given average discharge current, as expressed in equations 5-8, 5-9 and 5-10[157].

$$SOC = 1 - \frac{Q_e}{C(0,\theta)} \quad (5\text{-}9)$$

$$DOC = 1 - \frac{Q_e}{C(I_{avg},\theta)} \quad (5\text{-}10)$$

Where Q_e is the battery charge (A-s), C is the battery capacity (A-s), θ is the electrolyte temperature (^{0}C) and I_{avg} is the mean discharge current (A)

$$I_{avg} = \frac{I_m}{(\tau_1 S+1)} \quad (5\text{-}11)$$

Where I_M is the main branch current(A) and τ_1 is the main branch time constant (s)

Equation 5-11 expresses the estimated value of parasitic loss current during the battery charge cycle. The current is dependent on the parasitic branch voltage and the electrolyte temperature[157].

$$I_p = V_{PN} * G_{p\theta} \exp[\frac{\frac{V_{PN}}{\tau_p * S+1}}{V_{p\theta}} + A_p(1 - \frac{\theta}{\theta_f})] \quad (5\text{-}12)$$

Where I_P is the current loss in the parasitic branch (A), V_{PN} the voltage across the parasitic branch (V), $G_{p\theta}$ the constant, $V_{p\theta}$ is the constant (V), θ_f is the electrolyte freezing temperature (^OC)

Equation 5-12 is used to trace the amount of charge extracted from the battery as an integral of the main current. The initial extracted charge is essential for simulation purposes [156].

$$Q_e(t) = Q_{c_{init}} + \int_0^t -I_m(\tau)d\tau \quad (5\text{-}13)$$

5.2.3.3 The PWM converter model

The PWM converter model shown in Figure 5-8 represents a self-commutated, voltage source AC/DC converter. The VSC converts the DC-voltage from the battery to an AC-voltage through fast switching of the IGBT valves. [156]

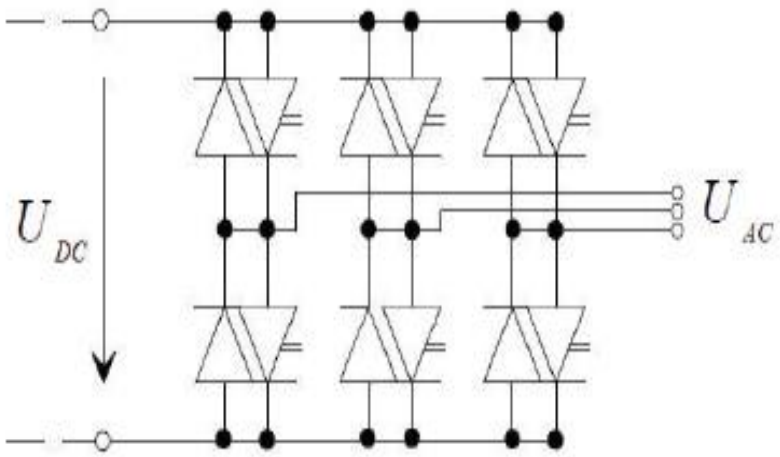

Figure 5-8: The PWM converter model

The converter's input DC voltage and the corresponding AC output voltage are described using equations 5-14 and 5-15.

$$U_{ACr} = K_O * PWM_r U_{DC} \quad (5\text{-}14)$$

$$U_{ACr} = K_O * PWM_i U_{DC} \quad (5\text{-}15)$$

Where U_{ACr} and U_{ACi} are real and imaginary AC voltage components respectively, K_O is the constant dependant on the nature of the PWM waveform, PWMr and PWMi are the real and imaginary modulation factor components, respectively, and, UDC is the DC voltage.

Summary

In this chapter, components for system modelling are presented and explained. This includes models of network elements and computational techniques as implemented in *DigSILENT™ - PowerFactory™ 2019*. A detailed study methodology is presented in Chapter 6.

CHAPTER 6: RESEARCH CASE STUDIES AND METHODOLOGY

Introduction

This chapter presents the case studies used in this research work as well as the corresponding simulations conducted using the network models presented in Chapter 5. The methodology and justification thereof are discussed in this chapter through and with emphasis on evaluating BESS impact on the grid.

6.1 Methodology

The simulations for the studies were conducted using the following methodology:

- Build and set the case studies and scenario network in *DigSILENT™ - PowerFactory™*.
- Run the base case through scenario 1 and scenario 2 described below in sections 6.2.1.1 and 6.2.1.2 respectively for initial and extreme conditions.
- Execute load flow, extract and record results for static and transient setup respectively.
- Integrate PV of specific size at specific locations and perform similar simulations as above and record results for further discussions.
- Integrate BESS of various sizes at specific locations and conduct Quasi-Dynamic simulations for the evaluation of the impact of BESS into the grid.
- Assess the economic impact through cost estimates
- Perform comparative analysis and draw conclusions.

Simulations conducted are justified by the following:

1. For stability analysis and electromagnetic transients for stability studies, RMS and EMT simulations are used in time-domain mode.
2. Static simulation mode aims to monitor critical parameters such as voltage profiles at bus terminals.
3. Dynamic transient simulations are executed for the assessment of transient stability, specifically the monitoring of generators' behaviours and transmission lines buses under disturbances.

4. P-V curves analysis is performed for the assessment of system loadability, active power margin or maximum loading as well as for the determination of system's point of collapse.
5. Quasi-Dynamic mode allows to perform several load flow calculations over a period of time, specifically when evaluating BESS contribution to voltage regulation and/or power system stability with regards to offsetting intermittency.

6.2 Case studies

6.2.1 Case 1 (Base or reference case): Network operation without RES and without BESS integration

6.2.1.1 Scenario 1: Initial conditions

This scenario is intended to provide the reference for the analysis and comparison of further cases. For the purposes of simulation, the model network IEEE 9-Bus as described in Figure 5-1 is built in *DigSILENT™ - PowerFactory™*. Firstly, the simulation is run in static steady state mode to investigate voltage profile, system loadability and system losses with no integration of solar system, no BESS or any other reactive power device for voltage support. Secondly, the transient behaviour is assessed with regards to system stability by monitoring: (1) the rotor angles and (2) the terminal voltages at some selected transmission lines buses. In this base case, the network analysis is performed with initial normal loading and the P-V curves are plotted for loadability assessment and determination load margin. The investigation of the network transient behaviour under normal conditions for further comparison and discussion, is achieved by applying a 3-phase fault at line 6-9. All the results and network behaviours for this base case scenario are recorded for comparison analysis and discussions with further cases.

6.2.1.2 Scenario 2: Extreme conditions

With no PV and BESS integrated to the grid, the system is stressed by a gradual increase of the total loading to create worst case conditions while performing load flow calculations. In *DigSILENT™*, a scaling factor of fifteen percent (15 %) increment is applied to the three loads and voltage magnitudes at all buses are determined to identify using sensitivity analysis, the weakest buses of the system. The weakest buses are then used as critical buses for the integration of RE sources and BESS, with the aim of comparing their respective impacts on the network with regard to system stability and power losses. Similar to scenario one the investigations are performed in steady state and dynamic transient state during fault and after

the fault incident has been removed. P-V curves are plotted for stability investigation to the determination of real power margins and loadability. Network losses and minimum mean voltage are obtained and all the results for this case are compared to scenario 1 and recorded for further discussions.

6.2.2 **Case 2: Solar PV integration without BESS**

In this case, under the same initial settings as in Scenario 2 of the base case above, the PV system is integrated at Bus 5. The aim is to investigate the extent to which voltage compensation and support can be achieved by injecting P at the distribution end or at load sides. The PV system is set to bring about the total power demand caused by the increase in load demand. As in the previous case, the voltage profile, the system stability and the power losses are monitored. Loadability of the system is also assessed using P-V curve analysis. The results of this case are analysed, discussed and compared to the base case.

In order to evaluate and assess the effects of the BESS, the best location of the PV system is determined through both static and dynamic transient simulations. The PV system is placed at one specific bus at the time and using voltage profile, loadability and stability condition as criteria the best PCC location is manually decided upon.

6.2.3 **Case 3: Solar PV integration with BESS**

This case aims to investigate the supportive or adverse impact of the integration of BESS on voltage regulation and power system stability conditions with reference to grid codes violations and mitigation solutions thereof by offsetting the intermittency of the solar PV energy. The voltage profile and the system stability is monitored. System loadability is also assessed using P-V curve analysis. The results of this case are analysed, discussed and compared respectively to Case 1 and Case 2 above.

6.2.3.1 Effects of BESS sizing and siting on system loadability and stability

6.2.3.1.1 Scenario 1: Concentrated integration

The objective of this case is to investigate the effect of BESS location on voltage and system stability and loadability. A single concentrated unit is used in this first scenario, where the same BESS capacity is considered, with the change of the PCC location while keeping the fault at the same fixed location as previously. The PV system and BESS are moved from the critical Bus 5 to all the other buses respectively and load flows are run after each position to assess the

voltage profile, system loadability and critical voltage collapse point through RMS/EMT simulations and P-V curves analysis respectively. Furthermore, in order to assess stability conditions, the results for the transient dynamic behaviour are recorded for each location, analysed with the aim to experimentally determine the optimal location of the BESS.

6.2.3.1.2 Scenario 2: Dispersed BESS integration

In this second scenario, the static and dynamic stability are assessed when the BESS capacity is disseminated at the best identified locations from scenario 1 above and the results are compared to the best of the results of scenario 1 of this current case.

6.2.4 Case 4: Determining system losses using Quasi-Dynamic Simulation mode

The aim of this case is to assess system performance through total losses determination over 24 hours without and with the integration of BESS. For this case, the IEEE 9-Bus test system is modified to insert time characteristics loads, with a 24-Hour load profile assigned to the three loads based respectively on typical residential, commercial and industrial load profiles. The resulting 24-hour system load curve is shown in Figure 6-1. Assessments similar to the ones performed in previous cases are performed and in addition, Quasi-Simulation is performed to achieve the aim of the case as stated above.

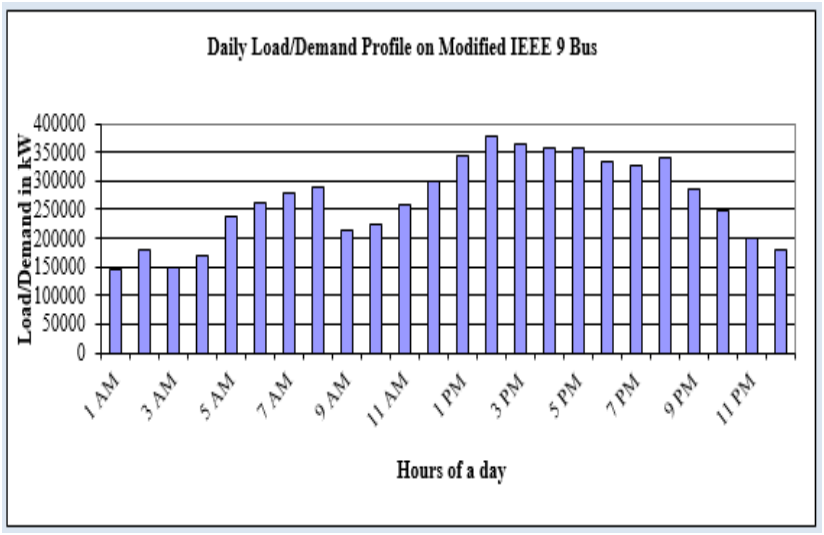

Figure 6-1: 24-hour system load generated by the DigSILENT™ - PowerFactory™ time characteristics functionality

Summary

In this chapter, four study cases and subsequent relevant scenarios are presented and explained. The aims and the purposes were provided to support and to substantiate each study case, together with the related simulation methodology. The results and justifications of the choice of simulation methodologies are discussed in Chapter 7.

CHAPTER 7: SIMULATION RESULTS AND DISCUSSIONS

Introduction

This chapter presents the simulation results for the cases presented in Chapter 6. For the first four cases, both static and dynamic transient RMS simulations are run under various conditions and the results are discussed with emphasis on system loadability, stability and network power losses. The last case discusses the financial evaluation of the BESS

7.1 Case 1: Network operation without RES and BESS

7.1.1 Scenario 1: Initial conditions

7.1.1.1 Steady-state analysis for voltage profile assessment

Firstly, the simulation is run in static steady state mode to investigate voltage profile, system loadability. The load flow is successfully run on the IEEE 9-Bus system. In *DigSILENT™ - PowerFactory™* the classical AC load flow is selected in positive sequence mode with balanced and symmetrical three-phase system to extract the results of active power and reactive power flow, current in lines and voltages at all bus bars of both test systems. With generator 1 set as the reference machine the RMS/EMT simulation is executed ensuring the network parameters are set at initial load conditions. The voltage magnitudes at all buses are measured and the corresponding graphs are displayed in Figure 7-1. From the displayed results, it can be noted that the minimum voltage of 0,979 p.u is measured at Bus 5 and it can be verified and confirmed that the maximum voltage of 1,040 p.u is measured at the slack bus (Bus 1).

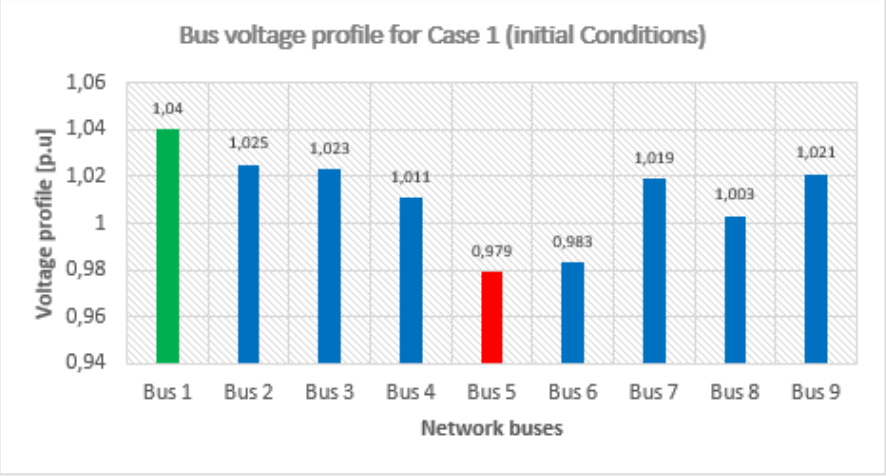

Figure 7-1: Voltage profile at all buses for Case 1 (initial conditions)

It can be noted that the voltage at Bus 5 is still above the standard required voltage of 0,95 p.u.

7.1.1.2 System loadability assessment and system losses

To assess system loadability, P-V curves analysis was performed with the aim of determining the maximum loadability point for different cases, the critical voltage collapse point and the calculation of the Megawatt distance to the critical point. Figure 7-2 presents the P-V curves extracted from *DigSILENT*™ - *PowerFactory*™ for this case and revealing a loadability of 829,93 MW at the critical voltage of 0,623 p.u. In other words, the system will collapse when the power demand increases to 829,93 MW and that will occur when the voltage reaches 0,623 p.u. This validates the convergence of the system voltage equations as presented in earlier sections.

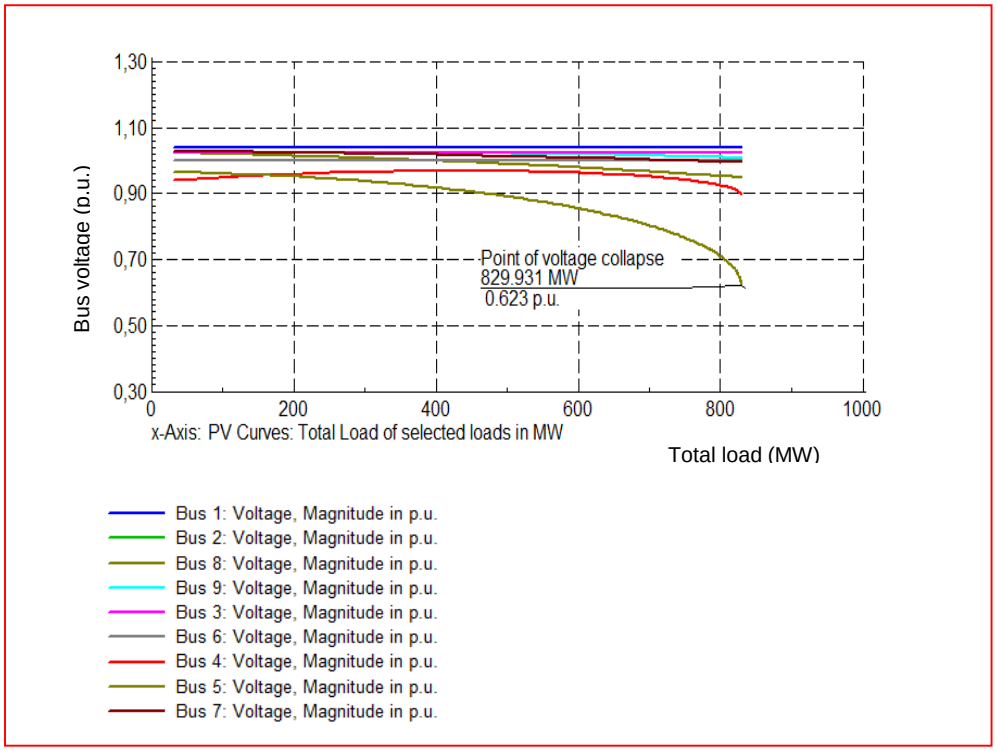

Figure 7-2: P-V curves for the Base Case Scenario 1 (initial conditions) of the 9-Bus network

With regards to losses, the total system summary is presented in Figure 7-4 below. The load losses are recorded at 46,4 MW for a total connected load of 206 MW.

| Total System Summary | Study Case: Nine-Bus N LOJI MEng DUT | Annex: / 1 |

No. of Substations	0	No. of Busbars	9	No. of Terminals	0	No. of Lines	6				
No. of 2-w Trfs.	3	No. of 3-w Trfs.	0	No. of syn. Machines	3	No. of asyn.Machines	0				
No. of Loads	3	No. of Shunts	0	No. of SVS	0						
Generation	=	216,74	MW	100,21	Mvar	238,78	MVA				
External Infeed	=	0,00	MW	0,00	Mvar	0,00	MVA				
Load P(U)	=	206,63	MW	172,50	Mvar	269,17	MVA				
Load P(Un)	=	206,63	MW	172,50	Mvar	269,17	MVA				
Load P(Un-U)	=	0,00	MW	0,00	Mvar						
Motor Load	=	0,00	MW	0,00	Mvar	0,00	MVA				
Grid Losses	=	10,11	MW	-72,29	Mvar						
Line Charging	=			-144,69	Mvar						
Compensation ind.	=			0,00	Mvar						
Compensation cap.	=			0,00	Mvar						
Installed Capacity	=	482,38	MW								
Spinning Reserve	=	265,64	MW								
Total Power Factor:											
Generation	=	0,91	[-]								
Load/Motor	=	0,77 / 0,00	[-]								

Figure 7-3: Total system summary for initial conditions (Case 1-Scenario 1)

7.1.1.3 Dynamic transient analysis

The analysis was performed using a fault event applied to the 9-Bus grid at mid-distance of Line 5 linking Bus 6 to Bus 9. After the determination of the critical fault clearing time (CFCT), which indicates the maximum fault time duration that, if exceeded the system will not recover pre-fault operating conditions, the fault event is set for a duration of 0,1 second with simulations to run for 11,99 seconds. The transient analysis is performed by monitoring the rotor angle of generators G2 and G3 with respect to the slack generator G1 as well as the voltage profile of transmission lines buses and load buses.

The results from Figure 7-4 indicate a considerable jump in the relative rotor angle deviation of both G2 and G3 with respect to the reference generator G1 at the application of the fault. After fault clearance, it is observed a substantially moderated damping oscillation which settles at 21,61 degrees at 11,45 seconds for G3 from the initial 16,12 degrees, prior the application of the fault. From pre-fault conditions, a new steady state operating point is reached showing that the system regained indeed stability.

Figure 7-5 shows the voltage profiles of the transmission lines and loads buses. It can be seen that voltages at all the buses dip down for the duration of the fault with the fault bus reaching a minimum of 0,25 p.u. After the fault has been cleared, the voltages increase and stabilise over time showing that the system has regained stability.

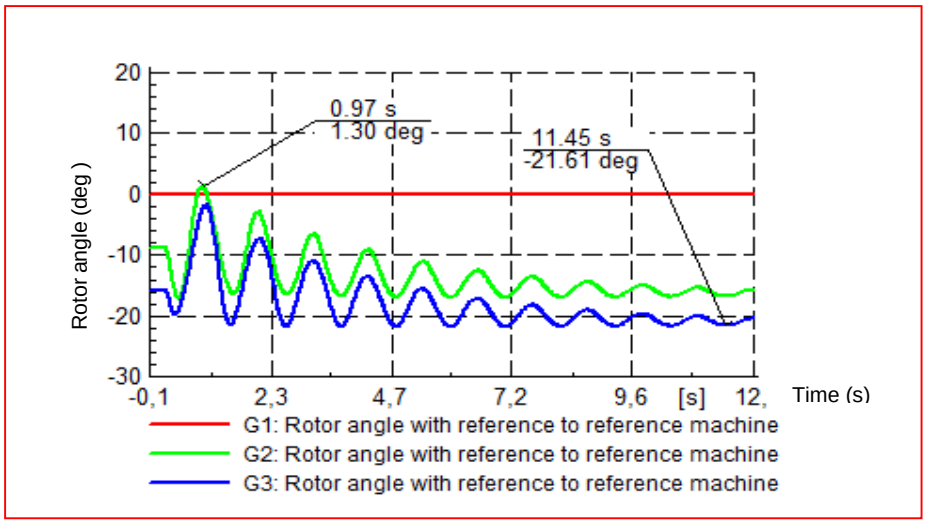

Figure 7-4: Rotor angle with respect to reference machine

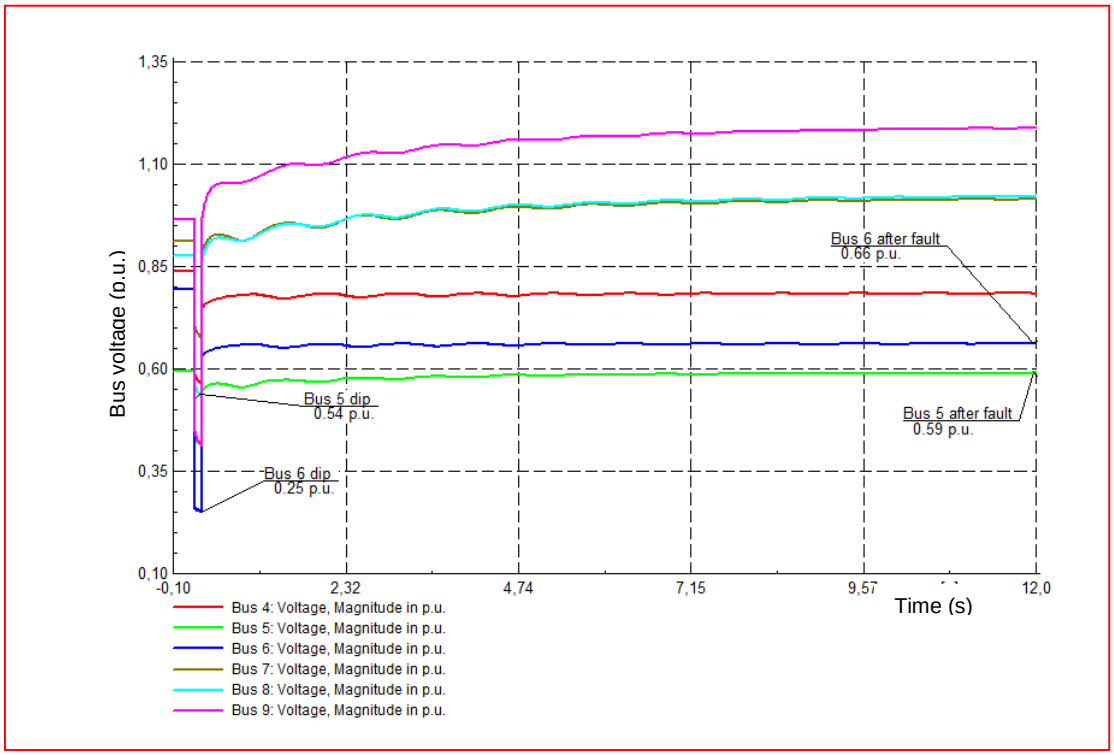

Figure 7-5: Voltage profile at transmission lines and load buses for Scenario 1 of Case 1 (initial conditions)

7.1.2 Scenario 2: Extreme conditions (worst case scenario)

7.1.2.1 Steady-state analysis for voltage profile assessment

Without any integration of any PV system or BESS, the network system is stressed by gradually increasing the total loading to create conditions that bring the test system close to stability limit. Figure 7-6 shows the results of the RMS/EMT simulations for the worst case scenario and it can be seen that Bus 5 is the weakest Bus recording the lowest voltage of 0,94 p.u. which is

below the prescribed 0,95 p.u. standard voltage requirement. This condition was reached at scaling factor 1,5 or 50 % load increase both in active and reactive power of initial loading.

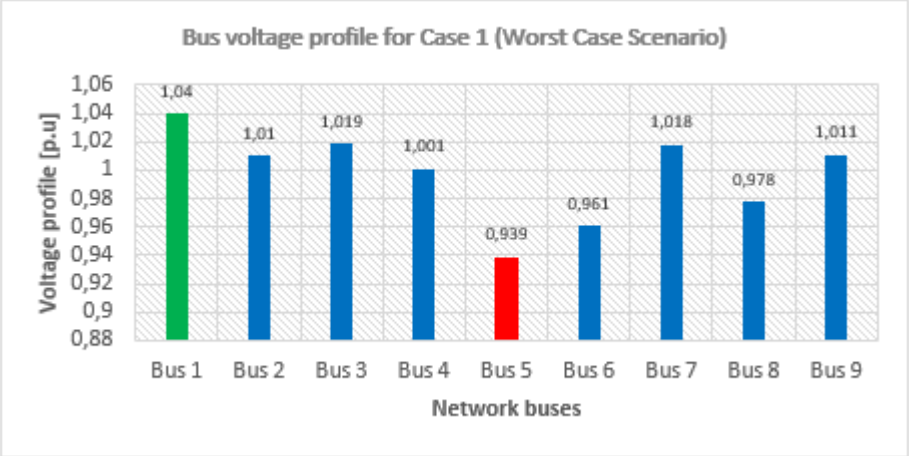

Figure 7-6: Voltage profile for worst conditions (Case 1-Scenario 2)

Figure 7-7 below presents a voltage profiles comparison between the two scenarios of Case 1 with Bus 5 being the Bus to be monitored going forward.

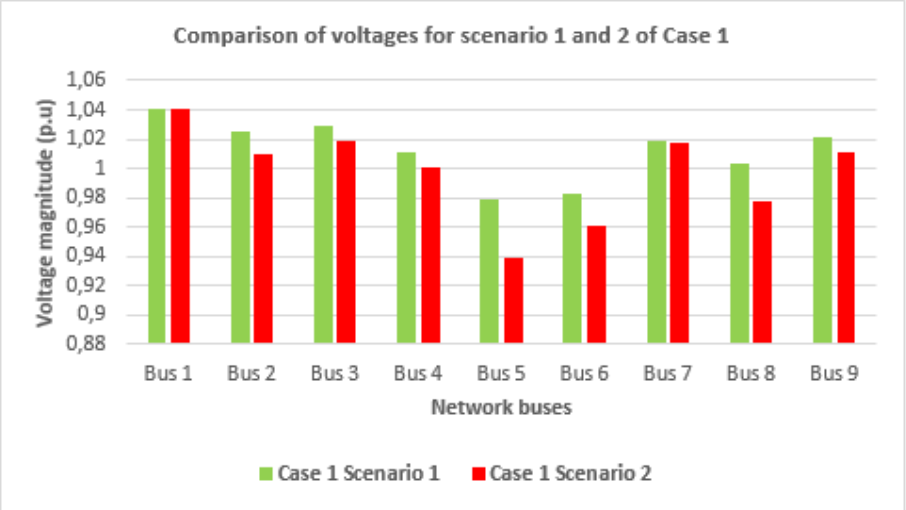

Figure 7-7: Comparison of voltage profiles for scenarios 1 and 2 of Case 1

7.1.2.2 System loadability assessment and system losses

The system loadability assessment was performed using P-V curves and the results are presented in Figure 7-8 below. indicate a reduction in the power system loadability from 829,93 MW to 714 MW and a critical voltage point increasing to 0.635 p.u. as shown in Figure7-7.

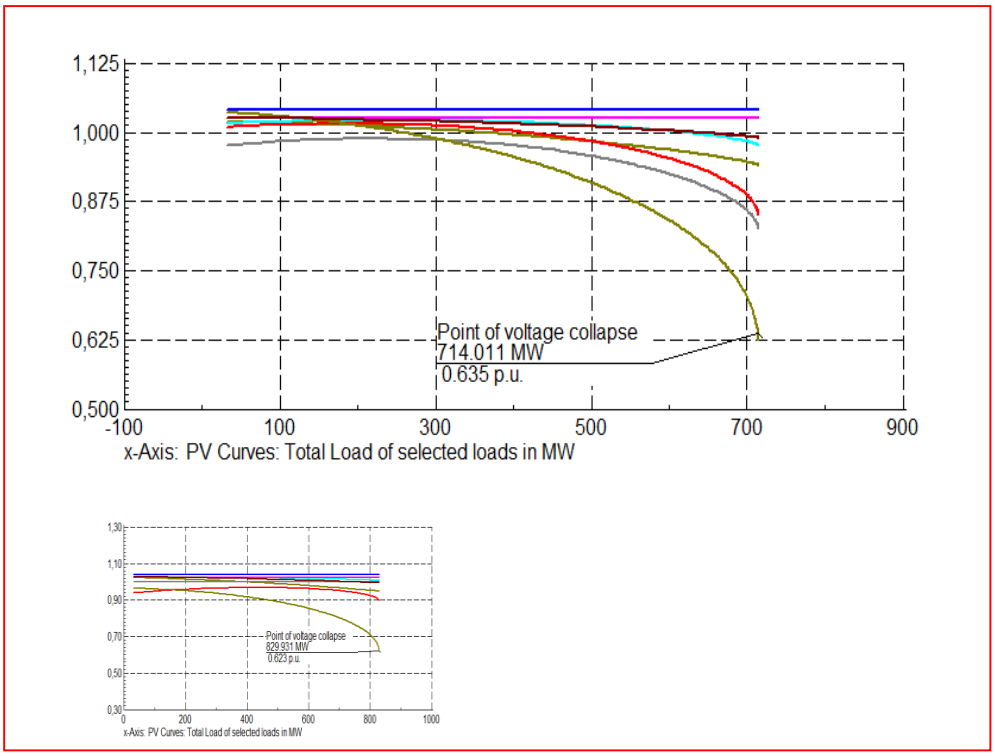

Figure 7-8: P-V curves for the base case under extreme conditions

The system power losses increase from 46,4 MW to 59,9 MW. with the 50 % load increase, implemented to create worst conditions scenario.

7.1.2.3 Dynamic transient analysis

A similar fault event as in section 7.1.1.3 is triggered and applied at the same location and for the same duration to investigate the transient behaviour under the setting as described in section 6.2.1.2 above. The relative rotor angle deviation of G2 and G3 with respect to the slack generator G1, is monitored and the results are presented in Figure 7-9. From the displayed results, it can be seen that the rotor angles of G2 and G3 oscillate at quite high frequency for the duration of the simulation between respectively -172 degrees and +177 degrees and the oscillations have no subsequent damping effect as in scenario 1, indicating the loss of stability. The instability condition of the network under study for the worst condition is further confirmed from the results in Figure 7-10, by the intense fluctuation of the transmission and load buses' voltages after the fault has been removed.

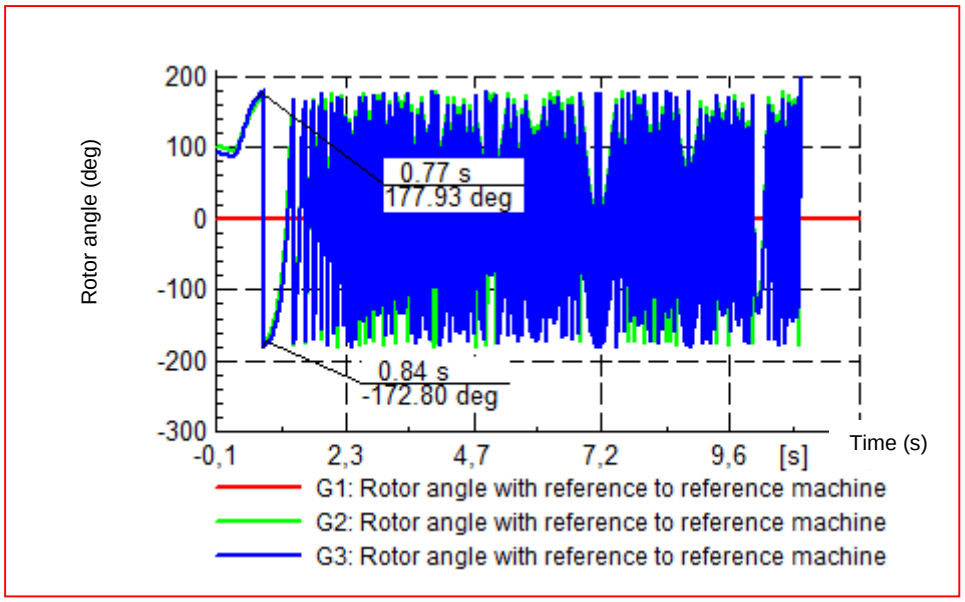

Figure 7-9: G2 and G3 relative rotor angles with respect to the slack generator G1

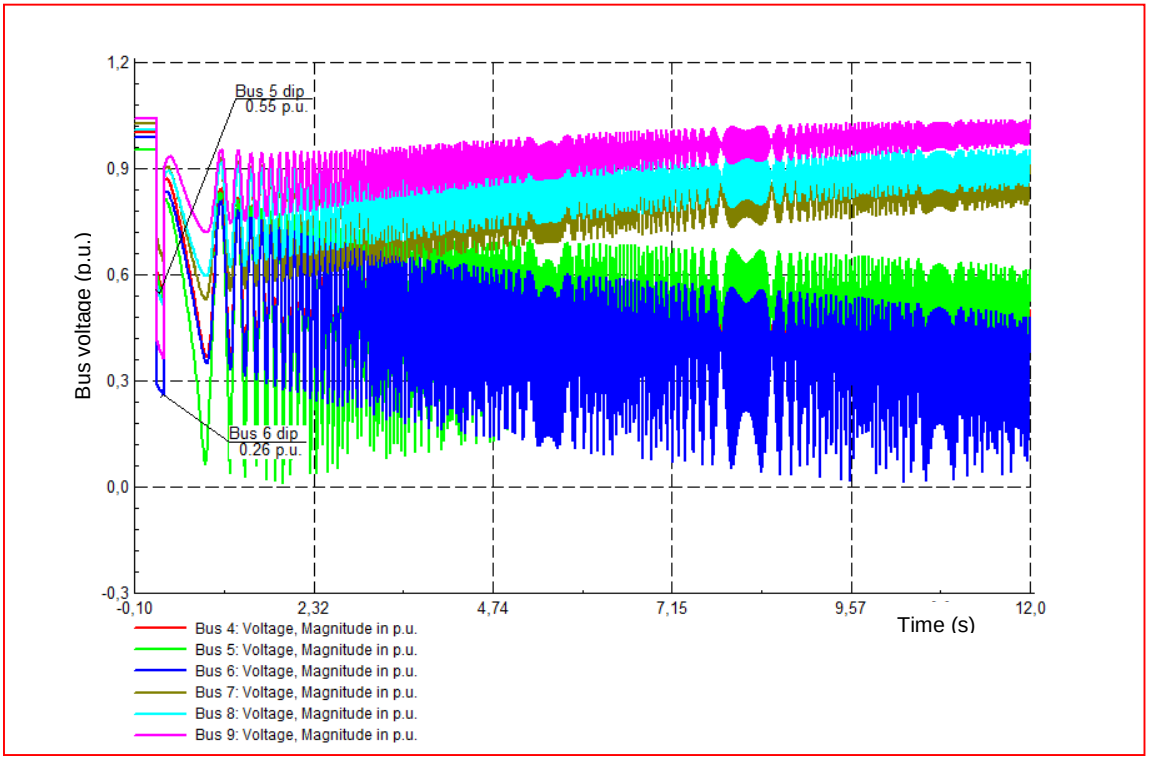

Figure 7-10: Voltage profile behaviour for transmission line and load buses

7.2 Case 2: Evaluation of the impact of PV integration without BESS

In this case, under the same settings as in scenario 2 of Base Case a 40 MW solar PV system is integrated at Bus 5 which was found in scenario 2 of the base case to be the weakest bus. The active power contribution of the PV system is determined by the need to compensate for the total P demand that was effected by the 50 % load increase as noted in section 7.1.2.1. Simulations are run both in steady-state and in dynamic modes with the aim of comparing the

results to those of Case 1 and it is expected that the worst condition results in scenario 2 will revert to near those of Scenario 1.

7.2.1 Impact of PV integration in steady-state analysis

7.2.1.1 Voltage profile assessment

The aim is to evaluate the impact of P injection from an inertia-less DG source at the distribution side on the voltage profile. The results of this case are compared to those of the Base case and recorded for the next case which will deal with the combination PV System – BESS.

Figures 7-11 and 7-12 show the results of the RMS/EMT simulation in static mode respectively for the voltage profile and voltage deviations

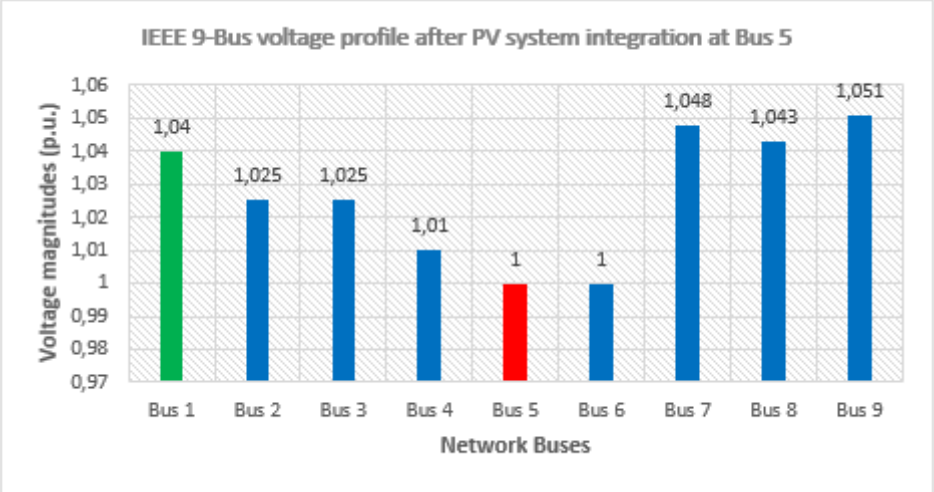

Figure 7-11: Voltage profile after Solar PV integration at bus 5

The results reveal that after the integration of the Solar PV system at critical Bus 5, a substantial voltage profile improvement is noticed at all the buses especially at the PCC bus where the voltage changes from 0,939 p.u to 1,000 p.u. equivalent to 6,49 %. It can also be observed that the voltage at Bus 9 increases by 3,9 %, from 1,011 p.u. to 1,051 p.u although the new voltage magnitude falls beyond 5 % of the nominal voltage, in violation of the standard requirement. This increase prompts the concern about overvoltage that may occur due to active power injection at the distribution side.

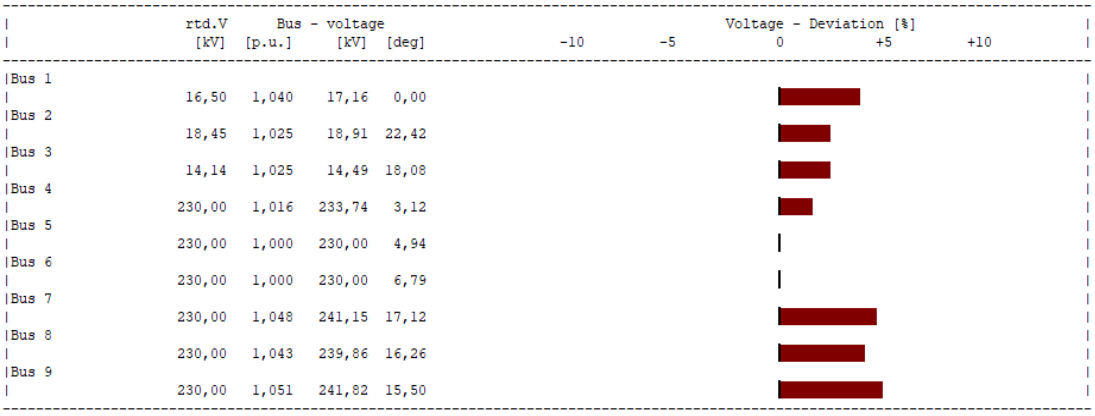

	rtd.V [kV]	Bus - voltage [p.u.]	[kV]	[deg]	Voltage - Deviation [%] −10	−5	0	+5	+10
Bus 1	16,50	1,040	17,16	0,00					
Bus 2	18,45	1,025	18,91	22,42					
Bus 3	14,14	1,025	14,49	18,08					
Bus 4	230,00	1,016	233,74	3,12					
Bus 5	230,00	1,000	230,00	4,94					
Bus 6	230,00	1,000	230,00	6,79					
Bus 7	230,00	1,048	241,15	17,12					
Bus 8	230,00	1,043	239,86	16,26					
Bus 9	230,00	1,051	241,82	15,50					

Figure 7-12: Bus voltage deviations for case 2: Solar PV integrated at bus 5

Figure 7-13 shows the comparison in voltage magnitude of the base case scenarios 1and 2 and with Solar PV integrated at Bus 5.

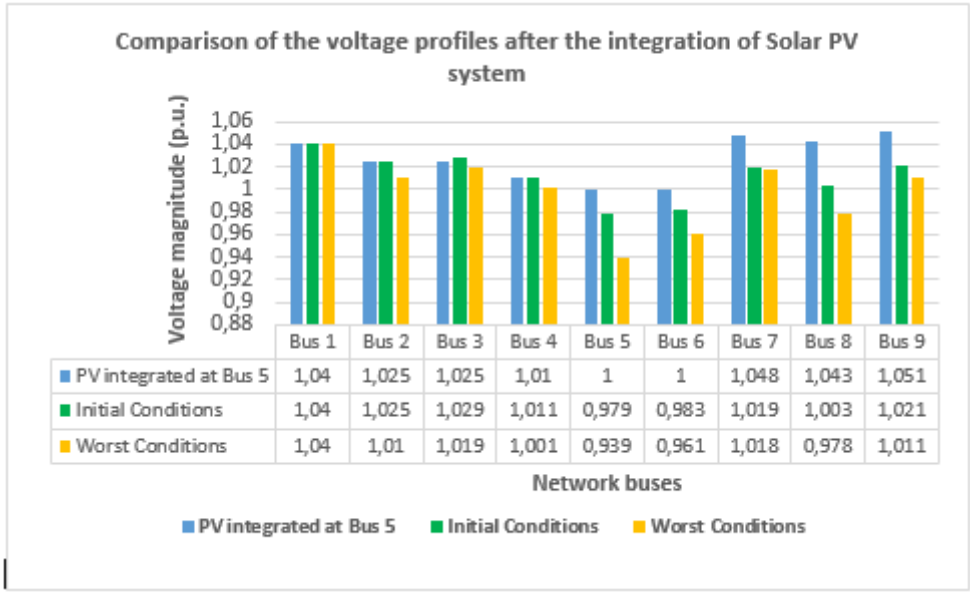

Figure 7-13: Voltage profile enhancement after integration of Solar PV system at critical Bus 5

7.2.1.2 System stability assessment using P-V curves analysis and system losses

Figure 7-14 presents the results of the system loadability assessment using P-V curve analysis in static approach. In comparison to the initial and worst conditions cases there is a 58,54 % increase in system loadability from the integration of the Solar PV system. The network's system loadability improves indeed from 714 MW in the worst condition scenario of Case 1 to 1132 MW with the integration of the Solar PV system impacting subsequently on the system's critical voltage collapse point.

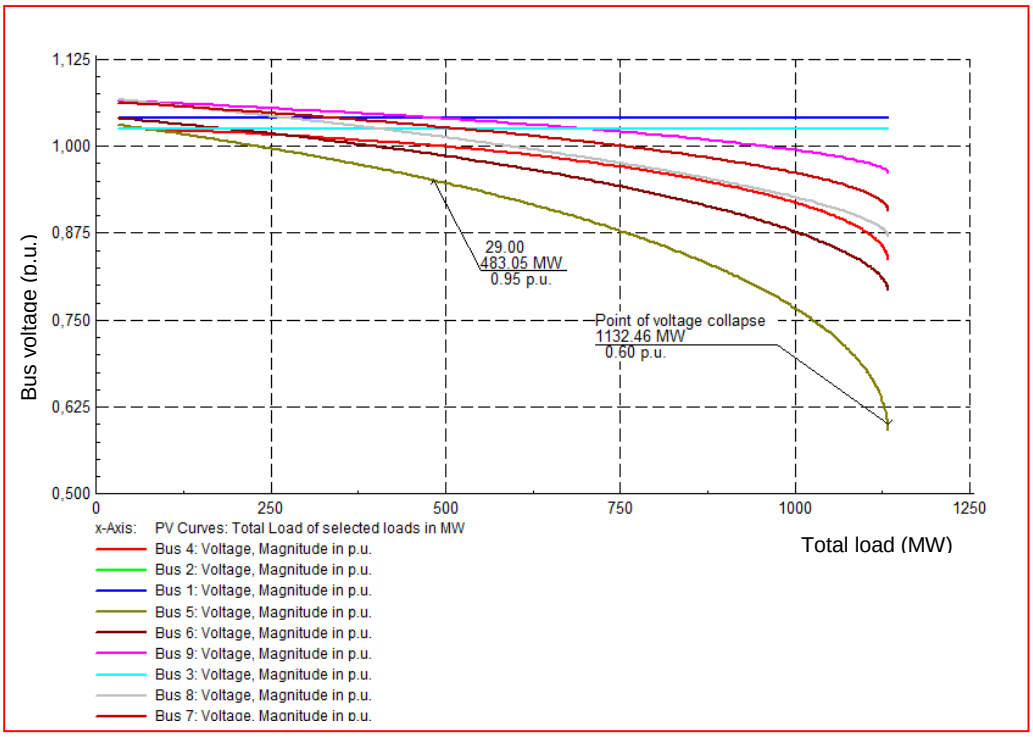

Figure 7-14: Impact of the integration of Solar PV system without BESS on system loadability

The total system losses reduced from 59,9 MW in the worst conditions scenario to 56,3 MW with the integration of the Solar PV system. This value however remains higher than the 46,3 MW losses recorded under initial conditions in scenario 1 of Case 1.

7.2.2 **Impact of PV integration in dynamic transient analysis**

Two scenarios were considered in order to prepare and perform the study of the impact of BESS incorporation on large scale integration at the best PCC Bus. Firstly, the determination of the optimal location of the Solar PV system and secondly, the determination of the optimal size the PV solar system. The results of the dynamic transient simulations are recorded to comparatively analyse them with those of Case 3 that evaluate the impact of the BESS.

7.2.2.1 Best PCC

The best PCC Bus was determined experimentally as the network in consideration, the IEEE-9-Bus System has a fairly minimal quantity of power systems components. Bus 4 was found to be the best PCC based on firstly, the requirement to keep the voltage level within standard margins, secondly, the need to improve system loadability while maintaining minimum losses and lastly, the dynamic transient stability response under emergency/fault condition. A PV system of the same size as in section 7.2.1.1 is placed alternately at all non-slack buses and simulations are run to assess the three criteria described above. The voltage at the weakest bus,

the percentage voltage improvement from the worst case as well as the point of voltage collapse and total losses are evaluated for each position of the Solar PV at various buses. Table 7-1 presents the results obtained and it can be seen that Bus 4, over buses 2 and 8, is the best PCC or optimal location under the assumptions made above, as it has the best voltage profile possible, acceptable losses and it regaining stability after fault disturbance during emergency/fault condition. Bus 4 indeed presented better improved percentage voltage from the worst case compared to Buses 2 and 8 respectively, and, a better voltage profile, 0,953 p.u. compared to Bus 2 and Bus 8 which have respectively 0,952 and 0,951.

To complete the determination of the best PCC process, transient stability was assessed for various locations using a three-phase fault that is applied at $t = 200ms$ for a duration of $100ms$ and then removed to monitor generators G2 and G3 rotor angles with respect to generator G1. Similar to the previous cases, the fault location remains unchanged at mid-distance of line 5 and for a total simulation time of 11,99 seconds. Figures 7-15 and 7-16 illustrate respectively, the unstable (Solar PV at buses 5,7,6,3 and 9) and stable (Solar PV at buses 2, 4 and 8) dynamic behaviour during the best PCC investigation. With the Solar PV system at buses 3, 5, 6, 7 and 9 it is observed as evidenced from the results in Figure 7-15 that the rotor angles of G2 and G3 with respect to G1 show stability just from the time the fault is removed to between 3,65 seconds to 6 seconds before falling into high oscillations, suggesting that the system will hardly regain stability. With the Solar PV at buses 2, 4 and 8 however, the oscillations of the rotor angles of G2 and G3 with respect to the rotor angle of the slack generator G1 are damped and progressively smoothen before stabilising at minus 10,75 degrees and minus 15,62 degrees from the reference generator respectively, evidencing that the system will regain stability after the simulation period.

Table 7-1: Summarised results of the PV system's optimal location on the 9-Bus transmission network

PCC	Solar PV @ Bus 5	Solar PV @ Bus 7	Solar PV @ Bus 6	Solar PV @ Bus 3	Solar PV @ Bus 9	Solar PV @ Bus 4	Solar PV @ Bus 2	Solar PV @ Bus 8
Voltage at the weakest bus [p.u.]	0,974	0,964	0,955	0,954	0,954	0,953	0,952	0,951
Voltage improvement from the worst [%]	4,1	2,7	2	1,9	1,9	1,8	1,7	1,6
Point of voltage collapse [MW]	1132,46	1138,22	1136,71	1134,49	1134,46	1134,33	1134,98	1132,44
Total MW losses	56,3	56,4	57,1	58.1	58,2	55,9	56,9	56,9
Dynamic Stability condition	**Unstable**	**Unstable**	**Unstable**	**Unstable**	**Unstable**	**Stable**	**Stable**	**Stable**

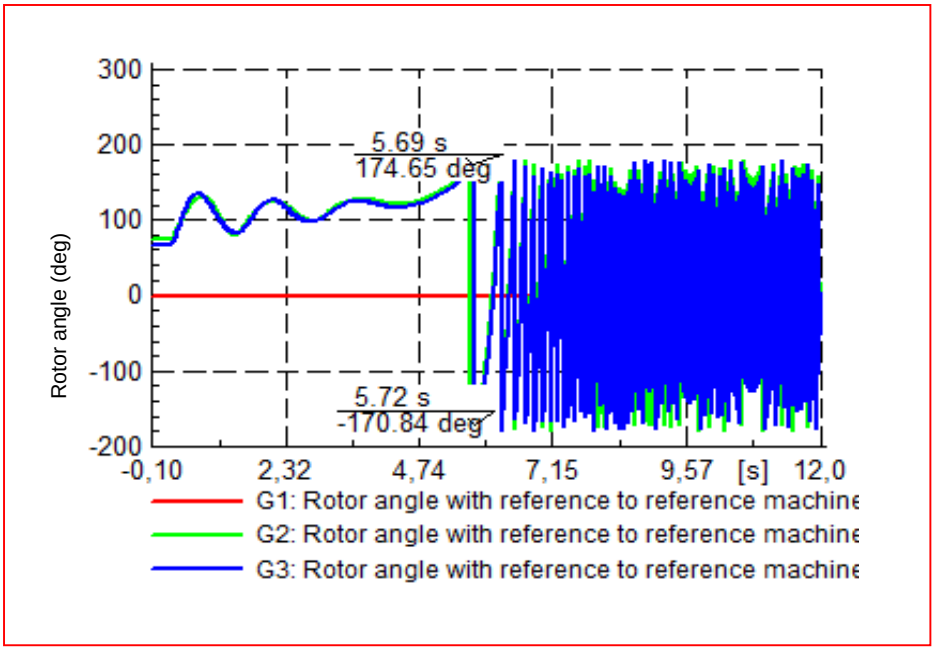

Figure 7-15: Unstable dynamic transient condition using rotor angle stability with the Solar PV system connected to bus3 (similar to Solar PV connected at buses 5, 6, 7 and 9)

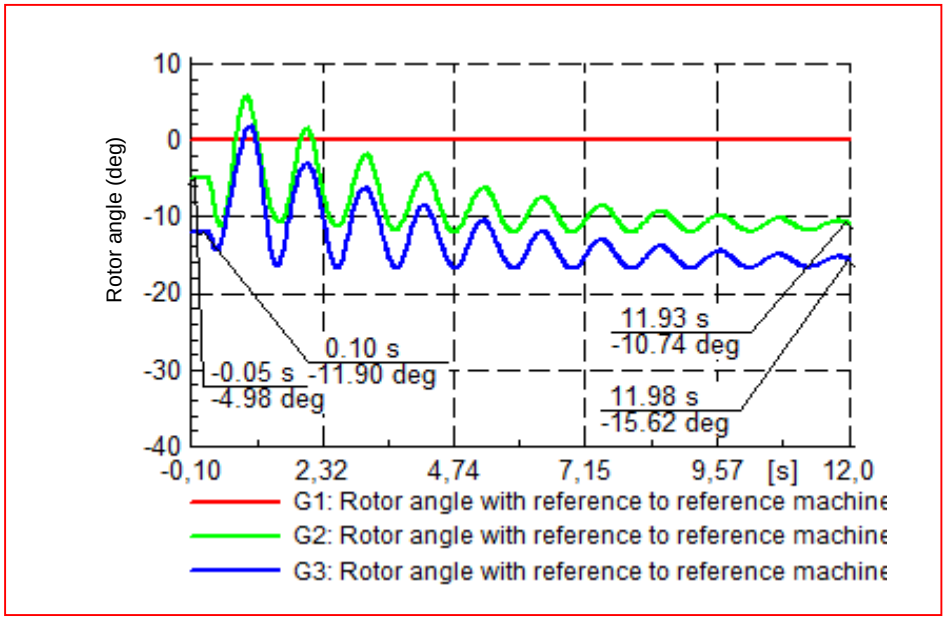

Figure 7-16: **Stable dynamic transient condition using rotor angle stability with the Solar PV system connected to bus 4 (similar to Solar PV at buses 2 and 8).**

7.2.2.2 Optimal size

The optimal PV sizing investigation was achieved by increasing the PV penetration level at 10 % increment at the best PCC, Bus 4 as identified in section 7.2.2.1. First, in the absence of a fault to determine static stability conditions by monitoring the voltage magnitude at the best PCC, the voltage magnitude at the critical bus, and the loadability and, secondly, the stability condition assessment in the presence of fault by monitoring the rotor angle stability.

The results of the investigation are consolidated in Table 7-2 and Figure 7-17 show the voltage magnitude trend as impacted by the increase capacity of the Solar PV system on the system.

Table 7-2: Impact of solar PV increasing capacity on bus voltages, loading margins and dynamic stability

PV penetration level	0 %	10 %	20 %	30 %	40 %	50 %	100 %	110 %	140 %
Bus 5 voltage magnitude	0,963	0,961	0,959	0,958	0,950	0,941	0,938	0,928	0,921
Best PCC (Bus 4) voltage	0,997	0,996	0,995	0,994	0,992	0,990	0,979	0,960	0,954
Loading margin I [MW]	591,02	590,68	588,11	587,13	586,65	586,01	585,64	584,99	577,09
Total losses	13,12	12,52	11,81	11,13	10,92	10,49	10,12	10,01	9,65
Dynamic transient stability condition	Stable					Unstable			NPFC (*)

(*): NPFC: No Power flow convergence

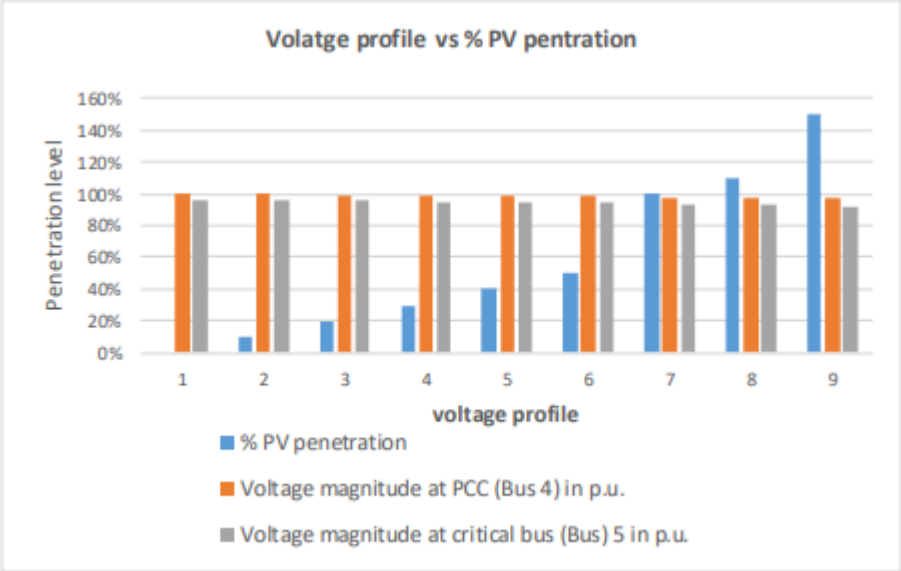

Figure 7-17: Impact of increased Solar PV capacity on voltage profile at the best PCC Bus and at the critical Bus respectively

The optimal penetration level is theoretically determined and constrained by fundamental stability conditions especially Bus 5 voltage magnitude as well as the dynamic transient stability condition of the system under fault application. The simulation results, show that at 40 % penetration level, Bus 5 magnitude was noted to be 0,95, and further increase made the voltage to plunge into values below the required standard magnitude voltage threshold of 0,95 p.u. The dynamic transient stability monitored through the rotor angle stability, indicates that the system is unstable from any Solar PV capacity over 40 % penetration level and from 140 % the results

show no power flow convergence. Figure 7-18 shows the results of unstable condition as per G2 and G3 rotor angle stability monitoring, illustrating 50 % Solar PV penetration.

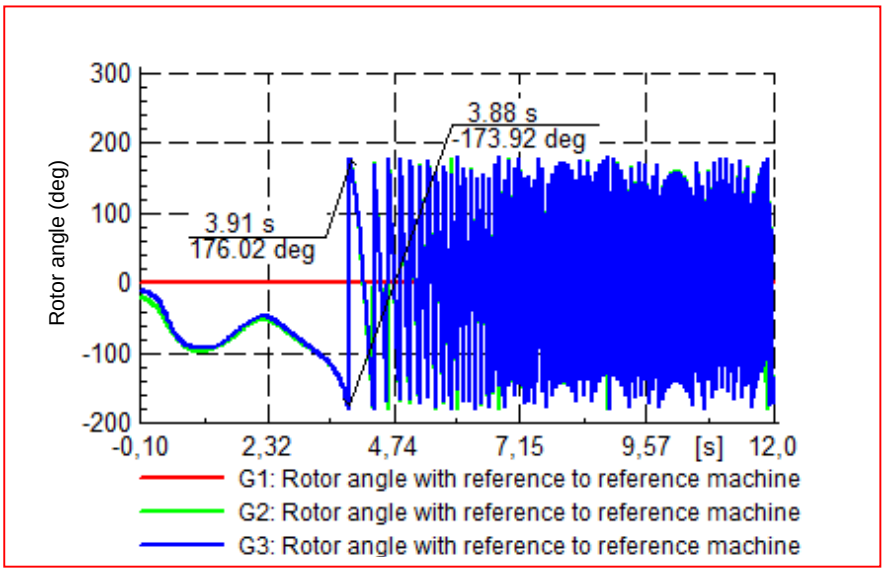

Figure 7-18: Unstable dynamic stability condition for 50 % Solar PV penetration without BESS

On the other hand, although the grid load margin improved with the integration of adequate Solar PV system from the worst case scenario as evidenced in section 7.2.1.2 above, the increase of Solar PV penetration level at a selected PCC, Bus 4 in this case, reveals that the system loadability and the point of voltage collapse, slightly decrease with the level of penetration. The above effect of increased Solar PV penetration on the IEEE-9 Bus system loadability is illustrated in Figure 7-19.

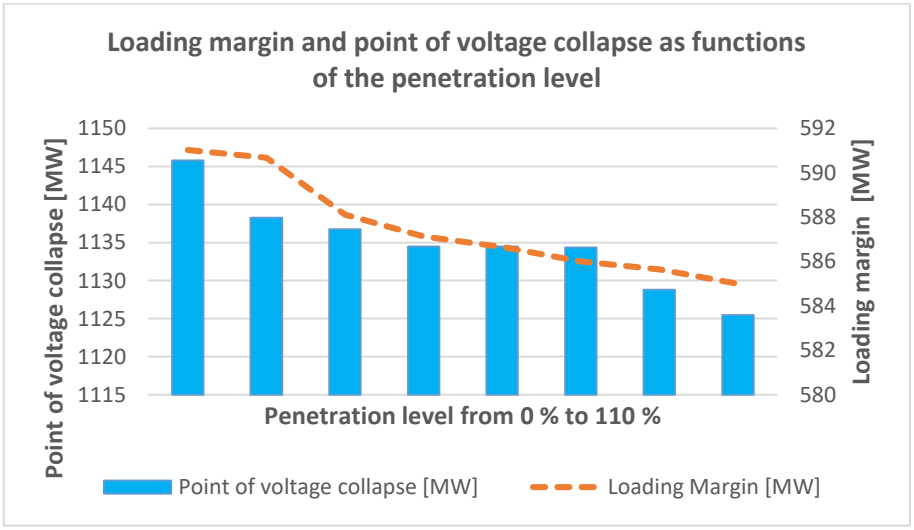

Figure 7-19: Effect of Solar penetration level on the IEEE 9-Bus system's loadability without BESS

.

7.3 Case 3: Evaluation of the impact of Solar PV integration with BESS

7.3.1 Impact of Solar penetration with BESS

Two scenarios are considered. Firstly, the impact of BESS is assessed in steady state for static stability and system loadability assessments and secondly the evaluation of BESS sizing and BESS location is assessed using dynamic transient stability analysis.

In both scenarios, the BESS are set up to be charged only by the solar PV system to assure that there is no reverse power flow, the effect of Solar PV intermittency is compensated by BESS absorption and there are no losses to account for in the case of BESS charging from the grid. To ensure that all available energy of the BESS is consumed up to the lower limits of the SOC, and peak shaving is achieved for reduction of further losses, the discharging process is set to happen during on-peak time from 13:30 to 17:30 as per Figure 6-1. In this way the energy stored in the BESS is fully utilized in one dispatch cycle (24 hours).

The hybrid PV-BESS system is placed at the critical Bus and several load flows are run to assess the voltage profile, system loadability and critical voltage collapse point through RMS/EMT simulations and P-V curves analysis are extracted. The results are consolidated and discussed below in points 7.3.1.1 and 7.3.1.2 below respectively.

The impact of BESS sizing and siting will be assessed further down using dynamic transient stability analysis under fault condition. For the purpose of this evaluation, the best PCC, the hybrid PV-BESS system was placed at Bus 4 which was found to be the best PCC.

7.3.1.1 On voltage stability

The load flow was run to assess the voltage profile at all the buses and the results are displayed in Figure 7-19. It can be seen that the combination PV-BESS impacts positively on the voltage profile as the voltage at all buses except the slack bus, improve slightly compared to the previous case where PV was integrated without BESS. Buses 7, 8 and 9 however experienced an overvoltage, in violation of the standard requirement with bus 9 reaching 1,065 p.u, compared to 1,051 p.u. recorded in the previous case where Solar PV was integrated to the grid without BESS. This can be explained by the proximity of these three buses to generators 2 and 3 as the voltage drops in lines 2,3, 4 and 5 are minimised with the support of the BESS at Bus 5.

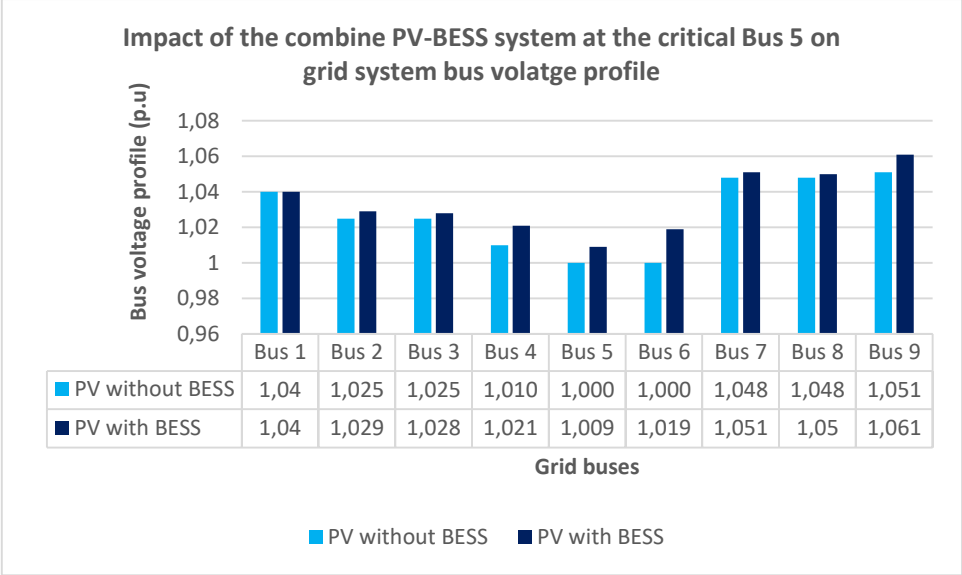

Figure 7-20: Grid voltage profile as effected by the combined PV-BESS at critical Bus 5

7.3.1.2 On system loadability

In Figure 7-21, P-V curves were extracted for the system loadability assessment of the impact of BESS. The analysis focused on the loading margin, the maximum loadability point and the point of collapse.

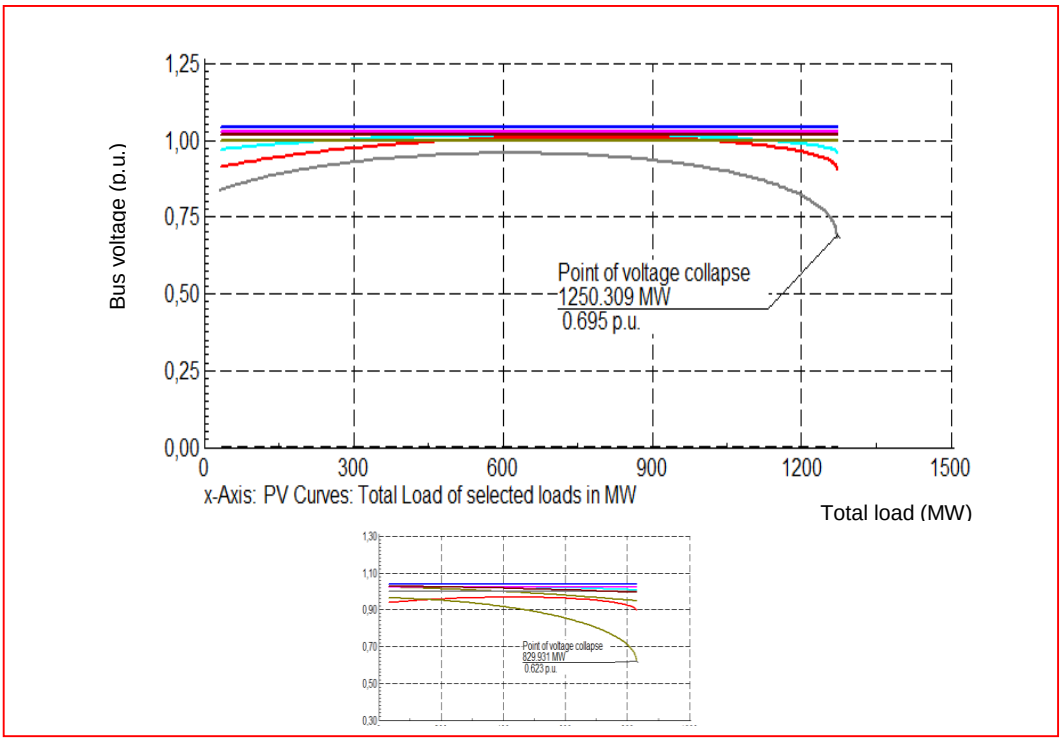

Figure 7-21: P-V curves with Solar PV combined with BESS at Bus 5 (from the initial worst case)

Results show that the incorporation of the BESS under the set conditions as described above improve substantially both the loading margin and the point of voltage collapse with respectively 16,9 % and 9,43 % while the maximum loadability point having a negligible improvement of 0,43 %.

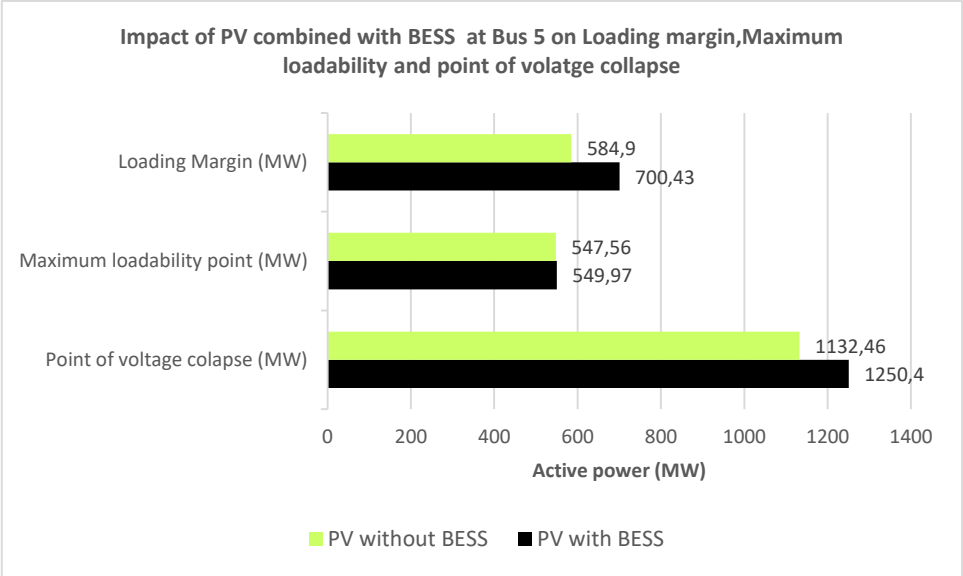

Figure 7-22: Comparison of the impact of the PV without BESS and PV with BESS on system loadability

7.3.2 **Dynamic transient evaluation of BESS sizing and siting on the PV penetrated grid**

To evaluate the impact of BESS sizing and siting on the PV penetrated grid, two scenarios that will be described later were considered. There was first a need to determine the size of BESS based on the grid generation capacity, Solar PV plant generation capacity and the average load requirement. Figures 7-23 and 7-24 provide respectively, the Solar PV plant generated energy and the average load consumption that subsequently will permit to determine the load time characteristics curves to be used for the Quasi-Dynamic Simulation tool. From the dynamic load flow on the network, the size of the BESS is determined from the excess power that is exported to the grid by the Solar PV system. The rational is that that excess power can be used to charge the BESS. The peak excess power was 3,3 MW for approximately 8 hours and the BESS chosen size was 4 MW.

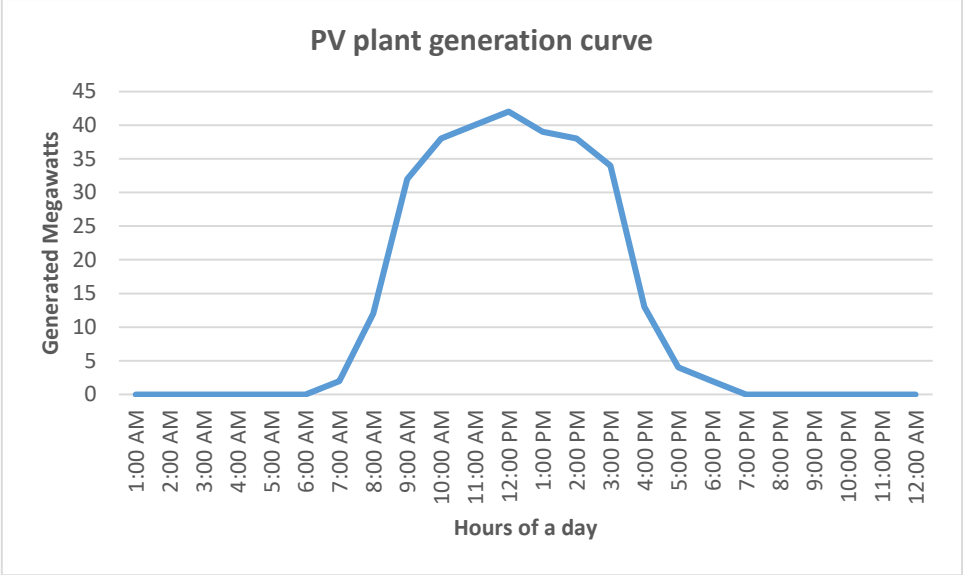

Figure 7-23: PV plant generation curve

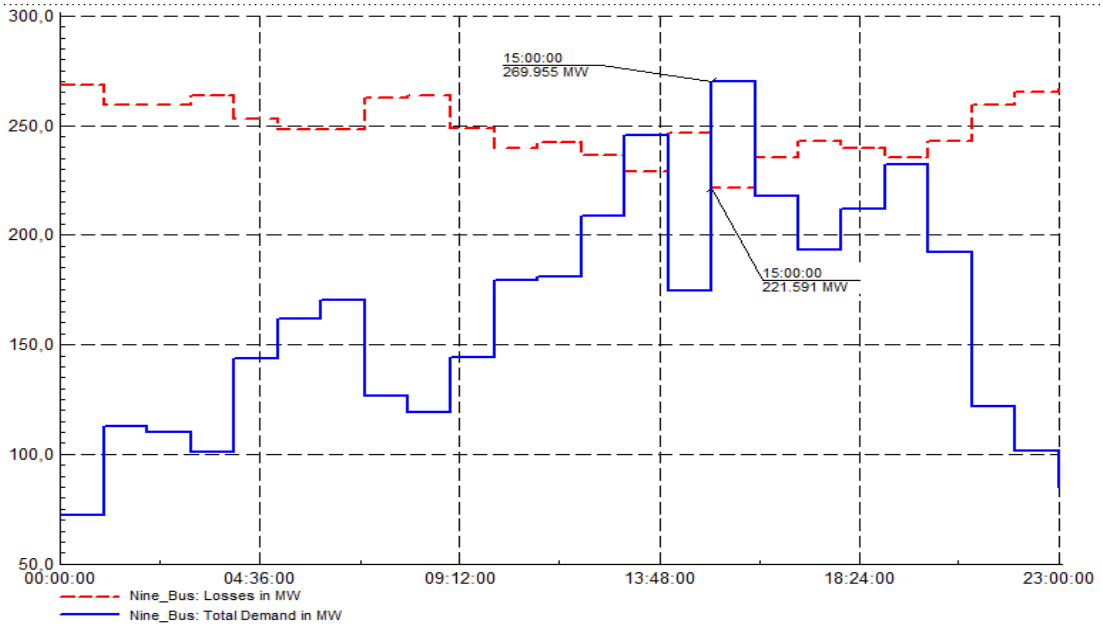

Figure 7-24: Overall average total demand on the IEEE 9-Bus

The assessment of the dynamic transient performance was performed by monitoring the rotor angle of G2 and G3 with reference to the slack generator G1 and the voltage profile at transmission line buses. To investigate the potential of grid-scale BESS as an enabler for large-scale renewable energy integration, the assessment starts with the unstable condition described in Figure 7-18 which presented a 50 % PV penetration. With different BESS sizes in 25 % increments, the dynamic stability is assessed using a three phase fault for 12 seconds. It is evidenced that the dynamic stability improves as the size of the BESS increases. From 0 % BESS added, up to just below 75 % of the size of the BESS, the network remained unstable as

shown in Figure 7-25 closely identical to Figure 7-18 when 50 % PV penetration was reached. The network regained stability after over 75 % of BESS was inserted to the PV as presented in Figure 7-26. Bus voltage profile was verified and it was noted that the voltage at the critical Bus 5, improved from 0,941 p.u to 0,956 p.u,

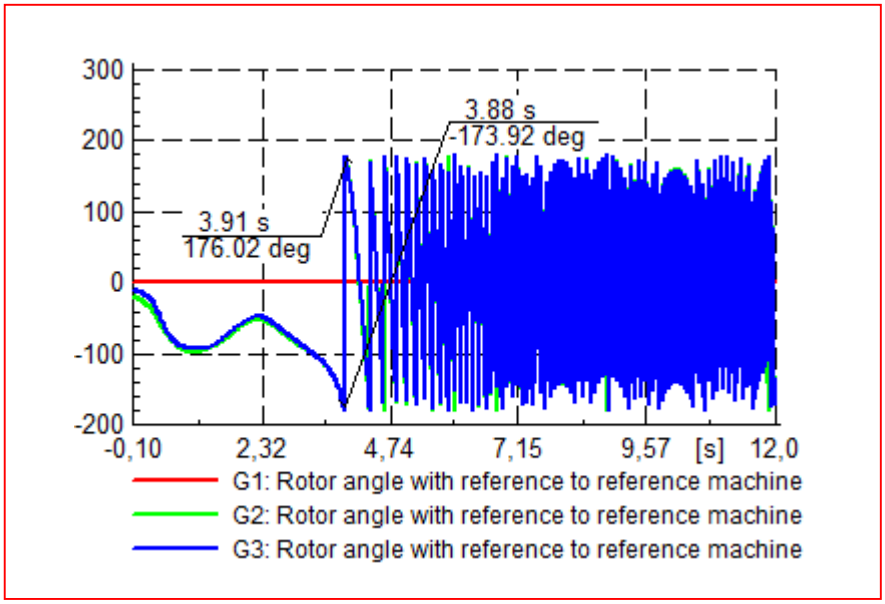

Figure 7-25: Unstable dynamic condition with 50 % PV penetration and 50 % BESS size

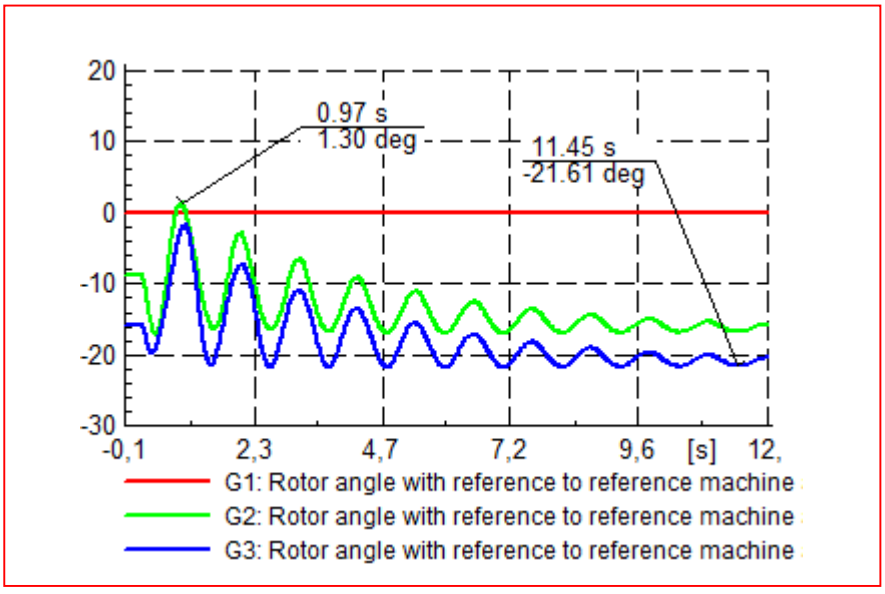

Figure 7-26: Stable dynamic condition with 50 % PV penetration and 75 % BESS size incorporated

Further increase of the BESS capacity till 125 % showed dynamic stability, but with over voltages recorded at buses 5,7,8 and 9. It can therefore be understood that under the limitations of voltage requirements, the size of BESS can impact positively on network stability and enable high Solar PV penetration.

7.4 Case 4: System losses determination using Quasi-Dynamic simulation

7.4.1 Power grid loss evaluation with no BESS incorporated

In this current case, Scenario 2 of Case One is considered as the base case. The Solar PV system is integrated at the critical Bus 5 with the aim to investigate to what extent voltage compensation and support can be achieved by injecting P at load ends. The Solar PV system is set to bring about the total power demand due to load increase and the load characteristic is modified to include time variant load for Quasi-simulation study.

The Quasi-simulation is performed to determine the total losses on the system for 24 hours. The results show that there is a further reduction in the losses from 59,9 MW to a maximum of 40,5 MW at 07:00 and a minimum loss of 32 MW at 15:00 as it can be seen from the graph in Figure 7-27. The maximum losses in this case are however closer to the losses in the base case scenario 1 with a higher gradient.

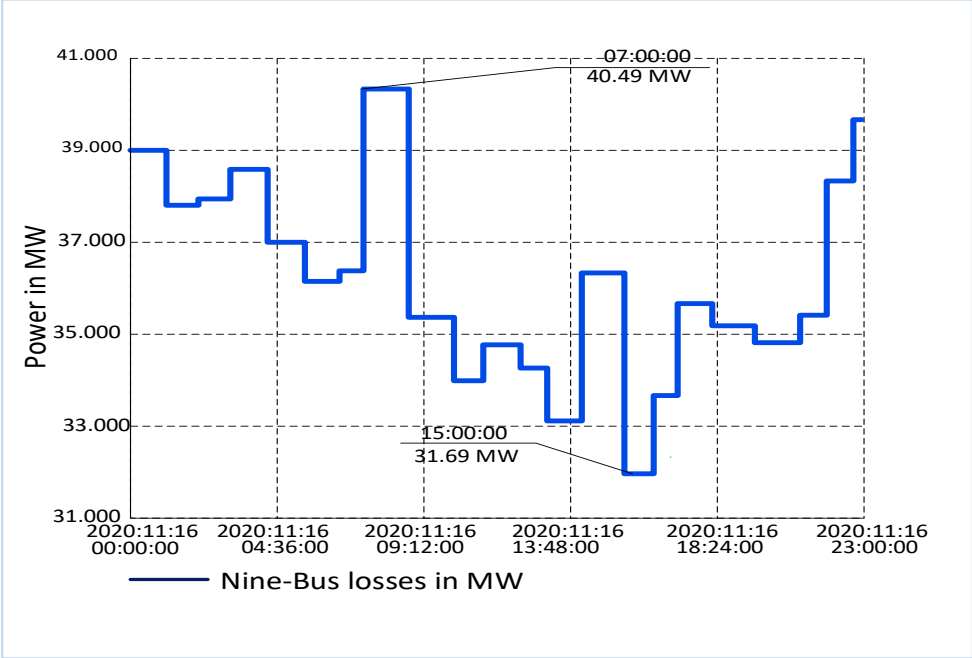

Figure 7-27: 24-hour Quasi simulation results for the PV penetrated test network system(without BESS)

7.4.2 PV integration with BESS

From the Quasi-simulation results presented in Figure 7-28, it is evidenced that the total system losses are minimal compared to all the previous cases reaching a high of 40 MW and a minimum of 38,7 MW with a very small gradient.

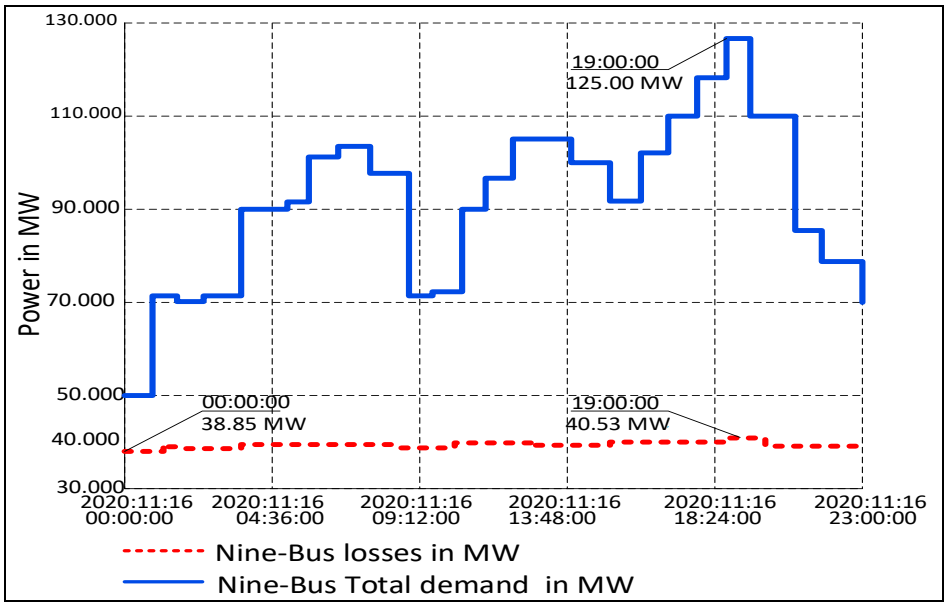

Figure 7-28: 24-hour Quasi simulation results PV integrated system with BESS

Summary

This chapter presents the results of the research work, based on 4 cases stated in the previous chapter. Conclusions are consolidated in the next chapter.

CHAPTER 8: CONCLUSION AND SUGGESTIONS FOR FURTHER RESEARCH

Introduction

This chapter presents conclusions based on the research questions and findings based on simulations executed. Further research topics and recommendations emanating from this dissertation are also suggested for considerations.

8.1 Findings

The studies were concerned with the evaluation of grid-scale BESS as an enabler for large-scale renewable energy integration. The evaluation focused on the impact of BESS on static and dynamic stability of a network and it was found that BESS have both negative and positive effects on grid stability.

Firstly, the simulations results confirmed that stability and loadability are dependent on the network structure, the location and size of the DG as well as the network fault conditions. Using a methodology based on the scenarios and cases comparison, four case were used to carry out the studies namely: (1) Network operating without DG, (2) Network operating with Solar PV system, (3) Impact of the BESS on stability and loadability, and, (4) Impact of BESS on system losses. Two scenarios were considered under Case one with the aim of creating reference cases for further comparison and analysis. From the two scenarios, Bus 5 was determined to be the critical bus from which the rest of the simulations were going to be based. Static and dynamic modes were used to assess in particular voltage stability and system loadability.

In Case 2, the incorporation of the Solar PV system, although with little reactive power generation capacity, revealed a voltage profile improvement, resulting particularly from the fact that converter-based technologies with appropriate control mechanisms can contribute to supporting voltage profile. Solar PV penetration also improved system loadability, loading margins and the point of voltage collapse. For the purpose of adequately placing the BESS for future cases, the studies analysed the impact of level of penetration using both the voltage profile and transient stability criteria, and, it was found that the best PCC was Bus 4. In Case 4, the impact of BESS was evaluated with regard to voltage profile and system loadability and simulations results were compared to those of Case 3. It was evidenced that voltage profile was improved but beyond standard values at some buses. System loadability also showed

improvement as the point of voltage collapse was pushed further to more power. The evaluation of the potential of grid-scale BESS as an enabler for large-scale renewable energy integration was achieved through an unstable case of 50 % PV penetration, which gained stability with the incorporation of BESS. However, that stability criterion was not enough and it was found that despite the positive impact on stability, the size of the BESS was limited by the voltage criterion at buses. The simulations results demonstrated the BESS function to act as generator or loads contributing subsequently to the overall power system stability by offsetting PV energy intermittency and allowing greater RE penetration.

In the last case, the load characteristic was modified to include time variant load for quasi-simulation of study cases and it was evidenced that the combined effect of the PV-BESS system, has a significant positive impact on the system loadability and the total power system losses.

8.2 Suggestions for further research

Since South Africa is striving towards a 2030 Smart grid goal, further research is necessary in certain aspects so that the objective is achieved. These are proposed topics:

- Advances in energy storage technologies within Southern Africa
- Techno-economic impact of the grid-scale BESS in the South African grid

REFERENCE LIST

[1] M. G. Molina, "Energy Storage and Power Electronics Technologies: A Strong Combination to Empower the Transformation to the Smart Grid," *Proceedings of the IEEE,* vol. 105, no. 11, pp. 2191-2219, November 2017, doi: 10.1109/JPROC.2017.2702627.

[2] L. Baker and J. Phillps, "Tensions in the Tansition: The Politics of Electricity Distribution in South Africa," *Environment and Planning C : Politics and Space* vol. 37, no. 1, pp. 177-196, 2019.

[3] Abdallah, L. and El-Shennawy, "Reducing Carbon Dioxide Emissions from Electricity Sector Using Smart Electric Grid Applications," *Journal of Engineering* January 2013.

[4] A. Miketa and D. Saygin, "Africa 2030: Roadmap for a Renewable Energy Future," *IRENA REmap 2030,* 2015.

[5] G. Pepermans, J. Driesen, D. Haesldnacks, R. Belmans, and W. D'haeseleer, "Distributed Generation Definition, Benefits and Issues," *Energy Policy*, vol. 33, no. 6, pp. 787-799, 2005.

[6] S. W. Blume, *Electric Power System Basics* (IEEE Press Series on Power Engineering). Wiley-InterScience, 2007.

[7] L. T. Berger and K. Iniewski, *Smart Grid: Applications, Communications, and Security*. New Jersey: John Wiley & Sons. , 2012.

[8] F. Katiraei and J. R. Aguero. (2011) Solar PV Integration Challenges. *IEEE Power Energy Magazine*. 69-71.

[9] N. Loji, K. Loji, R. Tiako, I. E. Davidson, and T. Akindeji, "Loadability Assessment of a Photovoltaic Penetrated Grid to Offset Intermittency and Reduce Total Losses using Battery Energy Storage System," presented at the SAUPEC/RobMech/PRASA Potchestroom, South Africa, January, 2021.

[10] B. Kroposki. (2015, September) Energy Storage in the Future Grid. *IEEE Electrification Magazine*. 94-65.

[11] P. Kundur, *Power System Stability and Control* (EPRI Engineering Series). Carlifonia: McGraw-Hill Inc., 1994.

[12] R. Ferroukhi, D. Gielen, G. Kieffer, M. Taylor, D. Nagpal, and A. Khalid, "REthinking Energy: Towards a New Power System " *IRENA Technical Report*, 2014.

[13] H. Wuester, R. Ferroukhi, L. El-Katiri, D. Saygin, T. Rinke, and D. Nagpal, "Rethinking Energy: Renewable Energy and Climate Change," *IRENA Technical. Report,* 2015.

[14] J. Cochran *et al.*, "Flexibility in 21st Century Power Systems," *NREL* no. TP-6A20-61721, May 2014.

[15] R. Adapa *et al.*, "Proposed Terms and Definitions for Flexible AC Transmission System (FACTS)," *IEEE Transactions on Power Delivery*, vol. 12, no. 4, pp. 1848-1853, October 1997.

[16] P. D. Lund, J. Lindgren, J. Mikkola, and J. Salpakari, "Review of Energy System Flexbility Measures to Enable High Energy Levels of Variable Renewable Electricity," *Renewable and Sustainable Energy Reviews*, vol. 45, pp. 785-807, February 2015, doi: 10.1016/j.rser.2015.01.057.

[17] M. Huber, D. Dimkova, and T. Hamacher, "Integration of Wind and Solar Power in Europe: Assessment of Flexibility Requirements," *Energy*, vol. 69, pp. 236-246, March 2014.

[18] E. Lannoye, D. Flynn, and M. O'Malley, "Evaluation of Power System Flexibility," *IEEE Transactions on Power Systems*, vol. 27, no. 2, pp. 922-931, May 2012.

[19] S. Impram, S. V. Nese, and B. Oral, "Challenges of renewable energy penetration on power system flexibility: A survey," *Energy Strategy Review*, vol. 31, August 2020.

[20] I. S. Jha, S. Sen, K. Bhambhani, and R. Kumar, "Grid Integration of Renewable Energy Sources," *Journal of Scientific and Technical Advancements*, vol. 1, no. 3, 2015.

[21] Y. G. Rebours, D. S. Kirschen, M. Trotigon, and S. Rossignol, "A Survey of Frequency and Voltage Control Ancillary Services—Part I: Technical Features," *IEEE Transactions on Power Systems*, vol. 22, no. 1, pp. 350-357, February 2007.

[22] H. Lund, A. N. Anderson, P. A. Ostergaard, B. V. Mathiesen, and D. Connolly, "From Electricity Smart Grids to Smart Energy Systems-A Market Operation Based Approach and Understanding " *Energy* vol. 42 pp. 96-102, 2012, doi: 10.1016/j..energy.2012.04.003.

[23] G. Wang *et al.*, "A Review of Power Electronics for Grid Connectionof Utility-Scale Battery Energy Storage Systems " *IEEE Transactions on Sustainable Energy*, vol. 7, no. 4, pp. 1778-1790, October 2016, doi: 10.1109/TSTE.2016.2586041.

[24] P. J. A. Lopez, N. Hatziargyriou, J. Mutale, P. Djapic, and N. Jenkins, "Integrating Distributed Generation into Electric Power Systems: A Review of Drivers, Challenges and Opportunities," *Electric Power Systems Research*, vol. 77, pp. 1189-1203, 2007, doi: 10.1016/j.epsr.2006.08.016.

[25] C. Sankaran, *Power Quality*. New York: CRC Press LLC, 2002.

[26] T. Kouskou, P. Bruel, T. El Rhafiki, and Y. Zeraouli, "Energy Storage : Applications and Challenges," *Solar Energy Materials and Solar Cells*, vol. 20, pp. 59-80, 2014.

[27] N. M. Tabatabei, A. J. Aghbolaghi, N. Bizon, and F. Blaabjerg, *Reactive Power Control in AC Power Systems: Fundamentals and Current Issues*. Cham, Switzerland: Springer International, 2017.

[28] F. H. Gandoman *et al.*, "Review of FACTS Technologies and Applications for Power Quality in Smart Grids with Renewable Energy Systems," *Renewable and Sustainable Energy Reviews*, vol. 82, pp. 502-514, 2018.

[29] M. Farhoodea, A. Mohammed, H. Shareef, and H. Zayandebroodi, "Power Quality Analysis of Grid-Connected Photovoltaic Systems in Distribution Networks," *Przeglad Elektrotechniczny* vol. 2013/2a, pp. 208-213, 2013.

[30] T. G. More, P. R. Asabe, and S. Chawda, "Power Quality Issues and It's Mitigation Techniques," *Journal of Engineering Research and Applications(IJERA)* vol. 4, no. 4, pp. 170-177, April 2014.

[31] S. Chattopadhyay, M. Mitra, and S. Sengupta, *Electric Power Quality*. Springer, 2011.

[32] S. Chowdbury and T. Matlokotsi, "Role of Grid Integration of Distributed Generation in Power Qualiy Enhancement : A Review," presented at the IEEE PES Power Africa, Livingstone, Zambia, 2016.

[33] A. De Almeida, L. Moreira, and J. Delgado, "Power Quality Problems and New Solutions," *Renewable Energy and Power Quality Journal* vol. 1, no. 1, pp. 25-33, November 2003.

[34] T. Matlokotsi, "Power Quality Enhancment in Electricity Networks Using Grid-Connected Solar and Wind Based DGs," Master of Science in Electrical Engineering, Department of Electrical Engineering, University of Cape Town, Cape Town, 2017.

[35] M. J. Ghorbani and H. Mokthari, "Impact of Harmonics on Power Quality and Losses in Power Distribution Systems " *International Journal of Electrical and Computer Engineering (IJECE)* vol. 4, no. 1, pp. 166-177, February 2015.

[36] A. Polycarpou, "Power Quality and Voltage Sag Indices in Electrical Power Systems," in *Electrical Generation and Distribution Systems and Power Quality Disturbances* G. Romero, Ed.: InTech, 2011.

[37] S. Ruiz-Romero, A. Colmenar-Santos, F. Mur-Perez, and A. Lopez-Rey, "Integration of Distributed Generation in the Power Distribution Network: The Need for Smart Grid Control Systems,Communication and Equipment for a Smart City—Use Cases," *Renewable and Sustainable Energy Reviews,* vol. 38, pp. 223-234, June 2014.

[38] S. W. Mohod, "Power Quality Issues and its Improvement in Wind Energy Generation Interface to th Grid," *MIT International Journal of Electrical and Instrumentation Engineering,* vol. 1, no. 2, pp. 116-122, 2011.

[39] A. Safdarian, M. Fotuhi-Firuzabad, and M. Lehtonen, "A General Framework for Voltage Sag Performance Analysis of Distribution Networks " *Energies,* vol. 12, July 2019.

[40] S. Gortz, "Battery Energy Storage for Intermittent Renewable Electricity Production: A Review and Demostration of Energy Storage Applications Permitting Higher Penetration of Renewables " Master of Science in Energy Technology, Department of Applied Physics and Electronics Umea University, Umea, Sweden, 2015.

[41] J. B. Gupta, *A Course in Power Systems : Generation and Economic Considerations, Transmission and Distribution, Switchgear and Protection*. New Delhi: SK Kataria & Sons, 2013.

[42] J. Machowski, J. W. Bialek, and J. R. Bumby, *Power System Dynamics: Stability and Control*, 2nd ed. New Delhi: John Wiley & Sons Ltd, 2008.

[43] T. Madhuranthaka and T. G. Manohar, "A Review on Power System Voltage Stability and Optimization Techniques," *Internaional Journal of Engineering Research and Application (IJERA),* vol. 6, no. 11, pp. 6-14, November 2016.

[44] P. Kundur *et al.,* "Definition and Classification of Power System Stabiity: IEEE/Cigre Joint Task Force on Stability Terms and and Definitions " *IEEE Transactions on Power Systems,* vol. 19, pp. 1387-1401, September 2004, doi: 10.1109/TPWRS.2004.825981

[45] R. Al-Abri, "Voltage Stability Analysis with High Distributed Generation(DG) Penetration," PhD, School of Electrical and Computer Engineering, University of Waterloo, Ontanio, 2012.

[46] C. D. Vourmas, P. W. Sauer, and M. A. Pai, "Relationships Between Voltage and Angle Stability of Power Systems," *Energy Systems,* vol. 18, no. 8, pp. 493-500, November 1996, doi: 10.1016/0142-0615(96)00009-9.

[47] B. S. Abdularaheem and C. K. Gan, "Power System Frequency Stability and Control: Survey," *International Journal of Applied Engineering Research,* vol. 11, no. 8, pp. 5688-5695, 2016.

[48] K. R. Padiyar, *Power System Dynamics Stability and Control*, 2nd ed. Hyderabad, India: BSP, 2008.

[49] Z. A. Kamuruzzaman and A. Mohammed, "Dynamic Voltage Stability of a Distribution System wih High Penetration of Grid-Connected Photovoltaic Type Solar Generators," *Journal of Electrical Systems,* vol. 12, no. 2, pp. 239-248, June 2016.

[50] M. Reza, P. H. Schavemaker, J. G. Slootweg, W. L. Kling, and V. d. Sluis, "Impacts of Distributed Generation Penetration Levels on Power Systems Transient Stability," presented at the IEEE Power Engineering Society Geeral Meeting, Denver,USA, June, 2004.

[51] J. G. Slootweg and W. L. Kling, "Impacts of Distributed Generation on Power System Transient Stability," presented at the IEEE Power Engineering Society Summer Meeting, Chicago, USA, September, 2002.

[52] L. Freris and D. Infield, *Renewable Energy in Power Systems*. New Jersey: Wiley & Sons Ltd, 2008.

[53] P. Daly, N. Cunniffe, and D. Flynn, "Inertia Considerations within Unit Commitment and Economic Dispatch for Systems with Non-Synchronous Penetration," presented at the IEEE Eindhoven Power Tech, Eindhoven, Netherlands, 2015.

[54] Z. A. Obaid, L. M. Cipcigan, L. Abrahim, and T. Muhssin, "Frequency Control of Future Power Systems: Reviewing and Evaluating Challenges and New Control Methods," *Journal of Mod. Power Systems Clean Energy*, vol. 7, no. 1, pp. 9-25, 2019.

[55] S. Sharma, K. R. Niazi, K. Verma, and T. Rawat, "A Bi-Level Optimization Framework for Investment Planning of Distributed Generation Resources in Coordination with Demand Response " *Energy Sources,Part A: Recovery, Utilization, and Environmental Effects,* May 2020, doi: 10.1080/15567036.2020.1758248.

[56] P. Daly, L. Ruttledge, M. Power, and D. Flynn, "Wind Power Emulated Inertial Respone: Ancillary Service Design & System Scheduling Considerations," presented at the CIGRE Session 46, Paris, France, 2016.

[57] M. Rezkalla and M. Marinelli, "Augmenting System Inertia Through Fast Acting Reserve: A Power Systems Case Study with High Penetration of Wind Power," presented at the 54th International Universities Power Engineering Conference IUPEC), Bucharest, Romania, September, 2019.

[58] S. Chakrabarti, "Notes on Power System Voltage Stability," January 2011.

[59] M. K. Jalboub, A. M. Ihbal, and R. A. Abd-Alhameed, "Determination of Static Voltage Stability Margin of the Power System Prior Voltage Collapse," presented at the 8th International Multi-Conference on Systems, Signals and Devices (SSD 2011), Sousse, Tunisia, 22-25 March, 2011.

[60] R. Kumar, A. Malik, and G. Dalakoti, "Power Flow & Voltage Stability Analysis Using MATLAB," *Internaional Research Journal of Engineering and Technology (IRJET),* vol. 4, no. 1, pp. 93-99, January 2017.

[61] M. R. Aghamohammadi, S. S. Hashemi, and M. S. Ghazizadeh, "A Novel Index for Online Voltage Stability Assessment Based on Correlation Characteristic of Voltage Profiles," *Iranian Journal of Electrical & Electronic Engineering* vol. 7, no. 2, pp. 131-139, June 2011.

[62] O. E. Oni, "Technical Perfomance and Stability Analysis of Eskom Power Network Using 600 kV,800 kV, and 1000 kV HVDC," Master of Science in Engineering, College of Agriculture, Engineering and Science, University of KwaZulu-Natal, Durban, South Africa, 2016.

[63] C. W. Taylor, *Power System Voltage Stability*. New York: McGrawhil, 1993.

[64] H. Chiang, I. Dobson, R. J. Thomas, J. S. Thorp, and L. Fekih-Ahmed, "On Voltage Collapse in Elecric Power Systems," *IEEE Transactions on Power Systems*, vol. 5, no. 2, pp. 601-611, May 1990.

[65] V. Ajjarapu and C. Christy, "The Continuation Power Flow: A Tool for Steady State Voltage StabilityAnalysis," *Transactions on Power Systems*, vol. 7, no. 1, pp. 416-423, February 1992.

[66] S. B. Bhaladhare, A. S. Telang, and P. P. Bedekar, "P-V, Q-V Curve - A Novel Approach for Voltage Stability Analysis," in *National Conference on Innovative Paradigms in Engineering & Technology*, 2013: International Journal of Computer Applications (IJCA), pp. 31-35.

[67] B. Gao, G. K. Morison, and P. Kundur, "Voltage Stability Evaluation Using Modal Analysis," *Transactions on Power Systems*, vol. 7, no. 4, pp. 1529-1542, November 1992.

[68] J. Kumar, C. Parthasarathy, M. Vasti, H. Laaksonen, M. Shafie-Khah, and K. Kauhaniemi, "Sizing and Allocation of Battery Energy Storage Systems in Aland Islands for Large-Scale Integration of Renewables and Electric Ferry Charging Stations," *Energies*, vol. 13, no. 317, January 2020, doi: 10.3390/en13020317.

[69] T. Van Cutsem and C. Vournas, *Voltage Stability of Electric Power Systems*. New York ,USA: Springer Science, 2008.

[70] M. R. Aghamohammadi, S. S. Hashemi, and M. S. Ghazizadeh, "A Novel Index for Online Voltage Stablity Assessment Based on Correlation Characteristic of Voltage Profiles," *Iranian Journal of Electrical and Electronic Engineering*, vol. 7, no. 2, pp. 131-140, June 2011.

[71] C. Reis and F. P. M. Barbosa, "A Comparison of Voltage Stability Indices," presented at the IEEE MELECON, Malaga, Spain, May, 2006.

[72] F. A. Althowibi and M. W. Mustafa, "Line Voltage Stability Calculations in Power Systems," presented at the IEEE International Conference on Power and Energy, Kuala Lampur, Malaysia, November, 2010.

[73] C. Sharma and M. G. Ganness, "Determination of the Applicability of Using Modal Analysis for the Prdition of Voltage Stability," presented at the IEEE PES Transmission and Distribution Conference and Exposition, Chicago, USA, April, 2008.

[74] Y. Tamura, H. Mori, and S. Iwamoto, "Relationship Between Voltage Instability and Multiple Load Flow Solutions in Electric Power Systems," *IEEE Transactions on Power Apparatus and Systems* vol. 102, no. 5, pp. 1115-1125, May 1983.

[75] N. Parsai and A. Thakur, "PV Curve-Approach for Voltage Stability Analysis," *International Journal of Information Technology and Electrical Engineering*, vol. 4, no. 2, pp. 46-52, April 2015.

[76] S. J. Thanekar, W. Z. Gandhare, and A. P. Vaidya, "Voltage Stability Assessment of a Transmission System - A Review," *International Journal of Electrical Engineering and Technology (IJEET)*, vol. 3, no. 2, pp. 182-191, July-September 2012.

[77] J. O. Petinrin and M. Shabaan, "Impact of Renewable Generation on Voltage Control in Distribution Systems," *Renewable and Sustainable Energy Reviews,* vol. 65, pp. 770-783, June 2016.

[78] T. Xu and P. C. Taylor, "Voltage Control Techniques for Electrical Distribution Networks Including Distributed Generation," in *17th IFAC World Congress* Seoul, Korea, July 6-11 2008, pp. 11967-11971.

[79] L. Kane and G. Ault, "A Review and Analysis of Renewable Energy Curtailment Schemes and Principles of Access: Transitioning Towards Business as Usual," *Energy Policy,* vol. 72, pp. 67-77, May 2014.

[80] L. Bird, J. Cochran, and X. Wang, "Wind and Solar Energy Curtailment: Experience and Practices in the United Sstates," *NREL Technical Report,* vol. TP 6A20 60983, March 2014.

[81] Y. Gu and L. Xie, "Fast Sensitivity Analysis Approach to Assessing Congestion Induced Wind Curtailment," *IEEE Transactions on Power Systems,* vol. 29, no. 1, pp. 101-110, 2014.

[82] D. J. Burke and M. J. O'Malley, "Factors Influencing Wind Energy Curtailment," *IEEE Transactions on Sustainable Energy,* vol. 2, no. 2, pp. 185-193, 2011.

[83] S. K. Tso, T. X. Zhu, Q. Y. Zeng, and K. L. Lo, "Evaluation of Load Shedding to prevent Dynamic Volateg Stability based on Extended Fuzzy Reasoning," in *IEE Proceedings on Generation, Transmission and Distribution,* 1996, vol. 144, no. 2: IEE, pp. 81-86.

[84] S. K. Tso, T. X. Zhu, Q. Y. Zeng, and K. L. Lo, "Evaluation of load shedding to prevent dynamic voltage instability based on extended fuzzy reasoning," *IEEE Proceedings,* vol. 144, no. 2, pp. 81-86, March 1997.

[85] H. Chen, T. N. Cong, W. Yang, C. Tan, Y. Li, and Y. Ding, "Progress in Eectrical Energy Storage System: A Critical Review," *Progress in Natural Science,* vol. 19, pp. 291-312, 2009, doi: 10.1016/j.pnsc.2008.07.014.

[86] F. Diaz-Gonzalez, A. Sumper, O. Gomis-Bellmunt, and R. Villafafila-Robles, "A Review of Energy Storage Technologies for Wind Power Applicatons," *Renewable and Sustainable Energy Reviews,* vol. 16, pp. 2154-2171, February 2012, doi: 10.1016/j.rser.2012.01.029.

[87] A. Eller and D. Gauntlett. (2017) Energy Storage Trends and Opportunities in Emerging Markets. *ESMAP*

[88] A. H. Al-Badi, R. Ahshan, N. Hosseinzadeh, R. Ghorbani, and E. Hossain, "Survey of Smart Grid Concepts and Technological Demonstrations Worldwide Emphasizing on the Oman Perspective," *Applied System Innovation,* vol. 3, no. 5, 2020, doi: 10.3390/asi3010005.

[89] P. Paliwal, N. P. Patidar, and R. K. Nema, "Planning of Grid Integrated Distributed Generators : A Review of Technology Objectives and Techniques," *Renewable and Sustainable Energy Reviews,* vol. 40, pp. 557-570, July 2014, doi: 10.1016/jrser.2014.07.20.

[90] H. Zhao, Q. Wu, S. Hu, H. Xu, and C. N. Rasmussen, "Review of Energy Storage System for Wind Power Integration Support," *Applied Energy,* vol. 137, pp. 545-553, 2015.

[91] P. Hayes and J. Arevalo, "Energy Storage: The Benefits Beyond the Integration of Renewables," *ABB Review,* vol. 4, pp. 42-49, 2015.

[92] S. N. Malival, "Optimal Location of SVC by Voltage Stability Index," *IJSRD- International Journal for Scientific Research & Development,* vol. 1, no. 10, pp. 2269-2271, 2013.

[93] N. G. Hingorani and L. Gyugyi, *Understanding FACTS : Concepts and Technology of Flexible AC Transmission Systems*. Wiley-IEEE Press, 2000.

[94] J. P. Dunlop, *Photovoltaic Systems*, 3rd ed. Illinios: American Technical Publishers, Inc., 2012.

[95] K. Zweibel, *Harnessing Solar Power: The Photovoltaic Challenges*. New York: Plenum Press, 1990.

[96] R. Messenger and J. Ventre, *Photovoltaic Systems Engineerig* Boca Raton: CRC Press LLC., 2000.

[97] T. Markvart, *Solar Electricity*, 2nd ed. West Sussex: John Wiley & Sons Ltd, 2008.

[98] H. L. Willis and W. G. Scott, *Distributed Power Generation: Planning and Evaluation*. New York, USA: CRC Press, 2000.

[99] E. T. Hashim and A. A. Abbood, "Temperature Effect on Power Drop of Different Photovoltaic Modules," vol. 22, no. 5, pp. 129-143, May 2016.

[100] K. C. Divya and J. Ostergaard, "Battery Energy Sorage Technology for Power Systems-An Overview," *Electric Power Systems Research*, vol. 79, pp. 511-520, 2009, doi: 10.1016/j.epsr.2008.09.017.

[101] P. Prakash and D. K. Khatod, "Oprimal Sizing and Siting Techniques for Distributed Generation in Distribution Systems: A Review " *Renewable and Sustainable Energy Reviews*, vol. 57, pp. 111-130, January 2016.

[102] J. M. Carasco *et al.*, "Power-Electronics Systems for the Grid Integration of Renewable Energy Sources: A Survey," *IEEE Transactions on Industrial Electronics*, vol. 53, no. 4, pp. 1002-1016, August 2006, doi: 10.1109/TIE.2006.878356.

[103] H. Wang, M. Liserre, and F. Blaabjerg, "Toward Reliable Power Electronics: Challenges, Design Tools and Opportunities," *IEEE Industrial Electronics Magazine*, vol. 7, no. 2, pp. 17-26, 2013, doi: 10.1109/MIE.2013.2252958

[104] R. E. Brown, "Impact of Smart Grid on Distribution System Design," presented at the Power and Energy Society General Meeting-Conversion and Delivery of Electrical Energy in the 21st Century, August, 2008.

[105] X. Luo, J. Wang, M. Dooner, and J. Clarke, "Overview of Current Development in Electrical Energy Storage Technologies and the Application Potential in Power System Operation," *Applied Energy*, vol. 137, pp. 511-536, 2015.

[106] F. R. Pazheri *et al.*, "Use of Renewable Energy Sources in Saudi Arabia through Smart Grid," *Journal of Energy and Power Engineering* vol. 6, pp. 1065-1070, 2012.

[107] A. Masembe, "Reliability Benefit of Smart Grd Technologies: A Case for South Africa," *Journal of Energy in Southern Africa*, vol. 26, no. 3, pp. 1-9, 2015.

[108] N. Phuangpornpitak and S. Tia, "Opportunities and Challenges of Integrating Renewable Energy Sources in Smart Grid System " *Energy Procedia*, vol. 34, pp. 282-290, 2013.

[109] F. Bignucolo, A. Cerretti, M. Coppo, A. Savio, and R. Turri, "Effects of Energy Storage Systems Grid Code Requirements on Interface Protection Performances in Low Voltage Networks," *Energies*, vol. 10, no. 387, pp. 1-20, March 2017, doi: 10.3390/en10030387.

[110] X. Fang, S. Misra, G. Xue, and D. Yang, "Smart Grid-The New and Improved Power Grid : A Survey," *IEEE Communication Surv Tutorials,* vol. 14, pp. 944-980, 2012.

[111] B. V. Mathiesen *et al.*, "Smart Energy Systems for Coherent 100% Renewable Energy and Transport Solutions," *Applied Energy,* vol. 145, pp. 139-154, February 2015, doi: 10.1016//j.apenergy.2015.01.075.

[112] K. Moslehi and R. Kumar, "Smart Grid - A Reliability Perspective," presented at the IEEE PES Conference on Innovative Smart Grid Technologies, Washington,DC, January, 2012.

[113] A. Evans, V. Strezov, and T. J. Evans, "Assessment of Utility Energy Storage Options for Increased Renewable Energy Penetration," *Renewable and Sustainable Energy Reviews,* vol. 16, pp. 4141-4147, March 2012, doi: 10.1016/j,rser.2012.03.048.

[114] R. Sebastian and P. R. Alzola, "Flywheel Energy Storage Systems: Review and Simulation for an Isolated Wind Power System," *Renewable and Sustainable Energy Reviews,* vol. 16, pp. 6803-6813, 2012, doi: 10.1016/j.rser.2012.08.008.

[115] P. F. Ribeiro, B. K. Johnson, M. L. Crow, A. Arsoy, and Y. Liu, "Energy Storage Systems for Advanced Power Applications," *Proceedings of the IEEE,* vol. 89, no. 12, pp. 1744-1756, 2001.

[116] L. Yao, B. Yang, H. Cui, J. Zhuang, and J. Xue, "Challenges and Progresses of Energy Storage Technology and its Application in Power Systems," *Journal of Modern Power Systems and Clean Energy,* vol. 4, no. 4, pp. 519-528, October 2016.

[117] A. Khaligh and Z. Li, "Battery, Ultra-Capacitor, Fuel Cell and Hybrid Energy Storage Systems for Electric, Hybrid Electric and Plug-in Electric Vehicles: State of the Art," *IEEE Transactions on Vehicular Technology,* vol. 59, pp. 2806-2814, 2010.

[118] G. Zini and B. Tartarini, "Hybrid Systems for Solar Hydrogen: A selection of Case Studies," *Applied Thermal Engineering,* vol. 29, pp. 2585-2595, 2009.

[119] R. Felseghi, E. Carcadea, M. S. Raboaca, C. N. Trufin, and C. Filote, "Hydrogen Fuel Cell Technology for the Sustainable Future of Stationary Applications," *Energies,* vol. 12, 2019, doi: 10.3390/en12234593.

[120] S. Weitemeyer, D. Kleinhans, T. Vogt, and C. Agert, "Integration of Renewable Energy Sources in Future Power Systems: The Role of Storage," *Renewable Energy* vol. 75, pp. 14-20, 2015, doi: 10.1016/j.renene.2014.09.028.

[121] D. O. Akinyele and R. K. Rayudu, "Review on Energy Storage Technologies for Sustainable Power Networks," *Sustainable Energy Technologies and Assessments,* vol. 8, pp. 74-91, 2014.

[122] E. Hossain, H. M. R. Faruque, S. H. Sunny, N. Mohammad, and N. Nawar, "A Comprehensive Review on Energy Storage Systems: Types, Comparison, Current Scenario, Applications, Barriers, and Potential Solutions, Policies, and Future Prospects," *Energies,* vol. 13, no. 365, July 2020.

[123] T. Bowen, I. Chemyakhovskiy, and P. Denholm, "Grid-Scale Battery Storage :Frequently Asked Questions," *NREL,* no. TP-6A20-74426, September 2019.

[124] M. S. Whittingham, "History, Evolution, and Future Status of Energy Storage," *Proceedings of the IEEE,* vol. 100, no. Special Centennial Issue, pp. 1518-1534, May 2012, doi: 10.1109/JPROC.2012.2190170.

[125] "EPRI-DOE Handbook of Energy Storage for Transmission & Distribution Applications " EPRI ,Palo Alto,CA, and the US Department of Energy, Washington DC,USA, 1001834, 2003.

[126] S. Vazquez, S. M. Lukic, E. Galvan, L. G. Franquello, and J. M. Carrasco, "Energy Storage Systems for Transport and Grid Applications," *IEEE Transactions on Industrial Electronics,* vol. 57, no. 12, pp. 3881-3895, December 2010, doi: 10.1109/TIE.2010.2076414

[127] J. Atherton, R. Sharma, and J. Salgado, "Techno-Economic Analysis of Energy Storage Systems foor Application in Wind Farms," *Energy,* vol. 135, pp. 540-552, June 2017.

[128] M. Pasta, C. D. Wessels, and R. A. Huggins, "A High Rate and Long Cycle Life Aqueous Electrolyte Battery for Grid-Scale Energy Storage," *Nature Communications*, vol. 3, pp. 1149-1168, 2012, doi: 10.1038/ncomms.2139.

[129] M. T. Lawder *et al.*, "Battery Energy Storage System (BESS) and Battery Management System (BMS) for Grid-Scale Applications," *Proceedings of the Cigre IEEE,* 2014.

[130] M. Begovic, A. Pregelj, A. Rohatgi, and D. Novosel, "Impact of Renewable Distributed Generation on Power Systems," *IEEE 34th Hawaii International Conference on System Sciences,* 2001.

[131] C. A. Hill, M. C. Such, D. Chen, J. Gonzalez, and W. M. Grady, "Battery Energy Storage for Enabling Integration of Distributed Solar Power Generation," *IEEE Transactions on Smart Grids,* vol. 3, no. 2, pp. 850-857, June 2012.

[132] G. A. Chown, "The Economic Analysis of Relaxing Frequency Control," Doctor of Philosophy, Faculty of Engineering and Built Enironment, University of Witwatersrand, Johannesburg , South Africa, 2007.

[133] A. A. A.. *et al.*, "DOE/EPRI 2013 Electricity Storage Handbook in Collaboration with NRECA," in "Sandia National Laboratoties," Oak Ridge USA, July 2013.

[134] *Draft Grid Connection Code for Battery Energy Storage Facilities (BESF) Connected to the Electricity Transmission System (TS) or the Distibution System (DS) in South Africa*, NERSA, January 2021.

[135] Y. Yang, H. Li, A. Aichhorn, J. Zheng, and M. Greenleaf, "Sizing Strategy of Distributed Battery Storage System with High Penetration of Photovoltaic for Voltage Regulation and Peak Load Shaving," *IEEE Transactions on Smart Grid,* vol. 5, no. 2, pp. 982-991, March 2014, doi: 10.1109/TSG.2013.2282504.

[136] Y. Yang, "Optimization of Battery Energy Storage Systems for PV Grid Integation Based on Sizing Strategy," Doctor of Phylosophy, Department of Electrical and Computer Engineering, Florida State University, Florida, 2014.

[137] "Handbook on Battery Energy Storage," in "Asian Development Bank (ADB)," Mandaluyong City, Phillipines, December 2018.

[138] E. Veldman, G. M., J. G. Slootweg, and W. L. Kling, "Technical Benefits of Distributed Storage and Load Management in Distribution Grids " presented at the PowerTech, Bucharest, Romania, 28 June -2 July, 2009.

[139] A. Alzahrani, H. Alharti, and M. Khalid, "Minimization of Power Losses through Optimal Battery Placement in a Distributed Network with High Penetration of Photovoltaics," *Energies,* vol. 13, no. 140, January 2020.

[140] T. H. Mehr, M. A. S. Massoum, and N. Jabalameli, "Grid-Connected Lithium-Ion Battery Energy Storage System for Load Leveling and Peak Shaving " presented at the Australasian Universities Power Engineering Conference, AUPEC 2013, Hobart, TAS, Australia, 29 September - 3 October 2013.

[141] G. Mokthari, G. Nourbakhsh, G. Ledwich, and A. Ghosh, "A Supervisory Load-Leveling Approach to Improve the Voltage Profile in Distribution Network," *IEEE Transactions on Sustainable Energy* vol. 6, no. 1, pp. 245-252, January 2015, doi: 10.1109/TSTE.2014.2367035.

[142] J. Makansi and J. Abboud, "Energy Storage: The Missing Link in the Electricit Value Chain," *Energy Storage Council White Paper*

2002.

[143] L. Lanuzza *et al.*, "RES and Energy Storage: New Opportunities for Emerging Markets," *RES4Africa*, vol. 1, pp. 1-23, 2016.

[144] X. Luo *et al.*, "Review of Voltage and Frequency Grid Code Specifications for Electrical Energy Storage Applications," *Energies*, vol. 11, pp. 1-26, April 2018, doi: 10.3390/en11051070.

[145] *Grid Code for Renewable Power Plants(RPPs) Connected to the Electricity Transmission System (TS) or the Disribution System (DS) in South Africa*.

[146] A. M. Elshurafa, "The Value of Storage in Electricity Generation: A Qualitative and Quantitative Review," *Journal of Energy Storage*, vol. 32, September 2020, doi: 10.1016/j.est.2020.101872.

[147] H. T. Kim, Y. G. Jin, and Y. T. Yoon, "An Economic Analysis of Load Leveling with Battery Energy Storage Systems (BESS) in an Electricity Market Environment: The Korean Case," *Energies*, vol. 12, no. 1608, April 2019, doi: 10.3390/en12091608.

[148] P. Gadhavi, "Battery Storage and a Framework for Africa," *Africa Energy Forum*, June 2019.

[149] DigSILENT, "DigSILENT PowerFactory2017 User Manual," in "DigSILENT PowerFactory," Gomarigen, Germany, June 2017.

[150] DigSILENT, "Niine Bus System," in "DigSILENT PowerFactory 2017," Heinrich-Hertz-Str. 9 72810 Gormaringen, Germany, 2016. [Online]. Available: www.digsilent.de

[151] A. G. Endegnanew, "Stability of High Voltage Hybrid AC/DC Power Systems," Ph. D Thesis, Department of Power Systems Laboratory, Swiss Federal Institute of Technology (ETH), Zurich, 2013.

[152] K. Loji, I. E. Davidson, and R. Tiako, "Voltage Profile and Power Losses Analysis on a Modified IEEE 9-Bus System with PV Penetration at the Distribution Ends," presented at the Southern African Universities Power Engineering Conference/Robotics and Mechatronics /Pattern Recognition Association of South Africa(SAUPEC/RobMech/PRASA), Bloemfontein, South Africa, January, 2019.

[153] D. J. Narang, J. Berdner, J. C. Boemer, and C. K. Vartanian, "IEEE Standard for Interconnection and Iteroperability of Distributed Energy Resources with Associated Electric Power Systems Interfaces : Amendment1," *IEEE Std 1547a - 2020*, April 2020.

[154] A. Ghosh, P. K. Saha, and G. K. Panda, "Chaos and Control of Chaos in Current Controlled Power Factor Connected AC-DC Boost Regulators," *International Journal of Modern Engineering Research*, vol. 2, no. 4, pp. 2529-2533, July-August 2012 2012.

[155] S. Hasan Saeed and D. K. Sharma, *Non-Conventional Energy Resources*. New Delhi: SK Kataria & Sons, 2012.

[156] DigSILENT, "Battery Energy Storage Systems," in "DigSILENT Powerfactory ", Germaningen,Germany, 2010.

[157] N. Moubayed, J. Kouta, A. El-Ali, H. Demayaka, and R. Outbib, "Parameter Identification of Lead-Acid Battery Model," presented at the 33rd IEEE Photovoltaic Specialists Conference, San Diego, Carlifonia, USA, June, 2008.